Federal Energy Regulatory Commission

Office of
Energy Projects

January 2013

Docket No. AD13-4-000

Recommended Parameters for Solid Flame Models for Land Based Liquefied Natural Gas Spills

Washington, DC 20426

Recommended Parameters for Solid Flame Models for Land Based Liquefied Natural Gas Spills

TABLE OF CONTENTS

TABLE OF CONTENTS (cont'd)

LIST OF APPENDICES

LIST OF TABLES

LIST OF FIGURES

LIST OF FIGURES (cont'd)

ACRONYMS & ABBREVIATIONS

ADB-10-07	Advisory Bulletin
ADL	Arthur D. Little
AGA	American Gas Association
BGCo	British Gas Corporation
CFR	Code of Federal Regulations
DOE	United States Department of Energy
DOS	disk operating system
DOT	Department of Transportation
FAC2	Factor of Two
FERC	Federal Energy Regulatory Commission
GDF	Gaz de France
GRI	Gas Research Institute
MG	Geometric Mean Bias
kg/m^2-s	kilogram per meter squared-seconds
kW/m^2	kilowatt per meter squared
LNG	liquefied natural gas
m	meter
m/s	meters per second
MRB	Mean Relative Bias
MRSE	Mean Relative Square Error
SEP	surface emissive power
SF	Safety Factor
SNL	Sandia National Laboratories
SPM	Statistical Performance Measure
U.S.	United States
USCG	United States Coast Guard
VG	Geometric Variance

SYMBOLS

AR	aspect ratio
C_m	measured parameter in SPM calculation
C_p	predicted parameter in SPM calculation
c_p	specific heat of air
d	diameter of pool fire
DR	drag ratio of fire
E_s	surface emissive power at flame surface
FR	Froude Number
FR'	modified Froude Number
$F_{12}(x)$	view factor at distance, x
g	gravitational acceleration, $9.81\ m/s^2$
h_c	heat of combustion of methane, $50x10^6\ J/kg$
θ	Flame tilt from vertical
l	length of pool fire
l_f	Flame length
$\dot{m}''_{burn}$	mass burning rate per unit area
$\dot{m}''_{\max}$	maximum mass burning rate
p	wind profile exponent dependant on Pasquill Stability Class
$\dot{q}''(x)$	radiant heat flux (thermal radiation) per unit area at distance x
$Q*$	dimensionless heat release rate
ρ_a	density of air, $\sim 1.2kg/m^3$
ρ_v	density of LNG vapor, $\sim 1.85kg/m^3$
T_a	temperature of air
$\tau(x)$	transmissivity in atmosphere at distance, x
u_{wr}	reference wind speed at reference height, z_r
$u_w(z)$	wind speed at height, z
w	width of pool fire

{THIS PAGE INTENTIONALLY LEFT BLANK}

EXECUTIVE SUMMARY

Sandia National Laboratories (SNL) was contracted by the U.S. Department of Energy (DOE) in 2007 to develop information for assessing the potential impacts associated with large liquefied natural gas (LNG) spills on water. DOE released the results of these studies in the report "Liquefied Natural Gas Safety Research Report to Congress," dated May 2012. Using data gathered from these tests and earlier methane gas burner tests, SNL developed recommendations on parameters, including mass burning rate, pool fire flame height, surface emissive power, and atmospheric transmissivity, appropriate for use in solid flame models for pool fires over water. The U.S. Department of Transportation's regulations at Title 49, Code of Federal Regulations (CFR), Part 193 requires use of the solid flame model LNGFIRE3 for predicting radiant heat from LNG pool fires on land. This document examines the effect of altering the LNGFIRE3 model based on SNL's recommendations regarding LNG pool fire modeling over water and on data provided by the largest LNG pool fire tests on land (Gaz de France Montoir tests) or water (SNL Phoenix tests).

As the calculation methods and parameters are fixed within LNGFIRE3 and cannot be changed by the user, staff of the Federal Energy Regulatory Commission (FERC) constructed a radiant heat calculation method which simulates LNGFIRE3 and which can be modified. By altering individual parameters for mass burning rate, pool fire flame height, surface emissive power, and atmospheric transmissivity, FERC staff investigated the effects of matching both individual parameters to measured experimental data and overall radiant heat predictions to measured results from field experiments.

While LNGFIRE3 under-predicts the mass burning rate, flame length, and the mean surface emissive power for large scale LNG fire tests, predicted distances to radiant heat levels are still close in agreement with the measured values from the experiments. This is primarily due to the over-prediction of the view factor inherent in the solid flame model representation of the flame as a cylinder. FERC staff concludes that LNGFIRE3, as currently prescribed by 49 CFR Part 193, is appropriate for modeling thermal radiation from LNG pool fires on land and is suitable for use in siting on-shore LNG facilities.

{THIS PAGE INTENTIONALLY LEFT BLANK}

1.0 INTRODUCTION

1.1 BACKGROUND

In 2007, Congress provided funding to the U.S. Department of Energy (DOE) to further develop information for assessing the potential impacts associated with large scale liquefied natural gas (LNG) spills on water. Sandia National Laboratories (SNL) was contracted by the DOE to conduct this research. Between 2008 and 2011, SNL conducted tests to simulate large-scale LNG spills and fires over water, cryogenic damage tests on ship structural components, and computer modeling of resulting LNG vessel damage. In May 2012, DOE released the results of this series of studies in "Liquefied Natural Gas Safety Research Report to Congress" [DOE 2012].

Although this effort was focused on examining public safety risks associated with the maritime transportation of LNG though U.S. waterways, it included the largest LNG pool fire tests, either on land or water, performed in the U.S. or internationally. The results of these fire tests are contained in the SNL report, "The Phoenix Series Large Scale LNG Pool Fire Experiments" [Blanchat 2010]. Using the data gathered from the Phoenix tests and earlier methane gas burner tests, SNL developed recommendations on parameters appropriate for use in solid flame models for pool fires over water.

The thermal radiation hazards from a pool fire depend on a number of parameters, including the mixing dynamics and chemical processes of the fuel and oxidant, and absorption and transmission of thermal radiation in the atmosphere. Quantification of these parameters and simulation of the processes, such as anisotropic turbulent mixing, non-equilibrium chemical kinetics, and non-uniform radiation spectra emitted by the fire and absorbed in the atmosphere, are difficult and computationally intensive. As a result, semi-empirical methods are often applied.

The solid flame model approach is currently the most commonly used methodology to model thermal radiation hazards for large open hydrocarbon fires. The solid flame approach approximates the geometric shape of a fire as a tilted cylinder, parallelepiped, or other simple geometry with characteristics based on experimentally derived values and correlations for mass burning rate, flame height, flame tilt, and flame drag. Corresponding geometric view factors for the simplified geometric shape and correlations for the surface emissive power (SEP) and atmospheric transmissivity are then multiplied together to estimate thermal radiation intensity at a specified distance. This approach is expressed by the following equation:

$$\dot{q}''(x) = SEP \cdot F_{12}(x) \cdot \tau(x) \quad (1)$$

where $\dot{q}''(x)$: radiant heat flux (thermal radiation) per unit area (kW/m^2) at distance x ($meters$)
SEP: surface emissive power (kW/m^2)
$F_{12}(x)$: view factor
$\tau(x)$: transmissivity in atmosphere

Using the data gathered from the Phoenix tests and earlier methane gas burner tests, SNL developed recommendations on parameters, including mass burning rate, pool fire flame height, SEP, and atmospheric transmissivity, appropriate for use in solid flame models for LNG pool fires over water. SNL's conclusions were detailed in report SAND2011-9415, "Recommendations on the Prediction of Thermal Hazard Distances from Large Liquefied Natural Gas Pool Fires on Water for Solid Flame Models" [Luketa 2011].

1.2 LNGFIRE3

Over the last 15 years, solid flame models have been incorporated into the federal safety standards for LNG facilities for evaluating thermal radiation hazards. In 1997, the U.S. Department of Transportation (DOT) revised its regulations at Title 49, Code of Federal Regulations, Part 193 (Part 193) to allow use of the LNGFIRE computer program based on the solid flame model described in Gas Research Institute Report GRI-89/0176 [Atallah 1990]. Unlike the previous calculation method specified in the regulation, LNGFIRE took into account wind speed, relative humidity and asymmetrical pool configurations [DOT 1997].

The LNGFIRE program required the specification of site specific parameters (e.g., LNG pool dimensions, flame base and target heights, and specific ambient conditions) and used default values for LNG properties such as molecular weight, liquid density, and boiling temperatures (although values for these properties could be altered). Using the provided ambient conditions and the pool shape and dimensions, the program determined a mass burning rate, flame length, flame tilt, flame drag ratio, and an effective SEP for the flame [Atallah 1990]. Report GRI-89/0176 indicated that results of the LNGFIRE program correlated well with data from pool fire experiments conducted during the 15 years prior to the model adoption. According to Report GRI-89/0176, the following data sets were used in that review [Atallah 1990]:

- Bureau of Mines, 1962;
- Tokyo Gas Company, 1967;
- University Engineers, Inc, 1971;
- Esso, 1973;

- Osaka Gas Company, 1973;
- American Gas Association (AGA), 1973;
- Japan Gas Association, 1976;
- United States Coast Guard (USCG), 1979;
- Shell, 1981;
- Shell, 1982;
- British Gas Corporation (BGCo), 1982;
- Gas Research Institute, Arthur D.
- Little, British Gas Corporation (GRI/ADL/BGCo), 1984; and
- Gaz de France (GDF) Montoir, 1989.

In 1993, Risk and Industrial Safety Consultants, Inc., the original model developers, updated the program and issued LNGFIRE2 in Gas Research Institute Report GRI-92/0532 [GRI 1992]. The DOT revised the Part 193 regulations in 2000 to allow use of the LNGFIRE3 model[1] and again in 2010 to incorporate Gas Technology Institute Report GTI-04/0032 [DOT 2000] [DOT 2010a].

1.3 SCOPE

After the completion of the Phoenix tests and issuance of the May 2012 DOE report to Congress, we recognized that although the tests were conducted over water, many of the parameters recommended by SNL could be applicable to pool fires over land.[2] Therefore, we evaluated which parameters for pool fires over water could be applicable (if any) to the current regulatory LNG pool fire model used for predicting thermal radiation distances from pool fires over land. Given the scarcity of large scale data and potential similarities in trends with the GDF Montoir and SNL data, we concluded that all four parameters (mass burning rate, flame length, SEP, and transmissivity), could potentially be argued to have some applicability to pool fires over land. Therefore, we examined each parameter in more detail with an emphasis on the final prediction of the thermal radiation intensity.

[1] Although the March 1, 2000 Final Rule incorporated LNGFIRE3 into Part 193, the regulation retained the reference to the original LNGFIRE documentation issued as Gas Research Institute Report GRI-89/0176. This text was corrected in an August 11, 2010 Final Rule to reference Gas Technology Institute Report GTI-04/0032. The regulations have never included LNGFIRE2.

[2] The pronouns "we," "us," and "our" used throughout this document refer to the staff of the FERC's Office of Energy Projects.

This document presents our examination of the effect of incorporating SNL's recommendations regarding LNG pool fire modeling over water into LNGFIRE3, the solid flame model required by DOT's regulations for examining contained LNG pool fires on land. As the first step in this examination, we created a version of LNGFIRE3's radiant heat calculation method in the engineering calculation software, Mathcad. This allowed us to investigate the effect of changing individual parameters for mass burning rate, pool fire flame height, SEP, and atmospheric transmissivity. In addition to the SNL recommendations, we examined potential approaches to better represent the effects of wind speed on flame tilt and flame drag on elevated fires. Using this adjusted model, we then conducted a validation study in conjunction with a sensitivity and parametric analysis for the mass burning rate, flame length, SEP, and thermal radiation intensities at various distances to assess overall model performance. In addition to the experimental data used to construct the original LNGFIRE formulation, which included the Montoir tests, this validation study included data from the Phoenix Series tests [Blanchat 2010]. Our goal was to determine whether the current LNGFIRE3 methodology and parameters remain suitable for use in siting LNG facilities or whether adjustments should be made to the LNGFIRE3 model.

Development of the alterable radiant heat calculation model is described in Section 2.0, "Mathcad Solid Flame Model." Sections 3.0 though 7.0 present our investigations on altering individual parameters or correlations: LNG mass burning rate; wind speed; flame tilt; flame drag; flame length; SEP; and transmissivity. Section 8.0, "Thermal Radiation," discusses the overall performance of both the altered model and LNGFIRE3 in predicting radiant heat measurements taken from experimental data. Based on the new data provided by SNL, we present our conclusions on the acceptability of the use of LNGFIRE3 for pool fires over land in Section 9.0, "Conclusions & Recommendations."

2.0 MATHCAD SOLID FLAME MODEL

In LNGFIRE3, the calculation methods for determining mass burning rate, flame length, SEP, transmissivity, and other parameters are fixed within the program and cannot be changed by the user. As a result, the LNGFIRE3 program could not be adjusted to analyze the effect of the SNL recommendations. In order to have a modeling approach where all of the parameters and correlations could be altered, we first constructed a radiant heat calculation method using Mathcad and termed this the "Mathcad Solid Flame Model." The model is shown in Appendix A. The native Mathcad file is available from FERC staff by request. This method was based on the solid flame model described in Gas Research Institute report GRI–89/0176, the only report to include the model source code.

Results for pool fires using the Mathcad Solid Flame Model were compared to results from the LNGFIRE3 computer program in order to verify the accuracy of the approach.

2.1 MODEL ALTERATIONS

The Mathcad Solid Flame Model allows for an explicit examination of any changes to each step in the LNGFIRE3 calculation methodology. Once confirmed to produce results comparable to LNGFIRE3, the following parameters were altered in the Mathcad Solid Flame Model to reflect the various SNL recommendations:

- mass burning rate;
- flame-height-to-diameter correlation;
- SEP; and
- transmissivity correlation.

In addition, we included modifications for the calculation of wind speed and flame drag to automatically calculate the wind speed that would occur at elevations higher than the wind speed reference height. This is discussed in Section 4.0, "Wind Speed and Flame Drag Modification."

2.2 STATISTICAL PERFORMANCE MEASURES

The validation results of the parametric analyses were evaluated using the same statistical performance measures (SPMs) and graphical analyses used in the model evaluation protocol set forth for vapor dispersion models in the DOT Advisory Bulletin ADB-10-07, "Liquefied Natural Gas Facilities: Obtaining Approval of Alternative Vapor-Gas Dispersion Models" [DOT 2010b] and the July 2011 FERC report, "Evaluation of DEGADIS 2.1 Using Advisory Bulletin ADB-10-07" [Kohout 2011].

The SPMs provide quantitative metrics for both a model's tendency to over-predict or under-predict experimental data and the degree of scatter of those predictions. The SPMs, shown in Table 2-1, were compared to the same quantitative criteria provided in the DOT Advisory Bulletin ADB-10-07 [DOT 2010b]. As noted in the Advisory Bulletin, the SPMs do not need to satisfy the quantitative criteria in order for the model to be acceptable. However, disagreement between the two may affect recommendations on safety factors [DOT 2010b].

Sections 3.0 through 7.0 present the evaluation and results for each parameter.

Table 2-1: Statistical Performance Measures

Safety Factor (SF) $0.5 \le \left\langle \frac{C_p}{C_m} \right\rangle \le 2.0$	Factor of Two (FAC2) $\sum \left(0.5 \le \frac{C_p}{C_m} \le 2.0 \right) \ge 50\%$
Mean Relative Bias (MRB) $-0.4 \le \left\langle \frac{C_m - C_p}{\frac{1}{2}(C_m + C_p)} \right\rangle \le 0.4$	Geometric Mean Bias (MG) $0.67 \le \exp\left\langle \ln\left(\frac{C_m}{C_p} \right) \right\rangle \le 1.5$
Mean Relative Square Error (MRSE) $\left\langle \frac{(C_p - C_m)^2}{\frac{1}{4}(C_p + C_m)^2} \right\rangle \le 2.3$	Geometric Variance (VG) $\exp\left\langle \left[\ln\left(\frac{C_m}{C_p} \right) \right]^2 \right\rangle \le 3.3$

3.0 LNG MASS BURNING RATE

3.1 BACKGROUND

The mass burning rate is the amount of gaseous fuel that is volatilized and burned in the pool fire. Higher mass burning rates will result in longer flame lengths and longer thermal radiation distances. For unconfined pools, such as spills over water, higher mass burning rates will also reduce the pool diameter (via mass balance) and subsequently may result in an overall reduction in the thermal radiation distance. However, most LNG pool fires over land would be directed to impoundments and would have constant pool dimensions. As a result, this competing effect would not occur. As mass burning rate is a function of heat transfer, it is possible that the rate will not change significantly between large LNG pool fires over water and large LNG pool fires over land because the function may be dominated by re-radiation and convection from the pool fire. For most solid flame models, the mass burning rate is derived and correlated from experimental data instead of heat transfer calculations. The mass burning rate is used primarily as an input parameter into calculating the flame length correlation and flame tilt.

3.2 LNGFIRE3 PARAMETER

For circular pool fires, LNGFIRE3 uses a semi-empirical mass burning rate correlation similar to the theoretical form of Burgess, Strasser, and Grumer [Atallah 1990] and correlated based on pool fires over land as small as 0.15 m diameter and up to a maximum of 20 m diameter (Shell tests), such that:

$$\dot{m}''_{burn} = \dot{m}''_{\max}\left(1 - e^{-0.46d}\right) \tag{2}$$

where $\dot{m}''_{burn}$: mass burning rate, *kg/m^2-s*
$\dot{m}''_{\max}$: maximum mass burning rate, *kg/m^2-s*
d : pool fire diameter, *m*

For rectangular geometries, LNGFIRE3 uses an empirical mass burning rate correlation parameterized by the product of the aspect ratio and modified Froude Number (AR·FR′) with an upper limit at low AR·FR′ capped by a maximum mass burning rate, such that:

$$\dot{m}''_{burn} = 0.043 + 0.068\left(AR \cdot FR'\right)^{-0.872} \quad \text{if } AR \cdot FR > 1 \tag{3a}$$

$$\dot{m}''_{burn} = \dot{m}''_{\max} \quad \text{if } AR \cdot FR \le 1 \tag{3b}$$

where $\dot{m}''_{burn}$: mass burning rate, *kg/m^2-s*
$\dot{m}''_{\max}$: maximum mass burning rate, *kg/m^2-s*

$AR = l / w$: aspect ratio of length, l, divided by width, w

$FR' = \frac{u_w(z)}{2 \cdot \sqrt{w \cdot g}}$: modified Froude Number

$u_w(z)$: wind speed, *m/s*, at height, z, *m*

g: gravitational acceleration, *9.81 m/s*^{2}

Experimental data indicates the measured mass burning rates can range significantly from 0.02 to 0.17 kg/m^2-s for pool fires over land, depending on the size and configuration of the pool fire and weather conditions. For both circular and rectangular pool fires, LNGFIRE3 uses a maximum mass burning rate of 0.11 kg/m^2-s for pool fires over land, based on the 20 m diameter Shell tests.

3.3 PARAMETER VARIATION

SNL recommends a mass burning rate of 0.15±0.4 kg/m^2-s for LNG pool fires over water based on the measured mass burning rate for one of the largest LNG pool fire tests over water (21.4 m diameter SNL Phoenix experiment[3]) [Blanchat 2010]. This mass burning rate is approximately the same as the 0.14 kg/m^2-s mass burning rate measured at the largest LNG pool fires over land (35 m diameter GDF Montoir experiments) [Malvos 2006], but is also in the range of the 0.11 kg/m^2-s used in LNGFIRE3. The similarity in mass burning rate appears to support the notion that, for large LNG pool fires, the burning rate is dominated by heat transfer from the fire to the pool and that a less significant contribution is from the heat transfer from the substrate.

However, wind would affect the convective heat transfer and re-radiation (due to flame tilt) which may also significantly affect the mass burning rate. The mass burning rate measured in the Shell tests was taken in a trial subject to wind speeds of approximately 7 m/s. The mass burning rate measured in the Phoenix tests was taken in a trial subject to low wind speeds of approximately 1.6 m/s. The mass burning rates measured in the GDF Montoir tests were approximately 0.14 kg/m^2-s for all three tests with wind speeds ranging from 2.7-4.8 m/s to 7.0-10.1 m/s, but measured higher heat fluxes back to the pool for wind speeds of 7.0-10.1 m/s [Malvos 2006]. Conversely, AGA trench fire tests indicated an inverse relationship with heat fluxes back to the pool and wind speeds [AGA 1974]. The difference in heat fluxes back to the pool among the Montoir and AGA trench fire tests highlight the influence of wind speed, but does not provide a clear trend. It is possible that the change in view factor and subsequent re-radiation due to flame tilt for the AGA trench fire tests from the wind and enhanced turbulent mixing and subsequent convective heat transfer from the wind have some competing effects.

[3] The 56 m diameter Phoenix test did not collect sufficient amount of data to determine a steady state mass burning rate.

As both the Montoir and SNL experiments indicate a potential maximum LNG mass burning rate that is similar and higher than the maximum mass burning rate of 0.11 kg/m^2-s used by LNGFIRE3, the mass burning rate measured at experiments were compared with those predicted with the Mathcad Solid Flame Model, using different maximum LNG mass burning rates. This comparison is shown in Figure 3-1, Figure 3-2 and Table 3-1.

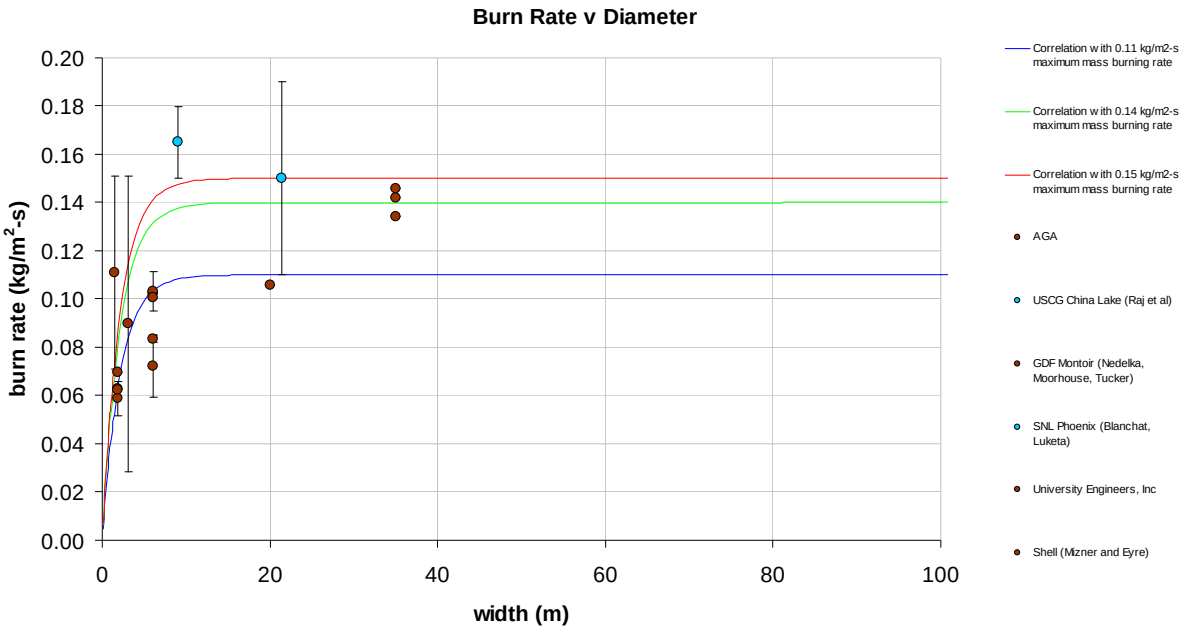

Figure 3-1 Circular Burn Rate Prediction Compared to Experimental Data

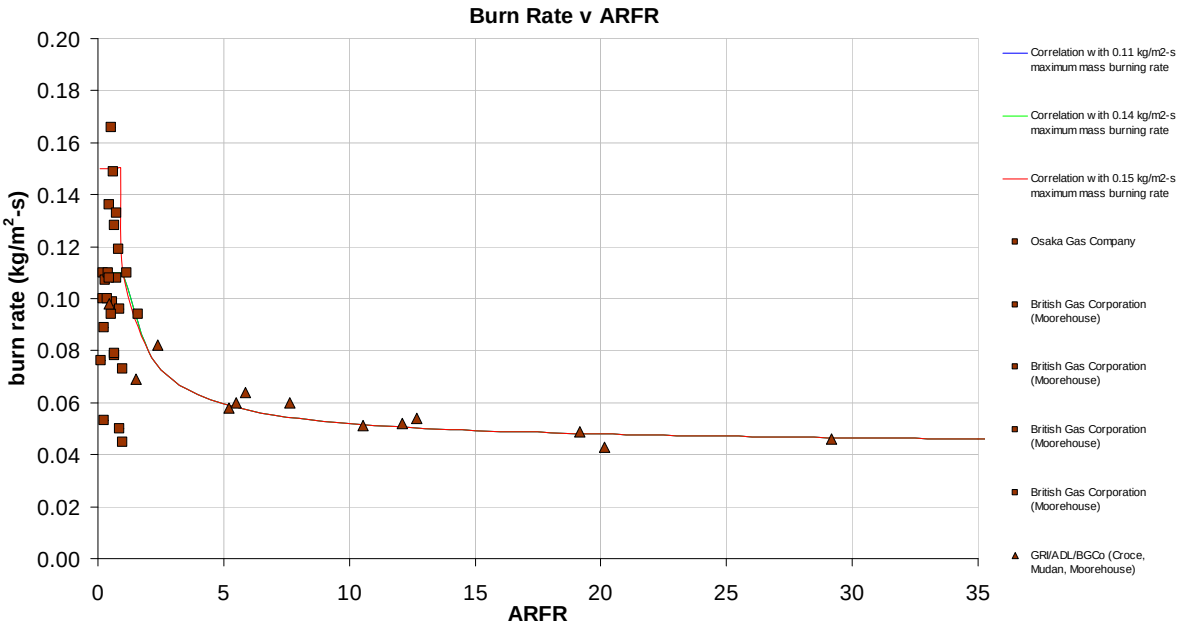

Figure 3-2 Rectangular Burn Rate Prediction Compared to Experimental Data

Table 3-1: Effect of Maximum Burn Rate on Burn Rate Prediction			
Statistical Performance Measure	**Burn Rate, kg/m^2-s**		
	0.11	**0.14**	**0.15**
SF	1.01	1.23	1.30
FAC2	86%	91%	91%
SF>1	48%	63%	69%
MRB	0.02	-0.10	-0.13
MG	1.07	0.89	0.84
MRSE	0.15	0.17	0.19
VG	1.20	1.22	1.24

As shown above, all three methodologies provide overall good agreement and are within the SPM criteria based on the average SPMs. The results also indicate increasing conservatism for increasing mass burning rates. However, the SPMs are averaged values and are largely influenced by the more abundant data recorded for small scale fires and trench fires that have lower mass burning rates.

When looking at the agreement with individual tests, LNGFIRE3 (or the Mathcad Solid Flame Model) shows reasonable agreement against all experimental data with the exception of: (1) the maximum burning rate reported in the Montoir pool fires; (2) the upper range of low aspect ratio rectangular fires over land; and (3) the mass burning rates reported for the USCG China Lake and SNL Phoenix pool fires over water. The mass burning rate measured in the Montoir tests were previously dismissed in the original LNGFIRE formulation and validation as it was not expected to change the output of the proposed model considerably. Additionally, any increase in the predicted flame length was thought to be offset in real fires by the increased sootiness of the flame observed at Montoir and reduction in the angle of tilt (Atallah, 1990). The mass burning rate measured in the USCG China Lake tests were previously dismissed in the original LNGFIRE formulation and validation because of the difference in behavior for pool fires over water. However, the reported China Lake burn rates have since been shown to be incorrect. According to SNL, the burn rates would rather fall within the 0.11 to 0.16 kg/m^2-s range, which is similar to the Phoenix tests and Montoir tests [Blanchat 2010]. This suggests the dominant heat transfer mode for large pool fires will be from re-radiation and convective heat transfer from the fire and may not be considerably affected by heat transfer from the water or ground. Provided this information, the increased burn rates reported in the Phoenix tests indicate that the an increased maximum mass burning rate should be reconsidered.

Increasing the mass burning rate to 0.14 kg/m^2-s or 0.15 kg/m^2-s from 0.11 kg/m^2-s would provide greater conservatism in predicting the mass burning rate for smaller pool fires over land. It would also provide better agreement with the Montoir tests over land and the upper range of low aspect ratio rectangular fires over land, as well as the USCG and SNL pool fires over water. However, maintaining the maximum mass burning rate at 0.11 kg/m^2-s provides more accurate predictions for smaller pool fires over land. While deference to the larger pool fires over land would normally be considered for model use in Part 193 siting analyses, as they are closer in size to the impoundments installed at land-based LNG facilities, it is important to understand the subsequent ramifications of this change to other parameters. Therefore, we explored additional parameters affected by the mass burning rate, including the flame tilt, Section 4.0, and flame length, Section 5.0.

{THIS PAGE INTENTIONALLY LEFT BLANK}

4.0 WIND SPEED, FLAME TILT & FLAME DRAG

4.1 BACKGROUND

Wind will cause a flame to tilt and drag along its base. Increasing wind speed will increase the flame tilt and flame drag. The wind speed at the location of the fire is typically a directly supplied parameter used to determine the amount of flame tilt and flame drag induced by the wind. Wind speed will typically change as the elevation changes. Most weather stations provide wind speeds at a 10 m height, but certain fires scenarios (e.g., tank top fires) would be at much higher elevations (e.g., 40 m). For flames at ground level (i.e., elevation of 0 m), the wind speed will not change significantly from the wind speed at the reference height and subsequently the flame tilt, flame drag, and thermal radiation will not change significantly. However, for elevated fires, the wind speed will increase based on the elevation above the wind speed reference height and the Pasquill Stability Class (A through F), as shown in Equation (4) and Figure 4-1 for a nominal wind speed of 1 m/s at a reference height of 10 m.

$$u_w(z) = u_w(z_r)\left(\frac{z}{z_r}\right)^p \tag{4}$$

where $u_w(z)$: wind speed at specified height, *m/s*, at height, z, *m*

$u_w(z_r)$: reference wind speed, *m/s*, at reference height, z_r, *m*

p: wind profile exponent dependant on Pasquill Stability Class, *0.10-0.35*

The increase in wind speed will subsequently increase the flame tilt and flame drag, and subsequently can increase the thermal radiation distances. Wind will result in flame tilt, which is the amount the fire is tilted by the wind, and flame drag, which is the amount the base of the fire is shifted or dragged by the wind. The flame tilt and flame drag will depend on the wind speed and size of the fire and is important to include as it causes the flame to become closer to downwind targets and subsequently increases the radiant heat intensity.

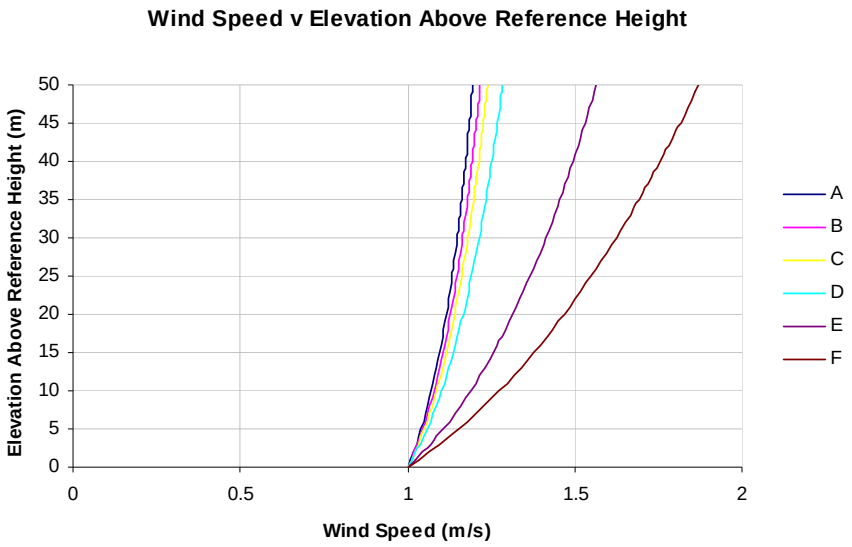

Figure 4-1 Wind Speeds for Elevation Above Reference Height

4.2 LNGFIRE3 PARAMETER

For circular fires, LNGFIRE3 uses a flame drag ratio correlation developed by Moorehouse parameterized by the wind speed and fire size as follows.

$$DR = 1.5\left(\frac{u_w(z)^2}{g \cdot d}\right)^{0.069} \tag{5}$$

where DR: drag ratio of fire
$u_w(z)$: wind speed, *m/s*
d : diameter of pool fire, *m*
g : gravitational acceleration, *9.81 m/s*^{2}

For rectangular fires, LNGFIRE3 uses a flame drag ratio correlation developed during the GRI/ADL/BGCo tests parameterized by the aspect ratio and a modified Froude number.

$$DR = 2.2 \cdot FR'^{0.33} \cdot AR^{0.2} \tag{6}$$

where DR: drag ratio of fire
$u_w(z)$: wind speed, *m/s*

$FR' = \dfrac{u_w(z)}{2 \cdot \sqrt{w \cdot g}}$: modified Froude Number

$AR = l / w$: aspect ratio of length divided by width

For circular and rectangular fires, the flame tilt is a function of wind speed, the pool size, and the mass burning rate. LNGFIRE3 uses the correlation developed by AGA, as shown below.

$$\theta = \cos^{-1}\left(\frac{1}{\sqrt{\frac{u_w(z)}{\left(\dot{m}''_{burn} \cdot g \cdot d / \rho_v\right)^{1/3}}}} \right) \tag{7}$$

where θ: Flame tilt from vertical, *degrees*
$u_w(z)$: wind speed, *m/s*
$\dot{m}''_{burn}$: mass burning rate per unit area, *kg/m^2-s*
d: size of the fire, taken as pool fire diameter, d, or width, w, *m*
ρ_v: density of LNG vapor, *~1.85kg/m^3* at boiling point
g: gravitational acceleration, *9.81 m/s^2*

4.3 PARAMETER VARIATION

In order to account for the change in wind speed based on the flame base elevation above the wind speed reference height, the wind speed parameter in the Mathcad Solid Flame Model automatically adjusts, based on the Pasquill Stability Class, for the height difference between the reference height of the wind speed and the elevation of the flame base. In addition, in constructing the Mathcad Solid Flame Model, flame drag was included at elevated fires, as the reason for dismissal of flame drag for elevated fires above 2 m in Gas Research Institute report GRI 89/0176 or Gas Technology Institute report GTI-04/0032 was not supported by any technical justifications.

Figures 4-2 and 4-3 show the effect of wind speed on flame drag for different pool sizes and aspect ratios with a much larger effect on high aspect ratios (note change in flame drag scales on vertical axes). However, there is a diminishing effect at high wind speeds and high aspect ratios are typically associated with trenches that are located near the ground where the wind speed will be close to the wind speed reference height. In addition, as can be seen by Equation (5) and (6), the flame drag is independent of the mass burning rate.

As shown in Figure 4-4 through Figure 4-7 and Table 4-1, LNGFIRE3 performs generally well with the limited data on flame drag and is well within the SPM criteria based on average SPMs.

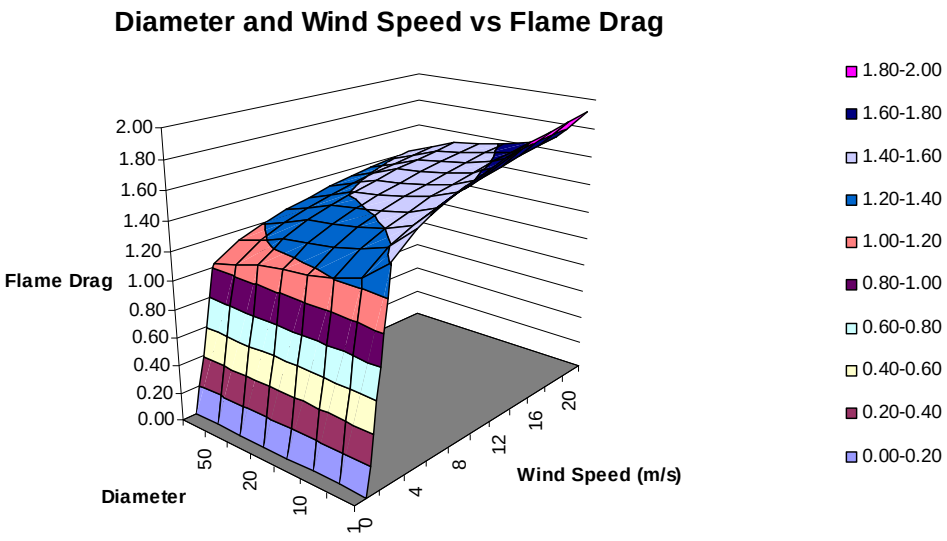

Figure 4-2 Flame Drag for Circular Pool Fires

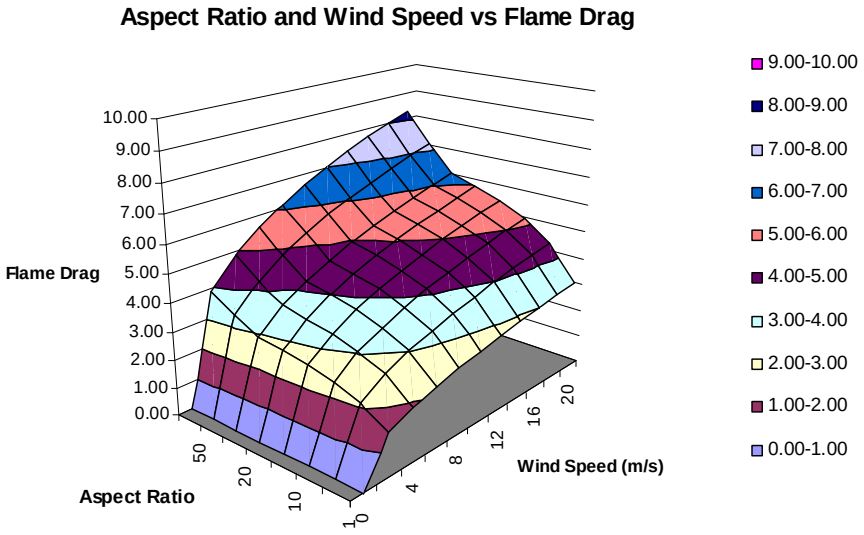

Figure 4-3 Flame Drag for Rectangular Pool Fires

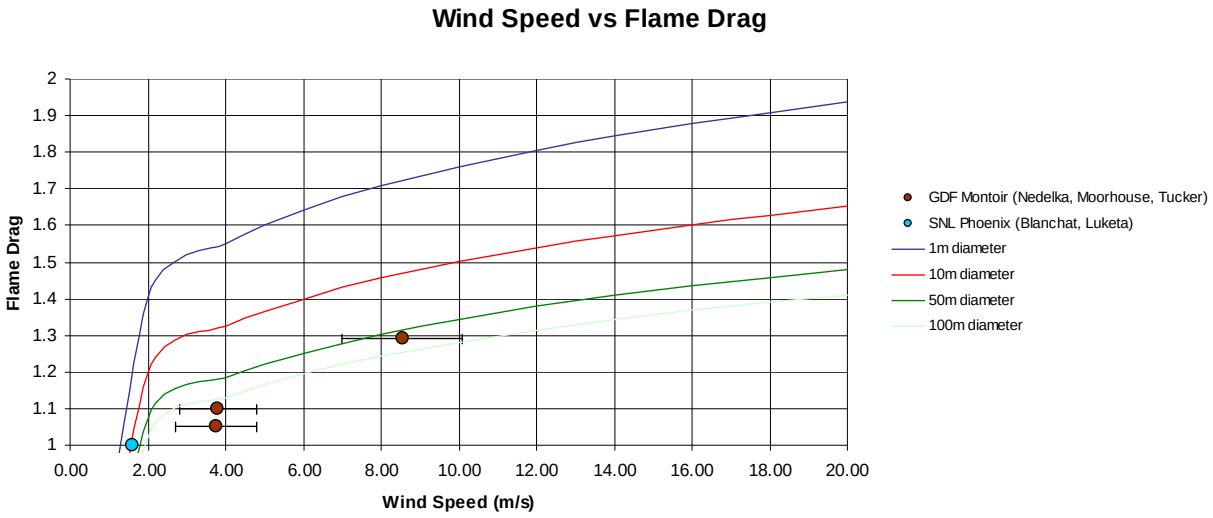

Figure 4-4 Flame Drag for Circular Pool Fires Predicted Compared to Experimental Data as a Function of Wind Speed

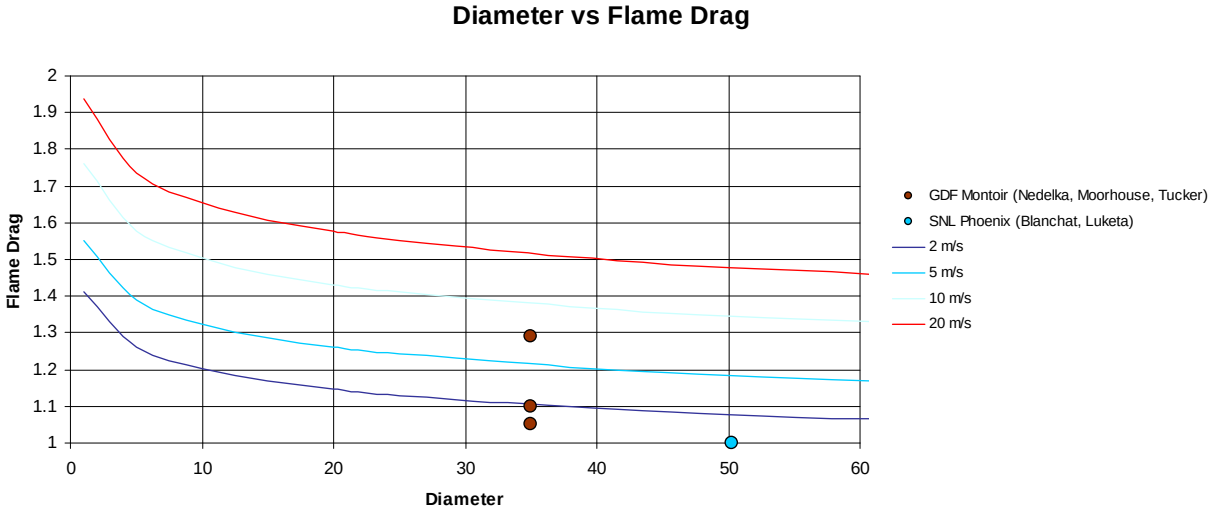

Figure 4-5 Flame Drag for Circular Pool Fires Predicted Compared to Experimental Data as a Function of Pool Diameter

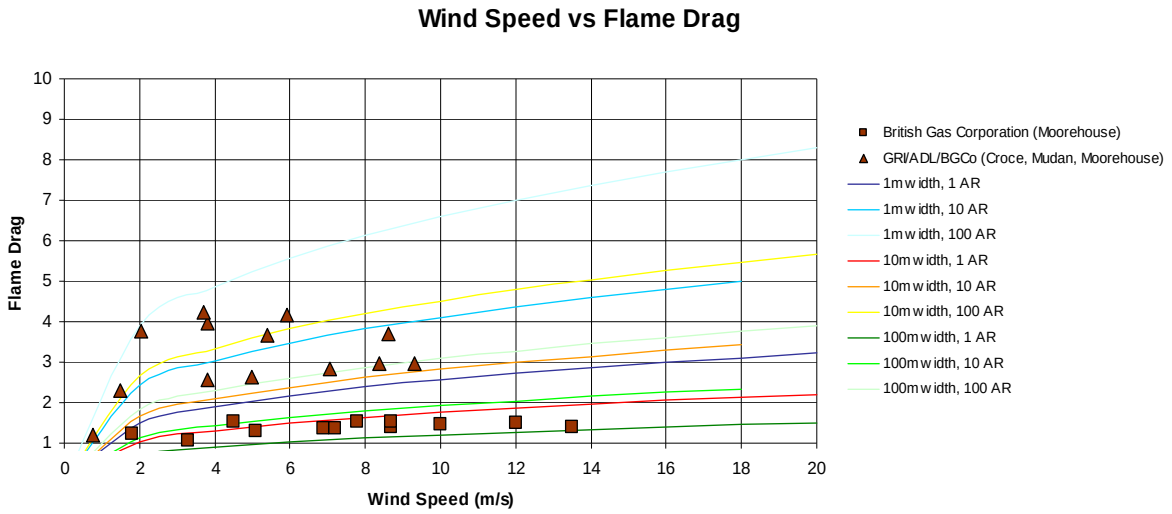

Figure 4-6 Flame Drag for Rectangular Pool Fires Predicted Compared to Experimental Data as a Function of Wind Speed

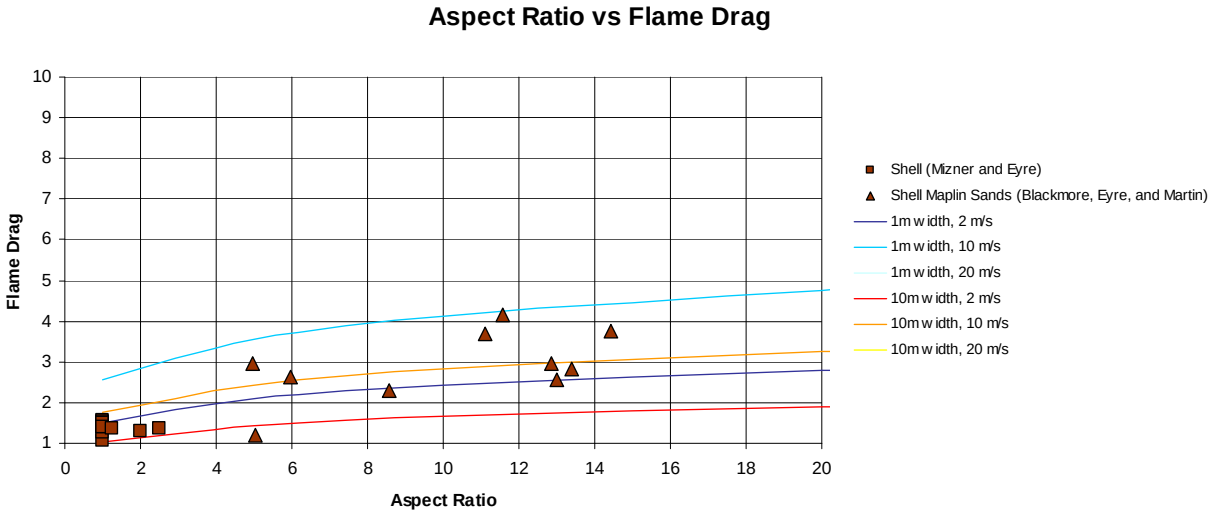

Figure 4-7 Flame Drag for Rectangular Pool Fires Predicted Compared to Experimental Data as a Function of Aspect Ratio

Table 4-1: Flame Drag Prediction	
SPM	**Flame Drag**
SF	1.09
FAC2	100%
SF>1	70%
MRB	-0.06
MG	0.96
MRSE	0.03
VG	1.07

Figure 4-8 shows the effect of wind speed on flame tilt for different pool sizes with a more pronounced effect from the wind speed. However, there is a diminishing effect of wind speed at high wind speeds that would be associated with tank top fires.

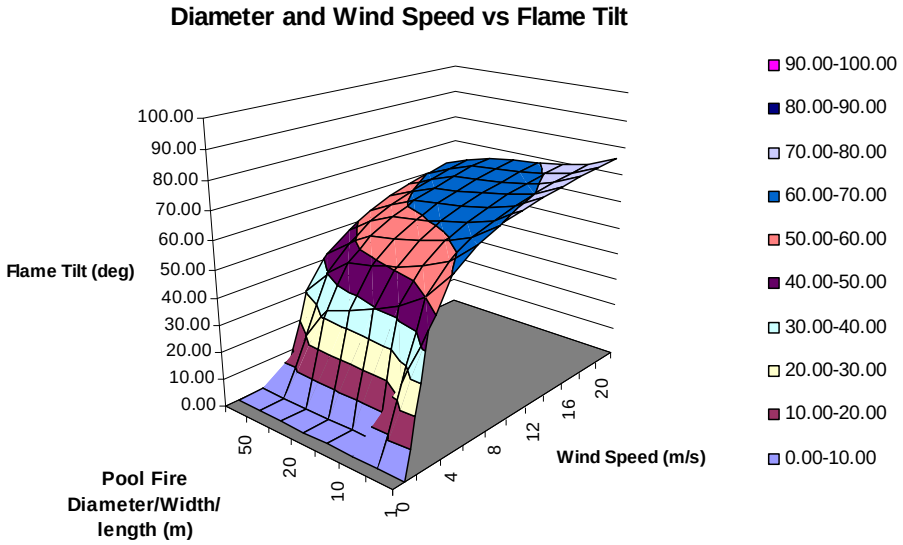

Figure 4-8 Flame Tilt for Pool Fires

As shown in Figure 4-9, Figure 4-10, and Table 4-2, LNGFIRE predicts the flame tilt fairly well and is within the SPM criteria for the various maximum mass burning rates. The results also indicate decreasing conservatism for increasing mass burning rates. However, the SPMs are averaged values and are largely influenced by the more abundant data recorded for small scale fires and trench fires that have higher flame tilts.

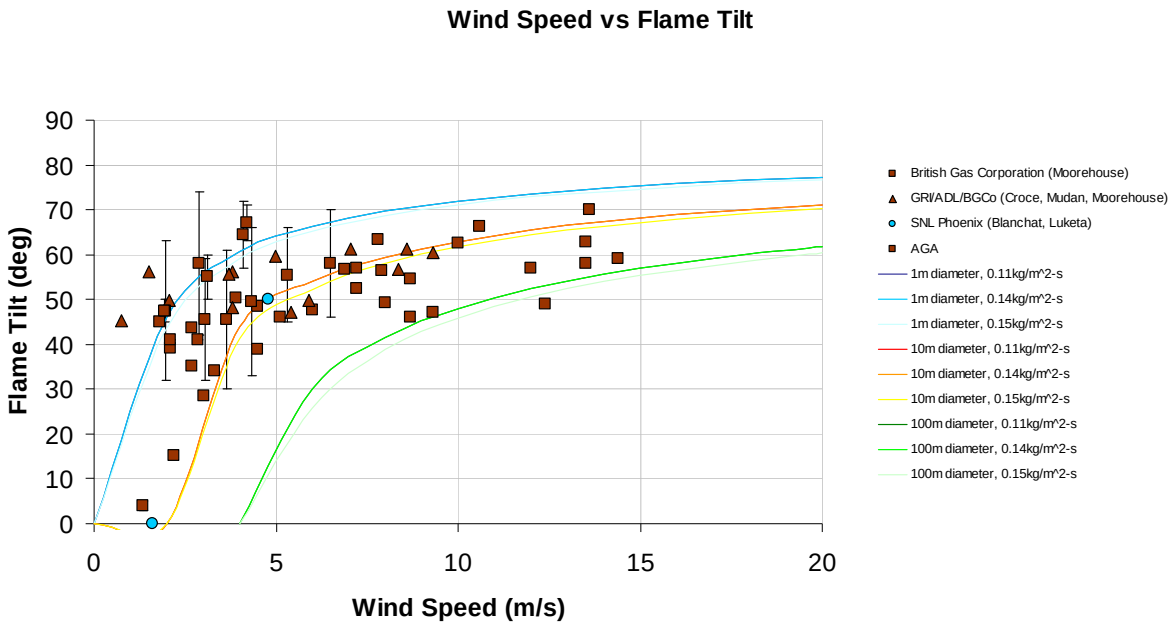

Figure 4-9 Flame Tilt for Pool Fires Compared to Experimental Data as a Function of Wind Speed

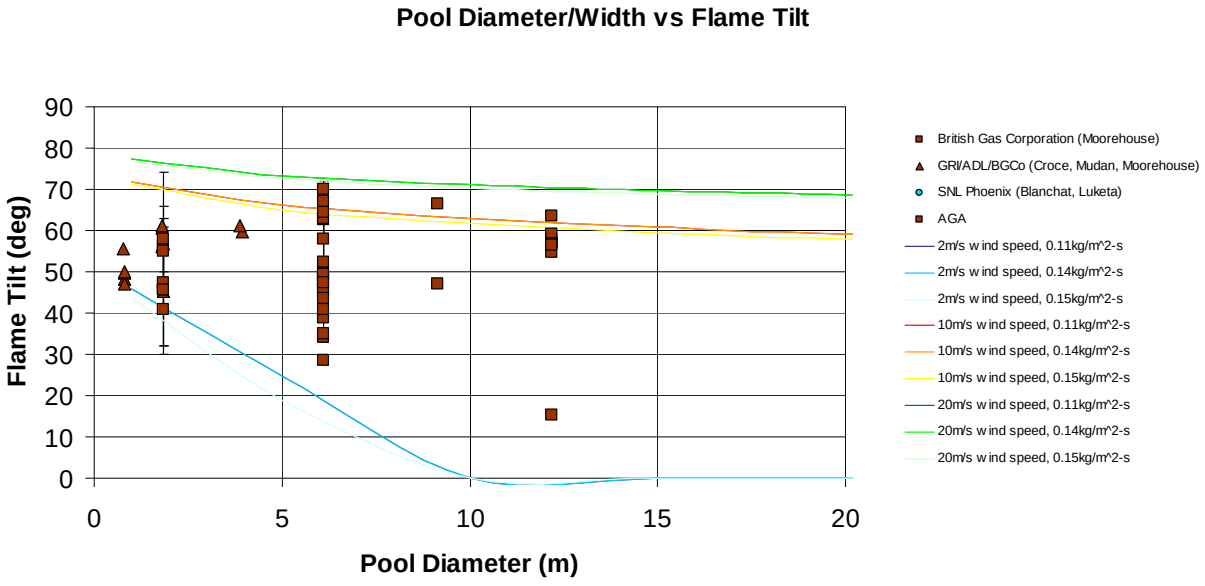

Figure 4-10 Flame Tilt for Pool Fires Compared to Experimental Data as a Function of Pool Fire Size

Table 4-2: Effect of Maximum Burn Rate on Flame Tilt Prediction				
Statistical Performance Measure	**Maximum Burn Rate, kg/m2-s**			
	measured	**0.11**	**0.14**	**0.15**
SF	1.15	1.10	1.06	1.05
FAC2	100%	100%	96%	96%
SF>1	83%	76%	65%	62%
MRB	-0.09	-0.06	-0.03	-0.02
MG	0.88	0.93	0.96	0.98
MRSE	0.05	0.05	0.06	0.07
VG	1.05	1.05	1.07	1.08

However, as will be discussed in Section 5.0, "Flame Length," the selection of a maximum mass burning rate greatly influences the prediction of the flame height and subsequent thermal radiation and therefore cannot be looked at in isolation.

{THIS PAGE INTENTIONALLY LEFT BLANK}

5.0 FLAME LENGTH

5.1 BACKGROUND

The flame length is the length of the flame as measured from the base of the fire. The flame length will vary for the turbulent diffusion flames present in large scale pool fires and therefore an average flame length is often reported for experimental data. Sometimes a maximum flame length or a flame length that occurs at a certain frequency (e.g., 95%) may be the only value reported for experimental data.

The flame length is a function of the mixing dynamics and chemical kinetics of the fuel and oxidant. For solid flame models, the flame length is typically calculated using empirical correlations based on the mass burning rate and diameter of the pool fire. For solid flame models, the flame height represents the height of the simplified geometry, and is accounted for in the view factor for calculating the distance to a specified thermal radiation level. Higher flame lengths will result in farther thermal radiation distances.

5.2 LNGFIRE3 PARAMETER

LNGFIRE3 uses the flame length correlation developed by Thomas for fires in the absence of wind. The Thomas correlation is based on a series of wood fire tests, and is shown below.

$$\frac{l_f}{d} = 42\left(\frac{\dot{m}''_{burn}}{\rho_a \sqrt{g \cdot d}}\right)^{0.61} \tag{8}$$

where l_f : Flame length, *m*

d : size of the fire, taken as pool fire diameter, d , or width, w , *m*

$\dot{m}''_{burn}$: mass burning rate per unit area, *kg/m^2-s*

ρ_a : density of air, *~1.2kg/m^3*

g : gravitational acceleration, *9.81 m/s^2*

5.3 PARAMETER VARIATION

For LNG pool fires over water, SNL recommends a new flame length correlation developed in the absence of wind for dimensionless heat release rates, Q*, of 0.1 to 1, corresponding to pool fire diameters of approximately 25 m to 2,200 m [Luketa 2011]. The SNL correlation is based on a series of 3 m gas burner tests using various flow rates

of methane and has been validated against the Phoenix trial LNG pool fire data. The SNL flame length correlation is shown below.

$$\frac{l_f}{d} = 4.196 \cdot Q^{*0.539} - 0.930 \quad \textbf{or} \quad \frac{l_f}{d} = 4.196 \left(\frac{\dot{m}''_{burn} \pi \frac{d^2}{4} h_c}{\rho_a c_p T_a \sqrt{g} \cdot d^{5/2}} \right)^{0.539} - 0.930 \tag{9}$$

where l_f : Flame length, *m*

d : diameter of pool fire, *m*

$\dot{m}''_{burn}$: mass burning rate per unit area, *kg/m^2-s*

h_c : heat of combustion of methane, *50x10^6 J/kg*

ρ_a : density of air, *~1.2kg/m^3*

c_p : specific heat of air, *1006 J/kg-K*

T_a : temperature of air, *K*

g : gravitational acceleration, *9.81 m/s^2*

However, as noted by SNL, the uncertainty on the flow measurements during the methane gas burner tests and the flame height data results in an uncertainty that can be represented by high and low correlations of similar form to the recommended SNL correlation as follows:

$$\frac{l_f}{d} = 4.828 \cdot Q^{*0.539} - 1.023 \text{ (high range of uncertainty)} \tag{10}$$

$$\frac{l_f}{d} = 3.623 \cdot Q^{*0.539} - 0.837 \text{ (low range of uncertainty)} \tag{11}$$

The flame length for pool fires over water and pool fires over land could be argued to be the same because the flame length is dominated by the mass burning rate and pool diameter. However, there could be some influence of the water vapor entrained into the fire that affects the flame length. As the SNL flame length correlation was developed based on methane gas burner tests (not over water), we examined the use of both correlations. Using the Mathcad Solid Flame Model, which incorporates both the Thomas and SNL flame length correlations, we performed a parametric analysis of mass burning rate and compared it against a wide array of LNG experimental data. The results are shown in Figure 5-1 and Table 5-1.

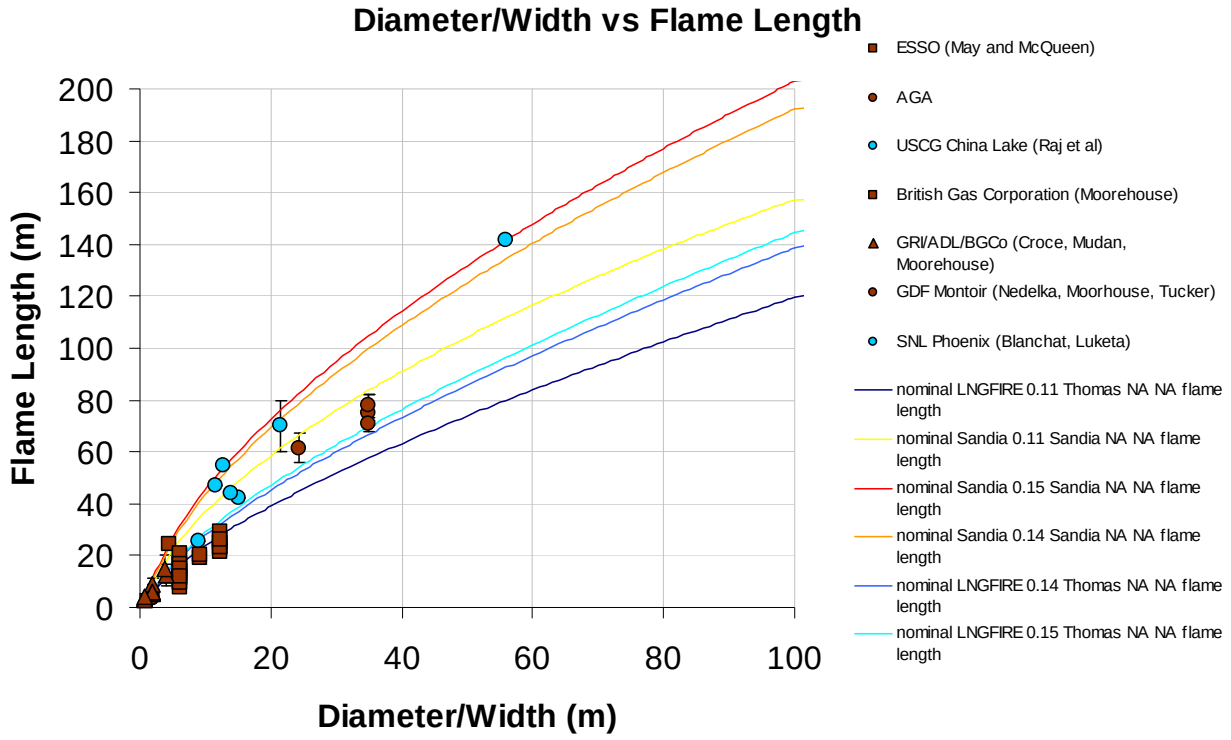

Figure 5-1 Flame Length Predictions Compared to Experimental Data

Table 5-1: Effect of Maximum Burn Rate and Flame Length Correlation on Flame Length Prediction

Statistical Performance Measures	Maximum Burn Rate, kg/m2-s							
	Exp		0.11		0.14		0.15	
	Thomas	SNL	Thomas	SNL	Thomas	SNL	Thomas	SNL
SF	1.07	1.66	1.05	1.63	1.19	1.86	1.23	1.93
FAC2	96%	86%	96%	81%	93%	58%	93%	54%
SF>1	57%	93%	55%	90%	63%	93%	66%	93%
MRB	-0.03	-0.33	-0.01	-0.31	-0.09	-0.40	-0.11	-0.43
MG	0.97	0.63	0.99	0.64	0.88	0.57	0.86	0.55
MRSE	0.08	0.28	0.10	0.28	0.12	0.39	0.14	0.43
VG	1.08	1.31	1.10	1.35	1.14	1.55	1.16	1.63

As shown above, the SNL recommended flame height correlation will result in higher flame heights compared to the Thomas flame height correlation. In addition, the use of the Thomas flame length correlation for pool fires using the 0.11 kg/m^2-s maximum mass burning rate provides the most accurate prediction of the flame length based on the SPMs overall. However, the SPMs are average values for all of the tests and are largely influenced by the more abundant data recorded for small scale fires and

trench fires. When examining larger scale fires that are of similar magnitude for fires that could be present at LNG facilities (greater than 10 m), the Thomas correlation can under-predict the measured flame length by almost a factor of 2 for LNG pool fires over land when coupled with the 0.11 kg/m^2-s mass burning rate. In contrast, the SNL correlation can over-predict the measured flame length by a factor of 2 for LNG pool fires over land when coupled with the 0.15 kg/m^2-s mass burning rate. The difference between the flame heights predicted by each correlation becomes even larger for pool fires up to 100 m.

Better agreement is shown with larger pool fires when using the SNL flame height correlation coupled with the 0.11 kg/m^2-s mass burning rate or when using the Thomas correlation coupled with the 0.15 kg/m^2-s mass burning rate, leading to an uncertainty on which maximum mass burning rate and flame length correlation to use. The uncertainty on the selection of the mass burning rate and the flame length correlation becomes even greater when considering the uncertainty ranges reported by SNL for the maximum mass burning rates and flame length correlation as shown in Figure 5-2, which includes a best fit flame length correlation within the SNL bands of uncertainty for pool fires over land using 0.14 kg/m^2-s as the maximum mass burning rate.

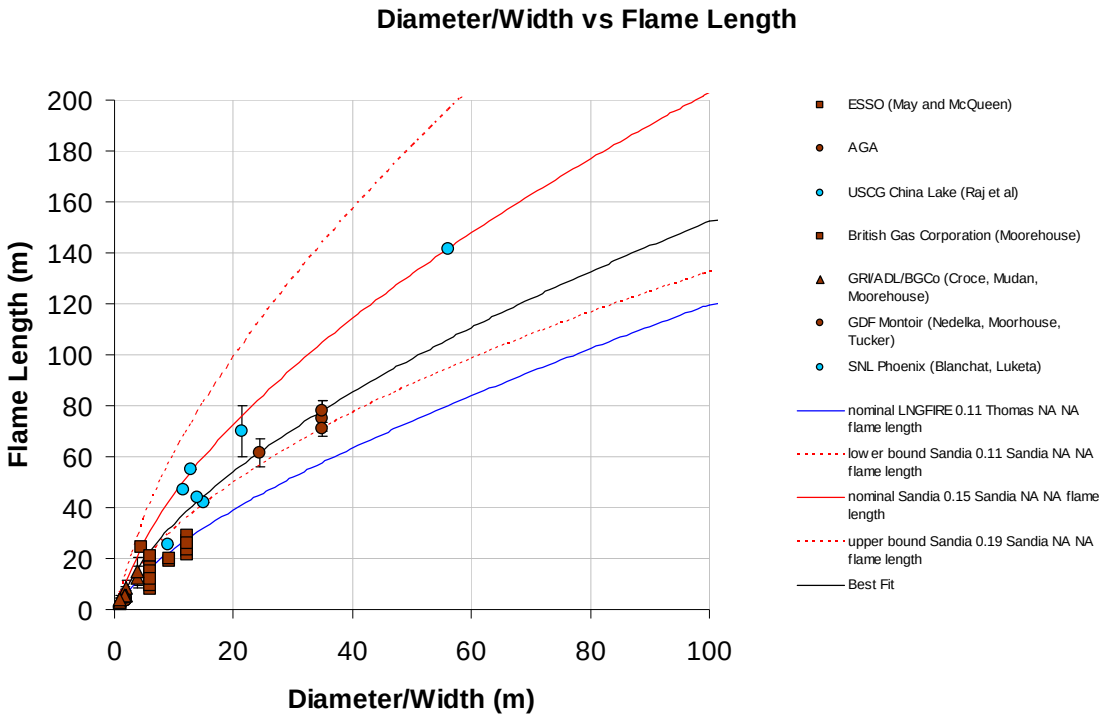

Figure 5-2 Flame Length Predictions and Uncertainties Compared to Experimental Data

Therefore, in order to properly evaluate the effect of these parameters, the selection of the maximum mass burning rate, flame length correlation, and SEP are evaluated in relation to the prediction of the thermal radiation in Section 8.0, "Thermal Radiation."

6.0 SURFACE EMISSIVE POWER

6.1 BACKGROUND

The SEP is the amount of thermal radiation emitted by the fire at its outer surface and is a function of the mixing dynamics and chemical kinetics of the flame. It is largely driven by the difference in soot production rates and soot oxidation rates occurring in the fire. As the pool fire diameter increases, the soot production rate increases, causing the flame to become optically thick. As the flame becomes optically thick, the SEP increases and heat radiates over greater distances from the pool. However, as the pool diameter increases further, the soot production rate begins to exceed the soot oxidation rate. This results in the flame becoming saturated and the soot (predominantly smoke particulates) escapes past the flame envelope and effectively reduces the SEP by obscuring the flame surface. As the SEP decreases, the distance over which heat radiates from the pool also decreases. As a result, there is a specific pool diameter which will generate a maximum possible SEP for a fire either over water or on land. Increases in pool size beyond this diameter will result in a lower SEP. In addition, as the soot is buoyant, the SEP is not homogeneous over the entire flame surface. Periodic smoke shedding due to wind will also provide moments of higher mean SEPs for smoke obscured flames.

As shown in the Equation (1), the SEP is a directly supplied parameter, along with the view factor and transmissivity, for determining the thermal radiation intensity. Higher SEPs will result in longer thermal radiation distances. Most solid flame models do not attempt to predict the production and oxidation of soot or the degree the soot can obscure and reduce the SEP for LNG pool fires, nor do they attempt to predict water vapor entrainment and its subsequent effects on the SEP for pool fires. Therefore, an average, or mean, SEP is typically used in solid flame models to describe the thermal radiation emitted by the fire. Most solid flame models will use a function based on the pool fire diameter and maximum mean SEP.

6.2 LNGFIRE3 PARAMETER

For circular pool fires, LNGFIRE3 uses a semi-empirical mean SEP correlation based on the flame emissivity as a function of optical thickness and a maximum mean SEP such that:

$$SEP = SEP_{\max} \cdot \varepsilon = SEP_{\max}\left(1 - e^{-\kappa \cdot d}\right) \tag{12}$$

where SEP : surface emissive power, kW/m^2
$SEP_{\max}$: maximum surface emissive power, kW/m^2
ε : emissivity of flame

d : optical thickness taken as pool fire diameter, d , width, w , or length, l , m
κ : attenuation coefficient, $0.3\ m^{-1}$

Experimental data indicates the SEP can range significantly from 20 kW/m^2 to over 300 kW/m^2 for pool fires over land depending on the size and configuration of the pool fire, the weather conditions, and the location on the flame. For both circular and rectangular pool fires, LNGFIRE3 uses a maximum mean SEP of 190 kW/m^2 for pool fires over land.

6.3 PARAMETER VARIATION

The large scale LNG fire tests conducted by SNL were measured to have a mean SEP of approximately 277±60 kW/m^2 and 286±20 kW/m^2 using wide angle radiometers and 238 kW/m^2 and 316 kW/m^2 using narrow angle radiometers with an uncertainty range of 248-326 kW/m^2 [Luketa 2011, DOE 2012]. For solid flame models of pool fires on water, SNL recommends the use of a nominal value of 286 kW/m^2 with parametric variation of 239-337 kW/m^2 [Luketa 2011]. However, as the Phoenix series were conducted over water, these tests are expected to yield different SEP values than LNG pool fires over land due to entrainment of water vapor into the fire (Luketa 2011). The entrainment of water vapor can reduce the soot production of the flame. This will reduce the luminosity and the SEP in smaller (optically thin) fires, but will also reduce the smoke production and increase the SEP in larger (optically thick) fires.

The increased SEP reported in the Phoenix tests suggest that an increased SEP should be re-considered for land based pool fires (i.e. LNGFIRE3). We compared the model against the large scale LNG fire tests conducted by GDF at Montoir, which were measured to have a SEP of approximately 257-273 kW/m^2 (265 kW/m^2 average) using wide angle radiometers [Atallah 1990] and a maximum SEP of approximately 316 kW/m^2 [Malvos 2006, Raj 2006] using narrow angle radiometers. Smoke obscuration was observed for the Montoir tests, while little or no smoke obscuration was observed for the Phoenix tests. This could indicate that the specific diameter associated with the maximum possible SEP for fires on land was reached in the Montoir tests (where the pool fire reached a diameter of 35 m), but not in the Phoenix tests over water (where the pool fire reached a diameter of 56 m). It is unclear whether the maximum mean SEP measured for LNG pool fires over land would be the same value as that measured for pool fires on water, albeit for different pool diameters.

As both the Montoir and SNL experiments indicate a potential maximum mean SEP that is similar and higher than the mean SEP of 190 kW/m^2 used by LNGFIRE3, the mean SEP determined from experimental data were compared with those predicted with the Mathcad Solid Flame Model, using different maximum mean SEPs. Using the Mathcad Solid Flame Model, which incorporated the various maximum mean SEPs, we

performed a parametric analysis of the SEP correlations and compared the results against a wide array of LNG experimental data, as shown in Figure 6-1, Figure 6-2, and Table 6-1.

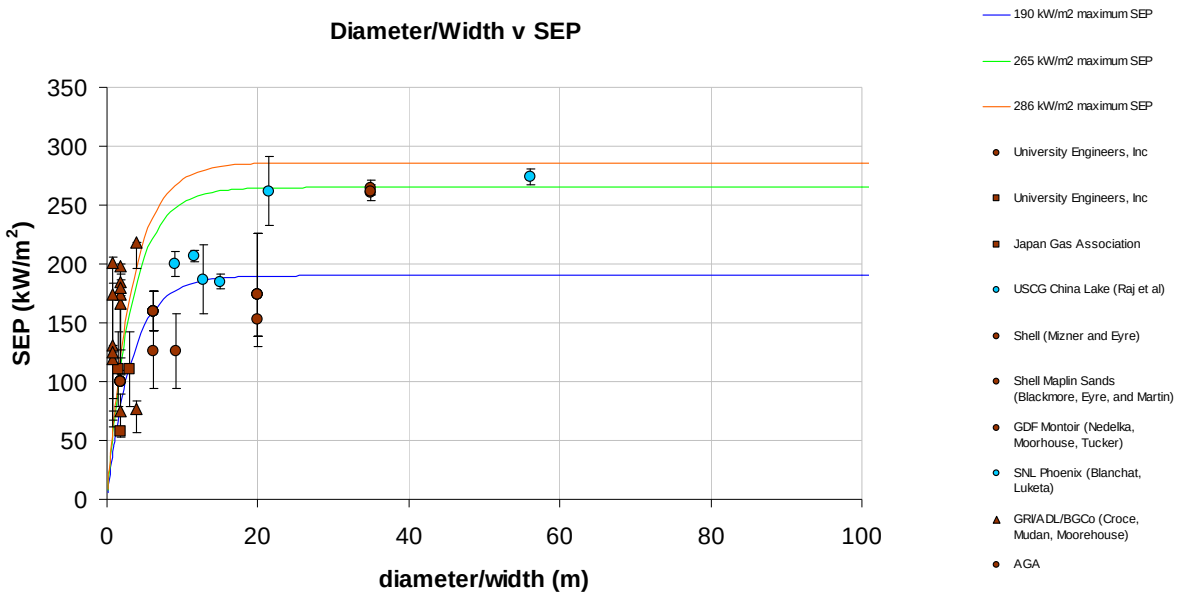

Figure 6-1 Surface Emissive Power Predicted Compared to Experimental Data as a Function of Pool Diameter and Width

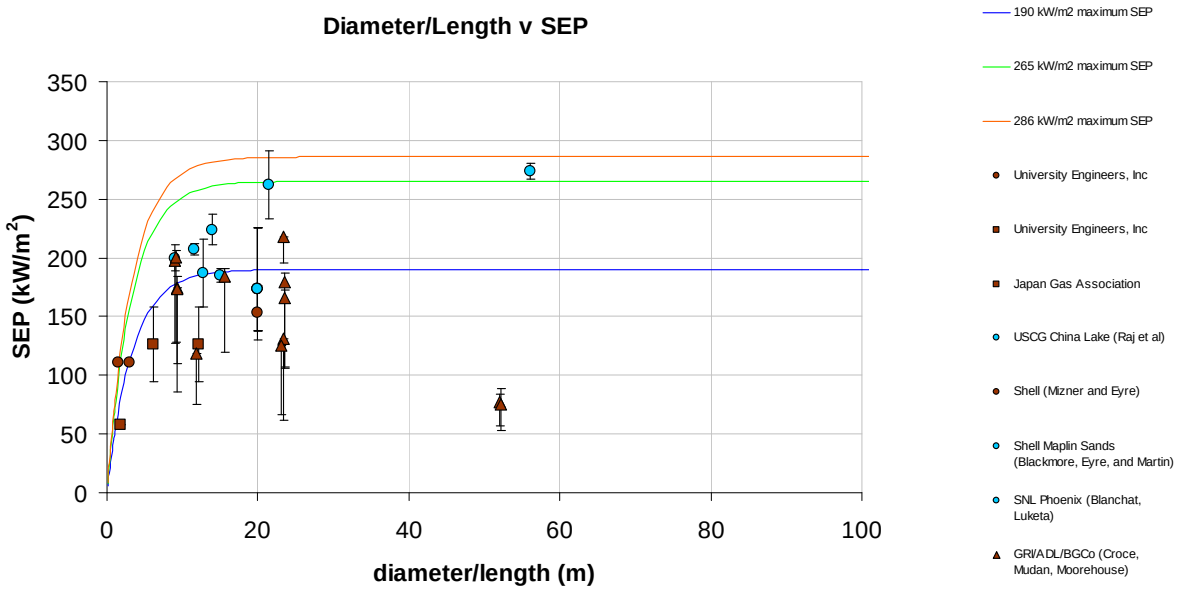

Figure 6-2 Surface Emissive Power Predicted Compared to Experimental Data as a Function of Pool Diameter and Length

Table 6-1: Effect of Maximum SEP on SEP Prediction			
Statistical Performance Measure	**SEP, kW/m^2**		
	190	**265**	**286**
SF	1.09	1.51	1.63
FAC2	94%	85%	83%
SF>1	45%	96%	98%
MRB	-0.03	-0.26	-0.31
MG	0.80	0.58	0.53
MRSE	0.09	0.20	0.25
VG	1.90	2.46	2.69

As shown above, the use of the 190 kW/m^2 for pool fires provides the most accurate prediction of the SEP based on the SPMs. However, the SPMs are average values for all of the tests and are largely influenced by the more abundant data recorded for small scale fires and trench fires. When evaluating individual experiments, the maximum SEP of 190 kW/m^2 would under-predict the SEP for the largest pool fires conducted over land (GDF Montoir tests). Increasing the maximum mean SEP to 286 kW/m^2 or 265 kW/m^2 from 190 kW/m^2 would provide greater conservatism for smaller pool fires over land and better agreement with the SNL and Montoir tests. However, as suggested by others [Blanchat 2010, Malvos 2006], the view factor for solid flame models that represent a fire as a cylinder will provide over-predictions compared to the actual flame shape. Typically, the SEP is adjusted SEP downward (same effect as adjusting view factor downward) to match the thermal radiation heat flux intensities at specified distances. As will be shown in Section 8.0, "Thermal Radiation," when taking this into account, the maximum mean SEP of 190 kW/m^2 provides the best overall agreement to thermal radiation measurements, including the Montoir tests, when coupled with the 0.11 kg/m^2-s maximum mass burning rate, Thomas flame length correlation, and transmissivity correlation utilized in LNGFIRE3.

7.0 TRANSMISSIVITY

7.1 BACKGROUND

The thermal radiation transmitted through the atmosphere will determine the thermal radiation that may be absorbed by an object. Transmissivity is the amount of thermal radiation that is transmitted through (and not absorbed by) the atmosphere. Transmissivity is a function of the presence of products in the atmosphere that absorb thermal radiation from the fire. It is largely driven by the amount of carbon dioxide and water vapor in the atmosphere. The amount of carbon dioxide in the air is dependent on the ambient temperature and the amount of water vapor in the air is dependent on both the relative humidity and ambient temperature. An increase in the amount of carbon dioxide and water vapor in the air decreases the transmissivity and subsequently decreases thermal radiation distances.

Most solid flame models will use a correlation to determine the amount of water vapor and subsequent absorption in the atmosphere, but the correlation may not include carbon dioxide absorption as it is not as dominant. As shown in the Equation (1), the transmissivity is a directly supplied parameter, along with the view factor and SEP, in solid flame models for determining the thermal radiation intensity. A higher transmissivity will result in longer thermal radiation distances.

7.2 LNGFIRE3 PARAMETER

LNGFIRE3 neglects absorption from carbon dioxide in the atmosphere and uses a common step-wise correlation for transmissivity based on a procedure described in McAdams, "Heat Transmission" [Atallah 1990] that accounts for water vapor content in the atmosphere only, as follows:.

$$\tau = 1 - \alpha_w \tag{13}$$

with

$$\alpha_w = \varepsilon_w \cdot \left(\frac{T_a}{T_{flame}} \right)^{0.45} \tag{14}$$

$$\varepsilon_w = 0 \qquad \text{if } 0 atm \cdot m < P_{vL} \le 0.00005 atm \cdot m$$

$$\varepsilon_w = 10^{-0.4685 + 0.34729 P_{\log} - 0.0864 P_{\log}^{\,2}} \cdot e^{\frac{\ln\left(0.72 + 0.16 \cdot P_{\log}\right) \ln\left(\frac{T_a}{500R}\right)}{\ln(3)}} \qquad \text{if } 0.00005 atm \cdot m < P_{vL} \le 10 atm \cdot m$$

$$\varepsilon_w = \left(1.24 - \frac{0.642}{P_{\log}}\right) \cdot e^{\frac{\ln\left(\frac{1.24P_{\log}-0.72}{1.24P_{\log}-0.642}\right)\cdot\ln\left(\frac{T_a}{500R}\right)}{\ln(3)}} \qquad \text{if } 10atm\cdot m < P_{vL} \le 453atm\cdot m$$

$$\varepsilon_w = e^{\frac{\ln\left(1.24-\frac{0.72}{P_{\log}}\right)\cdot\ln\left(\frac{T_a[R]}{500}\right)}{\ln(3)}} \qquad \text{if } 453atm\cdot m < P_{vL} \le 1000atm\cdot m$$

$$\varepsilon_w = 1 \qquad \text{if } P_{vL} > 1000atm\cdot m \qquad (15a\text{-}e)$$

$$P_{\log} = \frac{\ln(P_{vL})}{2.302585093} \qquad (16)$$

$$P_{v,L} = P_{v,water} \cdot \frac{T_{flame}}{T_a} \cdot (X - width) \qquad (17)$$

$$P_{v,water} = RH \cdot e^{14.4114 - \frac{9590.563}{T_a[R]}}\ atm \qquad (18)$$

where τ : transmissivity

α_w : absorptivity of water vapor

ε_w : emissivity of water vapor

T_a : ambient temperature, R

T_{flame} : flame temperature, R

$P_{v,L}$: amount of water vapor along path length, x

$P_{v,water}$: saturated water vapor pressure, atm

RH : relative humidity, $\%$

7.3 PARAMETER VARIATION

Based on the data from the Phoenix tests, SNL recommends the transmissivity correlation developed by Wayne with the saturated water vapor pressure determined based on the Antoine formula using the coefficients from Stull, as shown below [Luketa 2011]:

$$\begin{aligned}\tau = {} & 1.006 - 0.0117\log\left(\chi_{H_2O}(x)\right) - 0.02368\log\left(\chi_{H_2O}(x)\right)^2 \\ & - 0.03188og\left(\chi_{CO_2}(x)\right) + 0.001164\log\left(\chi_{CO_2}(x)\right)^2\end{aligned} \qquad (19)$$

with
$$\chi_{H_2O}(x) = \frac{2.8865 \cdot 10^2 \left(10^{4.65430 - \frac{1435.264}{T_a[K] - 64.848}} \cdot RH \right) [mmHg]}{T_a[K]} x[m] \quad (20)$$

$$\chi_{CO_2}(x) = \frac{273K}{T_a[K]} x[m] \quad (21)$$

where τ : transmissivity

$\chi_{H_2O}(x)$: amount of water vapor along path length, x

$\chi_{CO_2}(x)$: amount of carbon dioxide along path length, x

RH : relative humidity, $\%$

T_a : ambient temperature, K

The Wayne transmissivity correlation includes carbon dioxide absorption and will generally result in lower transmissivities compared to the transmissivity correlation used by LNGFIRE3, as shown in Figure 7-1.

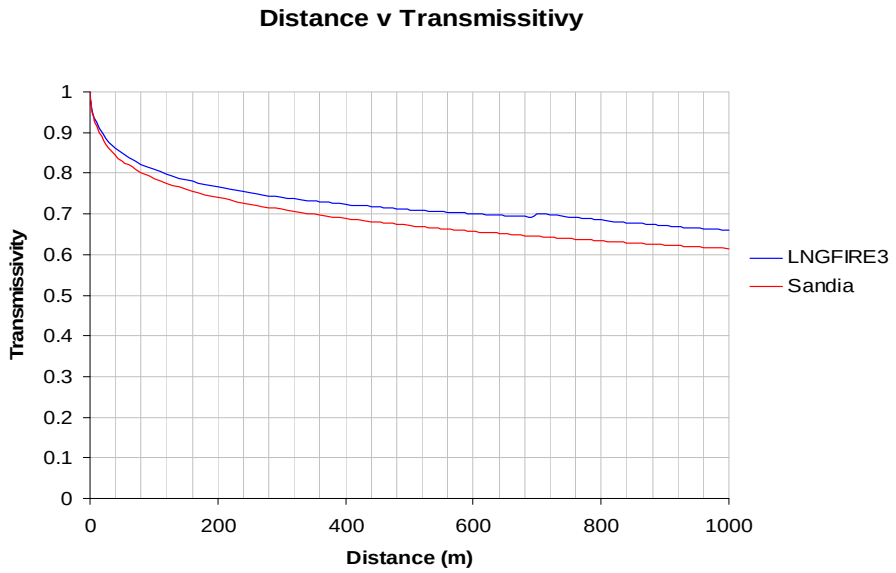

Figure 7-1 Transmissivity Predictions of LNGFIRE3 and SNL Recommendation

While the SNL recommended correlation is more accurate, the difference is relatively small and the LNGFIRE3 transmissivity correlation would be conservative. However, both transmissivity correlations were examined to determine their influence on the thermal radiation predictions.

{THIS PAGE INTENTIONALLY LEFT BLANK}

8.0 THERMAL RADIATION

Higher wind speeds, high burn rates, higher flame drags, higher flame tilts, higher predicted flame heights, higher SEPs, and higher transmissivities will all result in higher thermal radiation intensities and longer thermal radiation distances. In addition, a solid flame model that represents the fire as a tilted cylinder tends to over-predict the actual view factor compared to a real fire, resulting in higher thermal radiation intensities and longer thermal radiation distances. For this reason, the mean SEP is often adjusted downward to match the thermal radiation distances to account for the over-prediction resulting from assuming a simplified geometry.

In order to evaluate the effect of incorporating all of the SNL recommendations for LNG pool fires over water into the solid flame model LNGFIRE3, we compared downwind thermal radiation predictions by the Mathcad Solid Flame Model using various combinations of LNGFIRE3 parameters, SNL recommended parameters, and values in between that could reasonably be assumed against an assortment of LNG experimental data, as shown in Figure 8-1, Figure 8-2, Figure 8-3, Figure 8-4, and Table 8-1.

As shown, LNGFIRE3 performs fairly well, being within the SPM criteria for nearly all of the SPMs, and is generally conservative. However, the SPMs are averaged values and are largely influenced by the more abundant data recorded for small scale fires and trench fires that have lower thermal radiation intensities. When looking at individual experiments, LNGFIRE3 over-predicts the thermal radiation from trench fires by nearly a factor of 2 with decreasing conservatism for lower thermal radiation intensities. However, LNGFIRE3 also predicts the thermal radiation for Montoir tests much more accurately, but less conservatively. Moreover, LNGFIRE3 does a poor job predicting thermal radiation intensities for the Phoenix fire tests, and under-predicts by more than a factor of 2.

In addition, a model incorporating all of the SNL recommendations for fires over water performs well against the Phoenix fire tests (the only LNG pool fires over water evaluated with thermal radiation data), but vastly over-predicts thermal radiation intensities for LNG pool fires over land by more than a factor of 2.

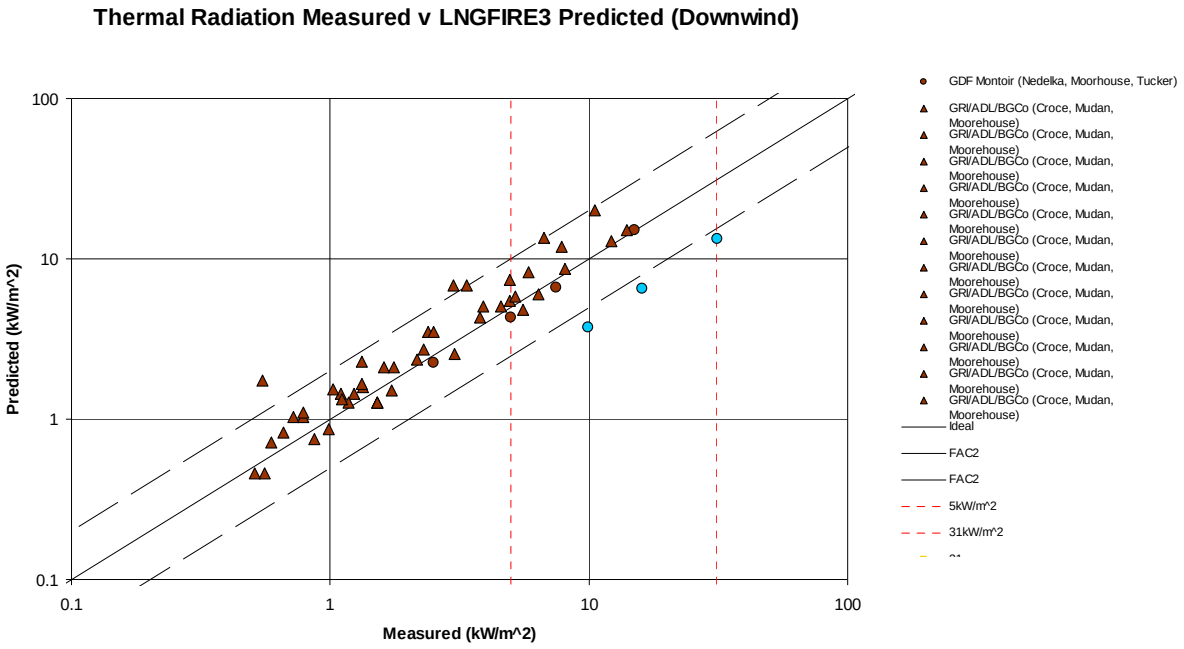

Figure 8-1: Mathcad Solid Flame Model / using LNGFIRE3 Values and Correlations (0.11 kg/m^2-s maximum mass burning rate, Thomas Flame Length Correlation, 190 kW/m^2 maximum SEP, water vapor only transmissivity)

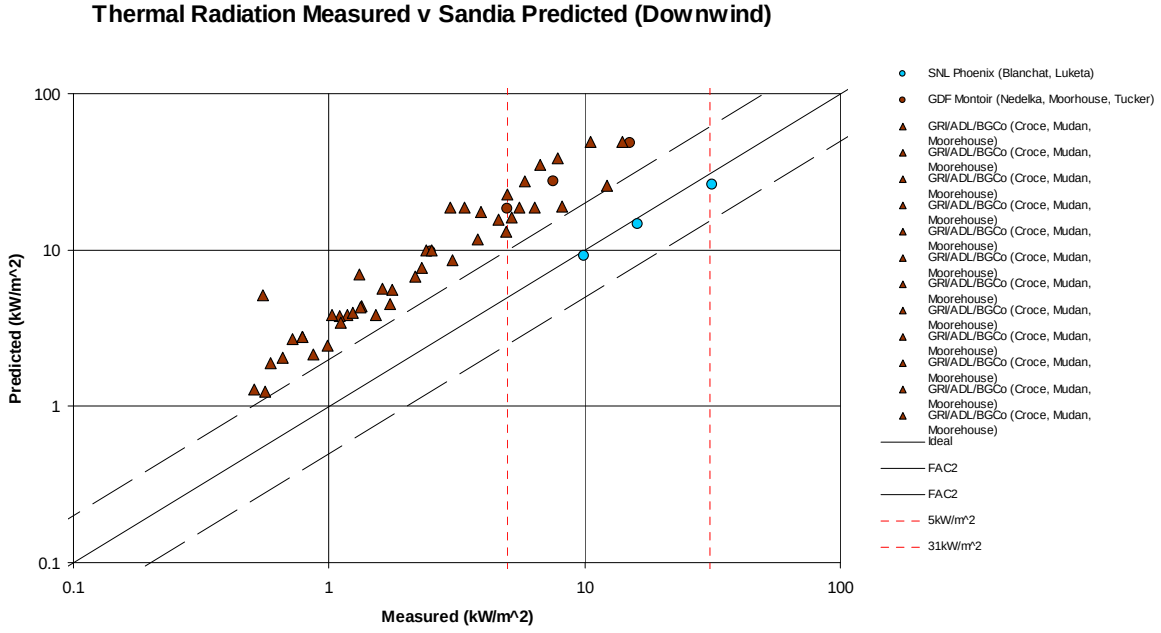

Figure 8-2: Mathcad Solid Flame Model using SNL Recommended Values and Correlations (0.15 kg/m^2-s maximum mass burning rate, SNL Flame Length Correlation, 286 kW/m^2 maximum SEP, Wayne transmissivity)

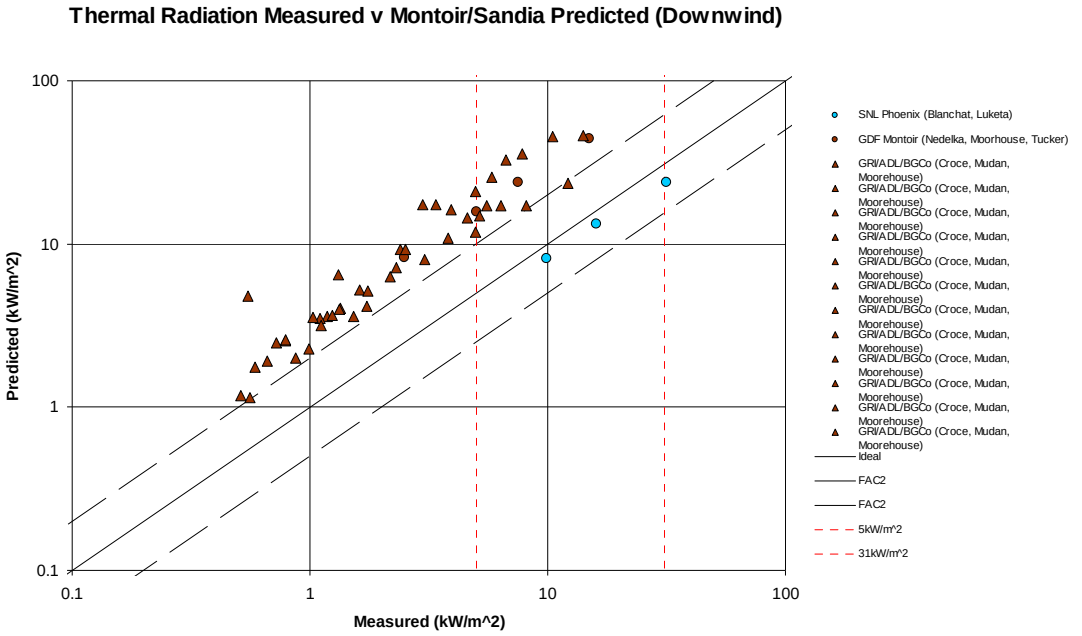

Figure 8-3: Mathcad Solid Flame Model using Montoir Values and SNL Correlations (0.14 kg/m^2-s maximum mass burning rate, SNL Flame Length Correlation, 265 kW/m^2 maximum SEP, Wayne transmissivity)

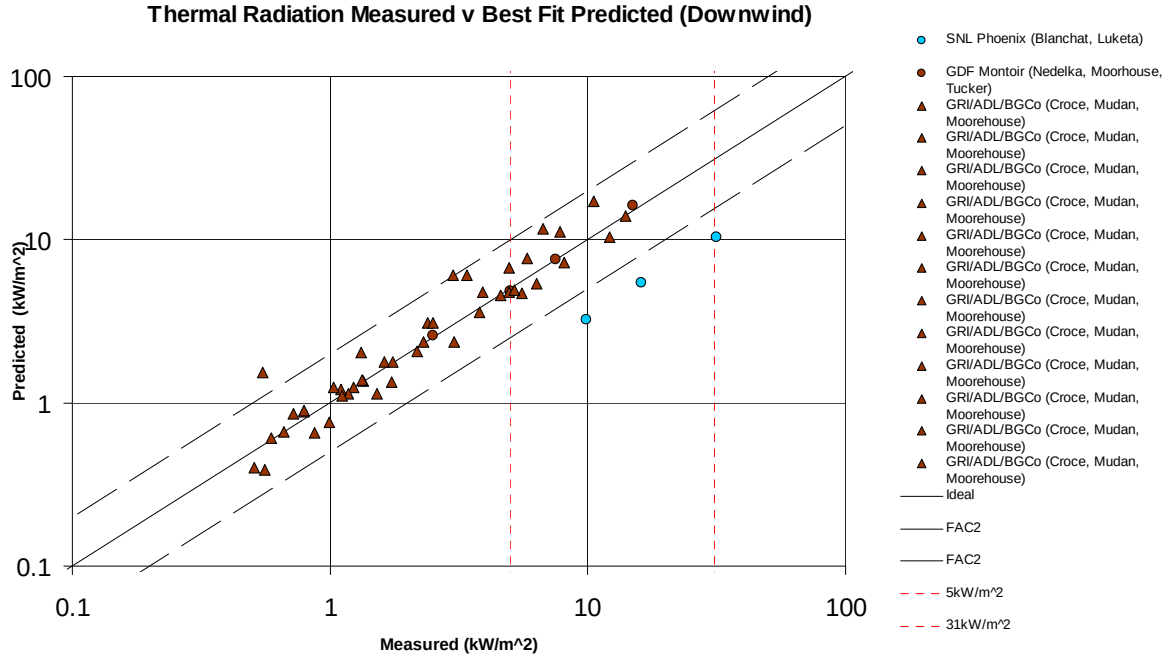

Figure 8-4: Mathcad Solid Flame Model using Best Fit Values and Correlations within SNL Range of Uncertainty (0.14 kg/m^2-s maximum mass burning rate, Best Fit Flame Length Correlation, 125 kW/m^2 maximum SEP, Wayne transmissivity)

Table 8-1: Effect of Parameters on Thermal Radiation Prediction				
SPM	**LNGFIRE3**	**SNL**	**Montoir**	**Best Fit**
SF	1.74	3.52	3.24	1.09
FAC2	70%	5%	7%	91%
SF>1	88%	95%	95%	57%
MRB	-0.25	-0.58	-0.55	0.00
MG	0.63	0.31	0.33	0.98
MRSE	0.38	1.18	1.07	0.12
VG	1.53	4.82	4.00	1.15

Using the Montoir mass burning rate and SEP with only the SNL recommendations for flame length and transmissivity does a better job at predicting the thermal radiation intensities, but would still over-predict thermal radiation intensities for LNG pool fires over land by more than a factor of 2.

Using best fit values within the SNL ranges of uncertainty for mass burning rate, flame length, and transmissivity, and then adjusting the view factor downward (via SEP) to better match the thermal radiation intensities measured would provide the most accurate predictions of the experimental data. However, this approach would be less conservative than LNGFIRE3 when compared to experimental data and would produce results -27% to +37% different than LNGFIRE3 for typically sized impoundments, full containment tanks, and single containment tank fire scenarios without any discernible decrease in uncertainty in the predictions.

9.0 CONCLUSIONS & RECOMMENDATIONS

While LNGFIRE3 under-predicts the mass burning rate, flame length, and the mean SEP for the Montoir tests, LNGFIRE3 predictions are still within the SPM criteria and uncertainty bands and are in close agreement with experimental data for thermal radiation due to the higher transmissivity predictions coupled with the over-prediction of the view factor when representing the flame as a cylinder. Adjusting the parameters to match the SNL recommendations would be less accurate and would over-predict thermal radiation intensities for pool fires over land. Adjusting the maximum mass burning rate and maximum mean SEP parameters coupled with the SNL recommendations for flame length and transmissivity to better fit the Montoir values would also be less accurate and over-predictive of thermal radiation intensities for pool fires over land, including the Montoir tests. Adjusting the parameters and correlations to best fit the mass burning rate, flame length, and mean SEP for the Montoir tests would still have similar over-predictive results due to the over-prediction of the view factor. The view factor could be adjusted downward (via SEP) to better match the thermal radiation for Montoir, but this approach would be less conservative than LNGFIRE3 when compared to other experimental data. This approach would not provide any additional certainty or discernibly more accurate predictions in thermal radiation intensity predictions for typically sized impoundments, full containment tanks, or single containment tank fire scenarios.

Therefore, we conclude that LNGFIRE3, as currently prescribed by 49 CFR Part 193, is appropriate for modeling thermal radiation from LNG pool fires on land and is suitable for use in siting on-shore LNG facilities.

{THIS PAGE INTENTIONALLY LEFT BLANK}

APPENDIX A: Mathcad Solid Flame Model

{THIS PAGE INTENTIONALLY LEFT BLANK}

Mathcad Solid Flame Model

Scenario Definition

Fire Definition

Pool shape
(1 = circle 2 = rectangle)

$p_s := 1$

Pool diameter
(if applicable)

$d := 35m = 114.829 \cdot ft$

Pool radius

$r := \frac{d}{2}$

Pool width
(if applicable)

$w := 1.81m = 5.938 \cdot ft$

Pool Length, if applicable
(length must be longer than width)

$l := 23.53m = 77.198 \cdot ft$

Aspect Ratio

$$AR := \begin{cases} AR \leftarrow 1 & \text{if } p_s = 1 \\ AR \leftarrow \frac{l}{w} & \text{if } p_s = 2 \\ AR \end{cases}$$

$AR = 1$

Flame Base Height

$Z_f := 0m$ $\quad Z_f = 0 \cdot ft$

Target Height

$Z_T := 0m$ $\quad Z_T = 0 \cdot ft$

Height Difference

$ZZ := Z_T - Z_f = 0 \cdot m$ $\quad ZZ = 0 \cdot ft$

Constants and Conversion Factors

Unit conversions

$kJ \equiv 1000 \cdot joule$ $\quad kgmole \equiv 10^3 mole$ $\quad kgmol \equiv 10^3 \cdot mol$

$kW \equiv 1000 \cdot watt$ $\quad gmole \equiv mole$ $\quad gmol \equiv mol$

$lbmole \equiv \frac{lb}{kg} 10^3 mole$

Universal gas constant

$R_u \equiv 8.314472 \cdot \frac{kJ}{kgmole \cdot K}$ $\quad R_u = 1545 \cdot \frac{ft \cdot lbf}{lbmole \cdot R}$

Material Properties

Molecular weight
(default=17kg/kgmole)

$MW_{LNG} := 17 \cdot \frac{kg}{kgmole}$

Heat of Combustion

$H_c := 50 \cdot 10^6 \frac{J}{kg}$

Specific Heat

$C_p := 1006 \frac{J}{kg \cdot K}$

Normal boiling point
(default=112K)

$T_b := 112 \cdot K$ $\quad T_b = 201.6 \cdot R$ $\quad T_b = -258.07 \cdot °F$ $\quad T_b = -161.15 \cdot °C$

Density of Liquid
(default 432kg/m^3)

$\rho_l := 432.00 \cdot \frac{kg}{m^3}$ $\quad \rho_l = 26.969 \cdot \frac{lb}{ft^3}$

Ambient Conditions

Ambient pressure	$p_a := 14.7psi$	$p_a = 14.7 \cdot psi$	$27.6mph = 12.338 \frac{m}{s}$
Wind speed	$u_{wr} := 8.55 \frac{m}{s}$	$u_{wr} = 19.13 \cdot mph$	
Ref. height for wind speed (10m for most weather stations)	$Z_r := 10 \cdot m$		
Ambient temperature	$T_a := (273.15 + 21)K = 294.15\,K$	$T_a = 21 \cdot °C$	
Relative humidity	$RH := 54\%$		
surface / ground roughness length/height	$z_R := 0.03m$		
Canopy Height	$h_{canopy} := 0m$		
Zero Plane Displacement	$d_{zp} := \frac{2}{3} h_{canopy}$		
von Karmen constant (typicall 0.41 for no-slip condition, DEGADIS uses 0.35)	$\kappa := 0.35$		
Insolation (1=clear night (default worse case), 2=cloudy night, 3=clear skies with slight rising or setting sun with solar angle between 15 and 35 degrees, 4=cloudy skies and all other clear skies, 5=clear skies with strong sun with solar angle greater than 60 degrees)	$Sun := 1$		

Pasquill Class

(1=A, 2=B, 3=C, 4=D, 5=E, 6=F)

$$\text{Class} := \begin{cases} 1 \text{ if } u_{wr} < 2\frac{m}{s} \wedge \text{Sun} = 5 \\ 2 \text{ if } \left[u_{wr} < 2\frac{m}{s} \wedge (\text{Sun} = 4 \vee \text{Sun} = 3)\right] \vee \left[\left(u_{wr} \geq 2\frac{m}{s} \wedge u_{wr} < 3\frac{m}{s}\right) \wedge (\text{Sun} = 4 \vee \text{Sun} = 5)\right] \vee \left[\left(u_{wr} \geq 3\frac{m}{s} \wedge u_{wr} < 5\frac{m}{s}\right) \wedge (\text{Sun} = 5)\right] \\ 3 \text{ if } \left[\left(u_{wr} \geq 2\frac{m}{s} \wedge u_{wr} < 3\frac{m}{s}\right) \wedge (\text{Sun} = 3)\right] \vee \left[\left(u_{wr} \geq 3\frac{m}{s} \wedge u_{wr} < 5\frac{m}{s}\right) \wedge (\text{Sun} = 3 \vee \text{Sun} = 4)\right] \vee \left[u_{wr} \geq 5\frac{m}{s} \wedge (\text{Sun} = 5)\right] \\ 4 \text{ otherwise} \\ 5 \text{ if } \left[\left(u_{wr} < 2\frac{m}{s}\right) \wedge (\text{Sun} = 2)\right] \vee \left[\left(u_{wr} \geq 2\frac{m}{s} \wedge u_{wr} < 3\frac{m}{s}\right) \wedge (\text{Sun} = 2)\right] \vee \left[\left(u_{wr} \geq 3\frac{m}{s} \wedge u_{wr} < 5\frac{m}{s}\right) \wedge (\text{Sun} = 1)\right] \\ 6 \text{ if } u_{wr} < 3\frac{m}{s} \wedge \text{Sun} = 1 \end{cases}$$

$\text{Class} = 4$

Monin Obukhov Length

$$\lambda := \begin{cases} \lambda \leftarrow -11.4 \cdot \left(\frac{z_R}{m}\right)^{0.10} \text{ if } \text{Class} \leq 1 \\ \lambda \leftarrow -26.0 \cdot \left(\frac{z_R}{m}\right)^{0.17} \text{ if } \text{Class} = 2 \\ \lambda \leftarrow -123 \cdot \left(\frac{z_R}{m}\right)^{0.30} \text{ if } \text{Class} = 3 \\ \lambda \leftarrow 1 \cdot 10^{10} \text{ if } \text{Class} = 4 \\ \lambda \leftarrow 123 \cdot \left(\frac{z_R}{m}\right)^{0.30} \text{ if } \text{Class} = 5 \\ \lambda \leftarrow 26.0 \cdot \left(\frac{z_R}{m}\right)^{0.17} \text{ if } \text{Class} \geq 6 \\ \lambda \cdot m \end{cases}$$

$\lambda = 1 \times 10^{10}\,m$

Friction velocity

$$\psi(z) := \begin{cases} \psi \leftarrow 2\ln\left[\frac{1+\left[1-15\left(\frac{z}{\lambda}\right)\right]^{\frac{1}{4}}}{2}\right] + \ln\left[\frac{1+\left[\left[1-15\left(\frac{z}{\lambda}\right)\right]^{\frac{1}{4}}\right]^{2}}{2}\right] - 2\,\mathrm{atan}\left[\left[1-15\left(\frac{z}{\lambda}\right)\right]^{\frac{1}{4}}\right] + \frac{\pi}{2} & \text{if Class} < 4 \\ \psi \leftarrow 0 \quad \text{if Class} = 4 \\ \psi \leftarrow -4.7\frac{z}{\lambda} \quad \text{if Class} \geq 5 \\ \psi \end{cases}$$

$$\psi(Z_r) = 0$$

$$u_{friction} := \frac{u_{wr}\cdot\kappa}{\left(\ln\left(\frac{Z_r + z_R}{z_R}\right) - \psi(Z_r)\right)} = 0.515\,\frac{m}{s}$$

Wind Profile Exponent

$$p_{guess} := \begin{cases} p \leftarrow 0.10 \quad \text{if Class} = 1 \\ p \leftarrow 0.11 \quad \text{if Class} = 2 \\ p \leftarrow 0.12 \quad \text{if Class} = 3 \\ p \leftarrow 0.14 \quad \text{if Class} = 4 \\ p \leftarrow 0.25 \quad \text{if Class} = 5 \\ p \leftarrow 0.35 \quad \text{if Class} = 6 \\ p \end{cases}$$

$$p_{guess} = 0.14$$

$$p_{wind}(z) := \mathrm{root}\left[u_{wr}\cdot\left(\frac{z}{Z_r}\right)^{p_{guess}} - \frac{u_{friction}}{\kappa}\left(\ln\left(\frac{z + z_R}{z_R}\right) - \psi(z)\right), p_{guess}\right]$$

$$p_{wind}(Z_r) = 0.14 \qquad p_{wind}(Z_f) = 0.14$$

Wind speed

$u_{wLNGFIRE3}(z) := u_{wr}$ $\quad u_{wFERC}(z) := u_{wr} \cdot \left(\frac{z + z_R - d_{zp}}{Z_r + z_R - d_{zp}} \right)^{p_{wind}(Z_r)}$

$u_{wLNGFIRE3}(Z_r) = 8.55 \frac{m}{s}$ $\quad u_{wFERC}(Z_r) = 8.55 \frac{m}{s}$

$u_{wLNGFIRE3}(Z_f + Z_r) = 8.55 \frac{m}{s}$ $\quad u_{wFERC}(Z_f + Z_r) = 8.55 \frac{m}{s}$

Molecular weight of air $MW_{air} := 28.84 \cdot \frac{kg}{kgmole}$

Ambient air density $\rho_a := 1.29 \frac{kg}{m^3} \cdot \frac{273K}{T_a}$ $\quad \rho_a = 0.075 \cdot \frac{lb}{ft^3}$ $\quad \rho_a = 1.197 \cdot \frac{kg}{m^3}$

Vapor density $\rho_v := \rho_a \cdot \frac{T_a}{T_b} \cdot \frac{MW_{LNG}}{MW_{air}}$ $\quad \rho_v = 0.116 \cdot \frac{lb}{ft^3}$ $\quad \rho_v = 1.853 \frac{kg}{m^3}$

Pool Fire

flame temperature
(default 1300K)

$T_{flame} := 1300K$ $T_{flame} = 1880 \cdot °F$ $T_{flame} = 1027 \cdot °C$

Modified Froude Number

$FR_{LNGFIRE3} := \frac{u_{wLNGFIRE3}\left(Z_f + Z_r\right)}{2\sqrt{w \cdot g}} = 1.015$ $FR_{FERC} := \frac{u_{wFERC}\left(Z_f + Z_r\right)}{2\sqrt{w \cdot g}} = 1.015$

$AR \cdot FR_{LNGFIRE3} = 1.015$ $AR \cdot FR_{FERC} = 1.015$

Burning rate

$m_{bmaxLNGFIRE3} := 0.11 \cdot \frac{k}{m}\, m_{bmaxSandia} := 3.5 \cdot 10^{-4} \cdot \frac{m}{s} \cdot \rho_l = 0.151 \frac{kg}{m^2 \cdot s}$

$m_{bmaxMontoir} := 3.25 \cdot 10^{-4} \cdot \frac{m}{s} \cdot \rho_l = 0.14 \frac{kg}{m^2 \cdot s}$ $m_{bmaxFERC} := 0.14 \frac{kg}{m^2 \cdot s}$

$$m_{bLNGFIRE3}\left(m_{bmax}\right) := \begin{cases} m_b \leftarrow m_{bmax} \\ m_b \leftarrow m_{bmax} \cdot \left(1 - e^{-0.46 \cdot \frac{d}{m}}\right) \text{ if } p_s = 1 \\ m_b \leftarrow \left[0.043 + 0.067 \cdot \left(AR \cdot FR_{LNGFIRE3}\right)^{-0.872}\right] \cdot \frac{kg}{m^2 s} \text{ if } AR \cdot FR_{LNGFIRE3} \geq 1 \wedge p_s = 2 \\ m_b \end{cases}$$

$m_{bLNGFIRE3}\left(m_{bmaxLNGFIRE3}\right) = 0.11 \cdot \frac{kg}{m^2 s}$

$m_{bLNGFIRE3}\left(m_{bmaxMontoir}\right) = 0.14 \frac{kg}{m^2 \cdot s}$

$m_{bLNGFIRE3}\left(m_{bmaxSandia}\right) = 0.1512 \cdot \frac{kg}{m^2 s}$

$$m_{bFERC}(m_{bmax}) := \left| \begin{array}{l} m_b \leftarrow m_{bmax} \\ m_b \leftarrow m_{bmax} \cdot \left(1 - e^{-0.46 \cdot \frac{d}{m}}\right) \text{ if } p_s = 1 \\ m_b \leftarrow \left[0.043 + 0.067 \cdot \left(AR \cdot FR_{FERC}\right)^{-0.872}\right] \cdot \frac{kg}{m^2 s} \text{ if } AR \cdot FR_{FERC} \geq 1 \wedge p_s = 2 \\ m_b \end{array} \right.$$

$$m_{bFERC}(m_{bmaxFERC}) = 0.14 \cdot \frac{kg}{m^2 s}$$

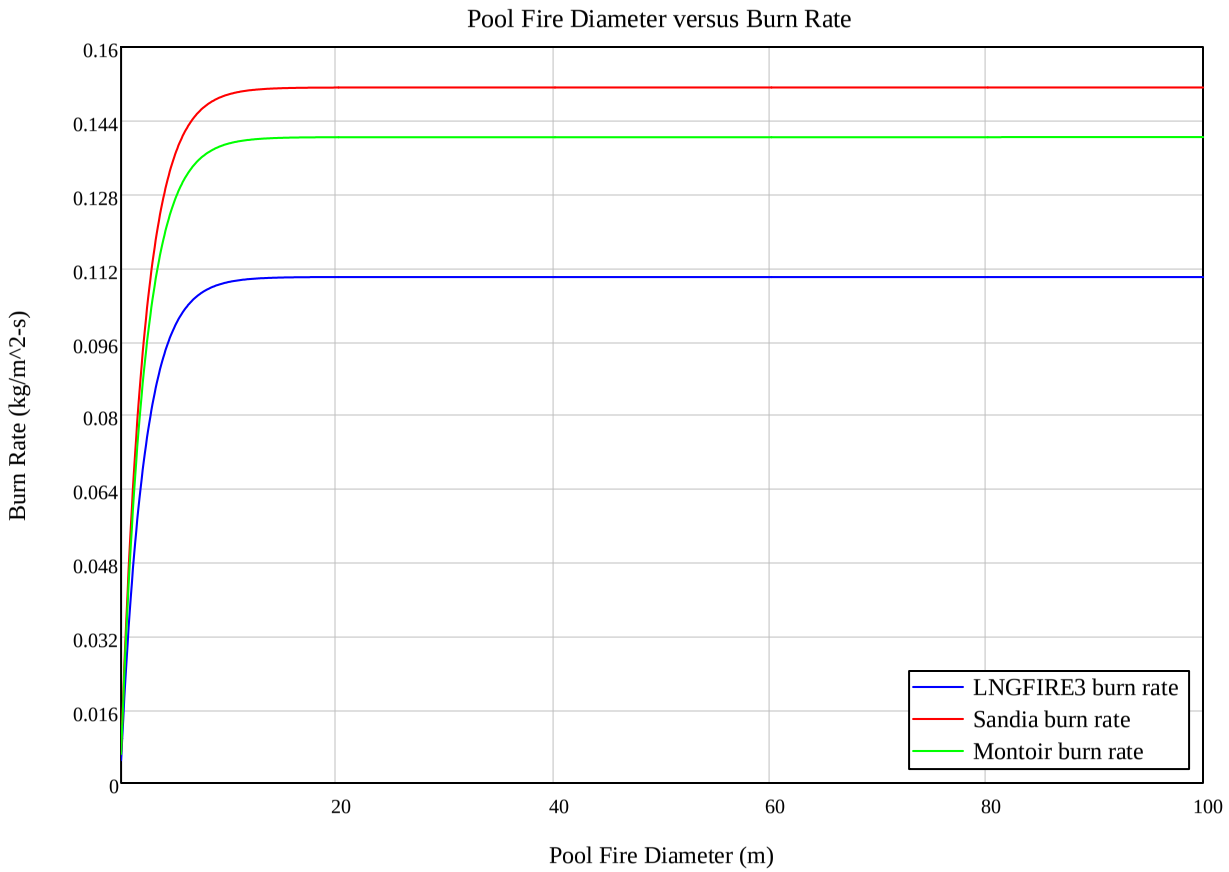
Pool Fire Diameter versus Burn Rate
Burn Rate (kg/m^2-s)
0.16
0.144
0.128
0.112
0.096
0.08
0.064
0.048
0.032
0.016
0
20
40
60
80
100
Pool Fire Diameter (m)
LNGFIRE3 burn rate
Sandia burn rate
Montoir burn rate

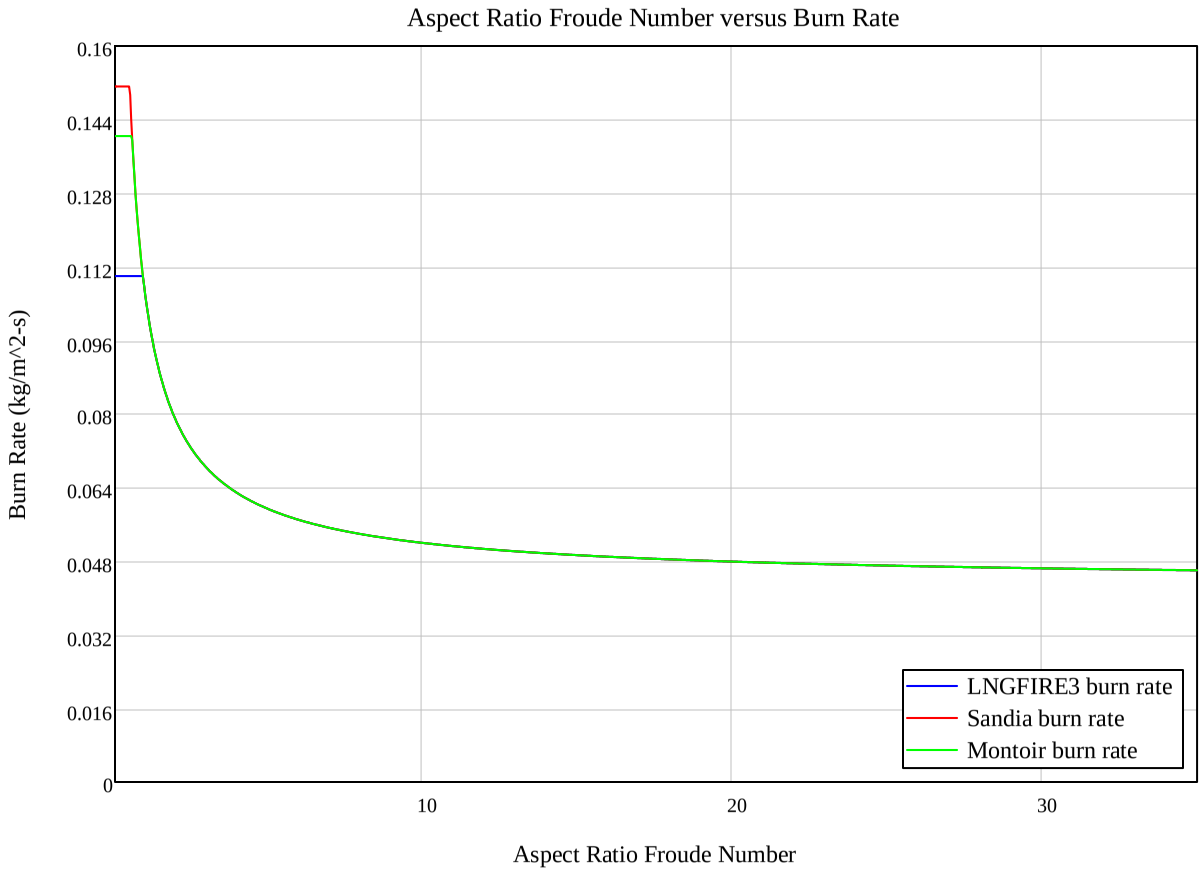
Aspect Ratio Froude Number versus Burn Rate
Burn Rate (kg/m^2-s)
0.16
0.144
0.128
0.112
0.096
0.08
0.064
0.048
0.032
0.016
0
10
20
30
Aspect Ratio Froude Number
LNGFIRE3 burn rate
Sandia burn rate
Montoir burn rate

Nondimensional wind velocity

$$u_{s.frontLNGFIRE3}(m_{burn}) := \begin{cases} u_s \leftarrow \dfrac{u_{wLNGFIRE3}(Z_f + Z_r)}{\left(\dfrac{g \cdot m_{burn} \cdot d}{\rho_v}\right)^{\frac{1}{3}}} & \text{if } p_s = 1 \\ u_s \leftarrow \dfrac{u_{wLNGFIRE3}(Z_f + Z_r)}{\left(\dfrac{g \cdot m_{burn} \cdot w}{\rho_v}\right)^{\frac{1}{3}}} & \text{if } p_s = 2 \\ u_s \end{cases}$$

$u_{s.frontLNGFIRE3}(m_{bLNGFIRE3}(m_{bmaxLNGFIRE3})) = 3.131$

$u_{s.frontLNGFIRE3}(m_{bLNGFIRE3}(m_{bmaxMontoir})) = 2.886$

$u_{s.frontLNGFIRE3}(m_{bLNGFIRE3}(m_{bmaxSandia})) = 2.816$

$$u_{s.sideLNGFIRE3}(m_{burn}) := \begin{cases} u_s \leftarrow \dfrac{u_{wLNGFIRE3}(Z_f + Z_r)}{\left(\dfrac{g \cdot m_{burn} \cdot d}{\rho_v}\right)^{\frac{1}{3}}} & \text{if } p_s = 1 \\ u_s \leftarrow \dfrac{u_{wLNGFIRE3}(Z_f + Z_r)}{\left(\dfrac{g \cdot m_{burn} \cdot l}{\rho_v}\right)^{\frac{1}{3}}} & \text{if } p_s = 2 \end{cases}$$

$u_{s.sideLNGFIRE3}(m_{bLNGFIRE3}(m_{bmaxLNGFIRE3})) = 3.131$

$u_{s.sideLNGFIRE3}(m_{bLNGFIRE3}(m_{bmaxMontoir})) = 2.886$

$u_{s.sideLNGFIRE3}(m_{bLNGFIRE3}(m_{bmaxSandia})) = 2.816$

$$u_{s.frontFERC}(m_{burn}) := \begin{cases} u_s \leftarrow \dfrac{u_{wFERC}(Z_f + Z_r)}{\left(\dfrac{g \cdot m_{burn} \cdot d}{\rho_v}\right)^{\frac{1}{3}}} & \text{if } p_s = 1 \\ u_s \leftarrow \dfrac{u_{wFERC}(Z_f + Z_r)}{\left(\dfrac{g \cdot m_{burn} \cdot w}{\rho_v}\right)^{\frac{1}{3}}} & \text{if } p_s = 2 \\ u_s \end{cases}$$

$$u_{s.frontFERC}(m_{bFERC}(m_{bmaxFERC})) = 2.889$$

$$u_{s.sideFERC}(m_{burn}) := \begin{cases} u_s \leftarrow \dfrac{u_{wFERC}(Z_f + Z_r)}{\left(\dfrac{g \cdot m_{burn} \cdot d}{\rho_v}\right)^{\frac{1}{3}}} & \text{if } p_s = 1 \\ u_s \leftarrow \dfrac{u_{wFERC}(Z_f + Z_r)}{\left(\dfrac{g \cdot m_{burn} \cdot l}{\rho_v}\right)^{\frac{1}{3}}} & \text{if } p_s = 2 \end{cases}$$

$$u_{s.sideFERC}(m_{bFERC}(m_{bmaxFERC})) = 2.889$$

Flame length

$$L_f(d, m_{burn}) := 42 \cdot d \cdot \left(\frac{m_{burn}}{\rho_a \cdot \sqrt{g \cdot d}} \right)^{0.61}$$

$L_f(d, m_{bLNGFIRE3}(m_{bmaxLNGFIRE3})) = 57.746 \cdot m$

$L_f(w, m_{bLNGFIRE3}(m_{bmaxLNGFIRE3})) = 7.37\,m$

$L_f(d, m_{bLNGFIRE3}(m_{bmaxMontoir})) = 67.014 \cdot m$

$L_f(w, m_{bLNGFIRE3}(m_{bmaxMontoir})) = 8.553\,m$

$$Q_{star}(d, m_{burn}) := \frac{m_{burn} \cdot \pi \cdot \frac{d^2}{4} \cdot H_c}{\rho_a \cdot C_p \cdot T_a \cdot \sqrt{g \cdot d} \cdot d^2}$$

$Q_{star}(d, m_{bLNGFIRE3}(m_{bmaxLNGFIRE3})) = 0.66$

$Q_{star}(w, m_{bLNGFIRE3}(m_{bmaxLNGFIRE3})) = 2.89$

$Q_{star}(d, m_{bLNGFIRE3}(m_{bmaxSandia})) = 0.9$

$Q_{star}(w, m_{bLNGFIRE3}(m_{bmaxSandia})) = 3.98$

$HD_{Sandia}(d, m_{burn}) := 4.196 \cdot Q_{star}(d, m_{burn})^{0.539} - 0.930$

$L_{fSandia}(d, m_{burn}) := HD_{Sandia}(d, m_{burn}) \cdot d$

$HD_{Sandialow}(d, m_{burn}) := 3.623 \cdot Q_{star}(d, m_{burn})^{0.539} - 0.837$

$L_{fSandialow}(d, m_{burn}) := HD_{Sandialow}(d, m_{burn}) \cdot d$

$HD_{Sandiahigh}(d, m_{burn}) := 4.828 \cdot Q_{star}(d, m_{burn})^{0.539} - 1.023$

$L_{fSandiahigh}(d, m_{burn}) := HD_{Sandiahigh}(d, m_{burn}) \cdot d$

$L_{fSandia}(d, m_{bLNGFIRE3}(m_{bmaxLNGFIRE3})) = 85\,m$

$L_{fSandia}(w, m_{bLNGFIRE3}(m_{bmaxLNGFIRE3})) = 12\,m$

$L_{fSandia}(d, m_{bLNGFIRE3}(m_{bmaxMontoir})) = 101\,m$

$L_{fSandia}(w, m_{bLNGFIRE3}(m_{bmaxMontoir})) = 14\,m$

$L_{fSandia}(d, m_{bLNGFIRE3}(m_{bmaxSandia})) = 107\,m$

$L_{fSandia}(w, m_{bLNGFIRE3}(m_{bmaxSandia})) = 14\,m$

$L_{fFERC}(d, m_{burn}) := \left(3.2 \cdot Q_{star}(d, m_{burn})^{0.539} - 0.65\right) \cdot d$

$L_{fFERC}(d, m_{bFERC}(m_{bmaxFERC})) = 79.048\,m$

$L_{fFERC}(w, m_{bFERC}(m_{bmaxFERC})) = 10.519\,m$

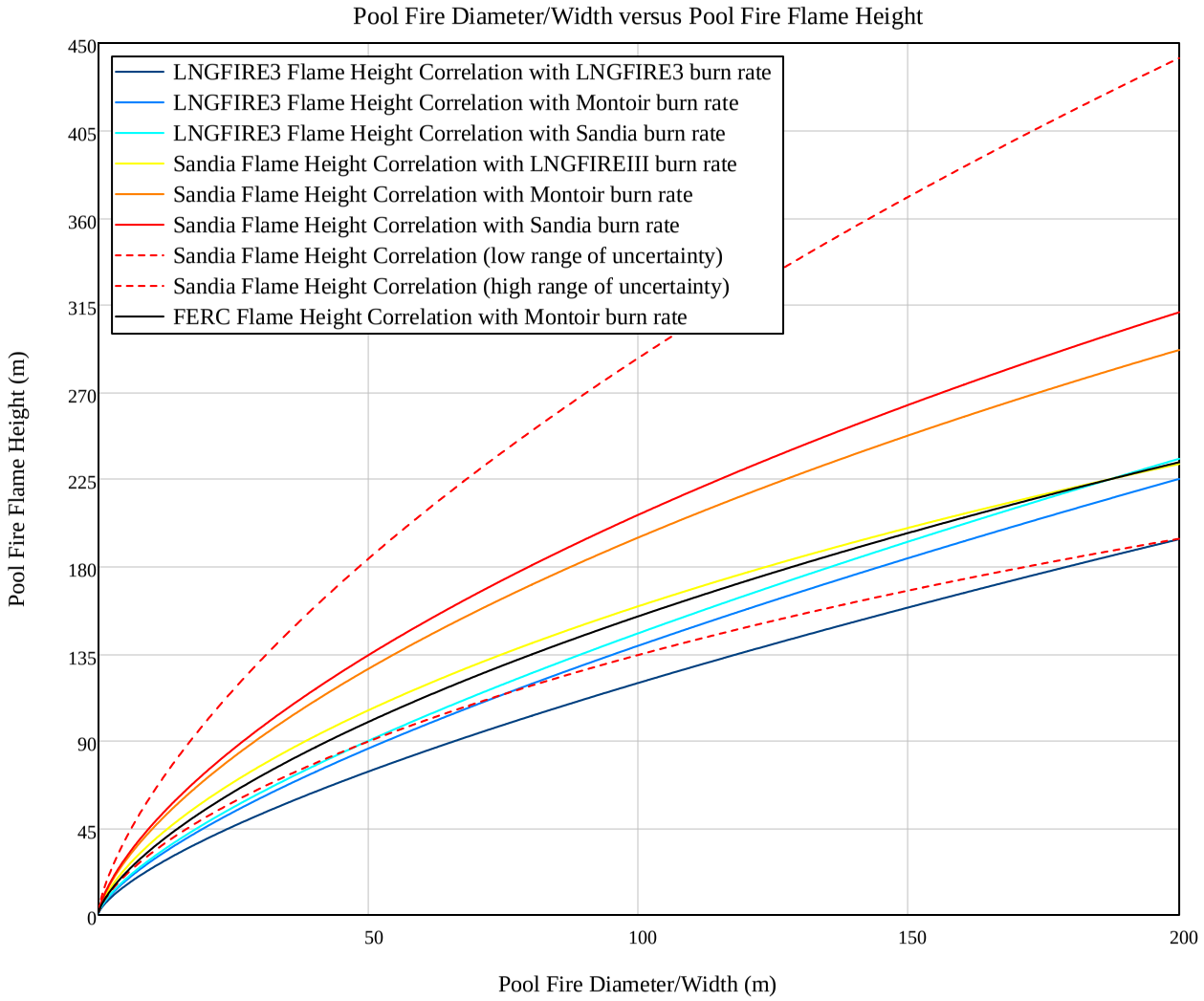
Pool Fire Diameter/Width versus Pool Fire Flame Height
LNGFIRE3 Flame Height Correlation with LNGFIRE3 burn rate
LNGFIRE3 Flame Height Correlation with Montoir burn rate
LNGFIRE3 Flame Height Correlation with Sandia burn rate
Sandia Flame Height Correlation with LNGFIREIII burn rate
Sandia Flame Height Correlation with Montoir burn rate
Sandia Flame Height Correlation with Sandia burn rate
Sandia Flame Height Correlation (low range of uncertainty)
Sandia Flame Height Correlation (high range of uncertainty)
FERC Flame Height Correlation with Montoir burn rate
Pool Fire Flame Height (m)
450
405
360
315
270
225
180
135
90
45
0
50
100
150
200
Pool Fire Diameter/Width (m)

Flame tilt angle from vertical

$$\alpha_{frontLNGFIRE3}(m_{burn}) := \begin{cases} \alpha_f \leftarrow \operatorname{acos}\left(\frac{1}{\sqrt{u_{s.frontLNGFIRE3}(m_{burn})}}\right)\cdot rad \quad \text{if } u_{s.frontLNGFIRE3}(m_{burn}) > 1 \\ \alpha_f \leftarrow \operatorname{acos}(1)\cdot rad \quad \text{if } u_{s.frontLNGFIRE3}(m_{burn}) \le 1 \\ \alpha_f \end{cases}$$

$\alpha_{frontLNGFIRE3}(m_{bLNGFIRE3}(m_{bmaxLNGFIRE3})) = 55.586\cdot deg$ $\alpha_{frontLNGFIRE3}(m_{bLNGFIRE3}(m_{bmaxSandia})$

$$\alpha_{sideLNGFIRE3}(m_{burn}) := \begin{cases} \alpha_s \leftarrow \operatorname{acos}\left(\frac{1}{\sqrt{u_{s.sideLNGFIRE3}(m_{burn})}}\right)\cdot rad \quad \text{if } u_{s.sideLNGFIRE3}(m_{burn}) > 1 \\ \alpha_s \leftarrow \operatorname{acos}(1)\cdot rad \quad \text{if } u_{s.sideLNGFIRE3}(m_{burn}) \le 1 \\ \alpha_s \end{cases}$$

$\alpha_{sideLNGFIRE3}(m_{bLNGFIRE3}(m_{bmaxLNGFIRE3})) = 55.586\cdot d$ $\alpha_{sideLNGFIRE3}(m_{bLNGFIRE3}(m_{bmaxSandia})) = 53.$

$$\alpha_{frontFERC}(m_{burn}) := \begin{cases} \alpha_f \leftarrow \operatorname{acos}\left(\frac{1}{\sqrt{u_{s.frontFERC}(m_{burn})}}\right)\cdot rad \quad \text{if} \quad u_{s.frontFERC}(m_{burn}) > 1 \\ \alpha_f \leftarrow \operatorname{acos}(1)\cdot rad \quad \text{if} \quad u_{s.frontFERC}(m_{burn}) \le 1 \\ \alpha_f \end{cases}$$

$$\alpha_{frontFERC}(m_{bFERC}(m_{bmaxFERC})) = 53.96\cdot deg$$

$$\alpha_{sideFERC}(m_{burn}) := \begin{cases} \alpha_s \leftarrow \operatorname{acos}\left(\frac{1}{\sqrt{u_{s.sideFERC}(m_{burn})}}\right)\cdot rad \quad \text{if} \quad u_{s.sideFERC}(m_{burn}) > 1 \\ \alpha_s \leftarrow \operatorname{acos}(1)\cdot rad \quad \text{if} \quad u_{s.sideFERC}(m_{burn}) \le 1 \\ \alpha_s \end{cases}$$

$$\alpha_{sideFERC}(m_{bFERC}(m_{bmaxFERC})) = 53.96\cdot deg$$

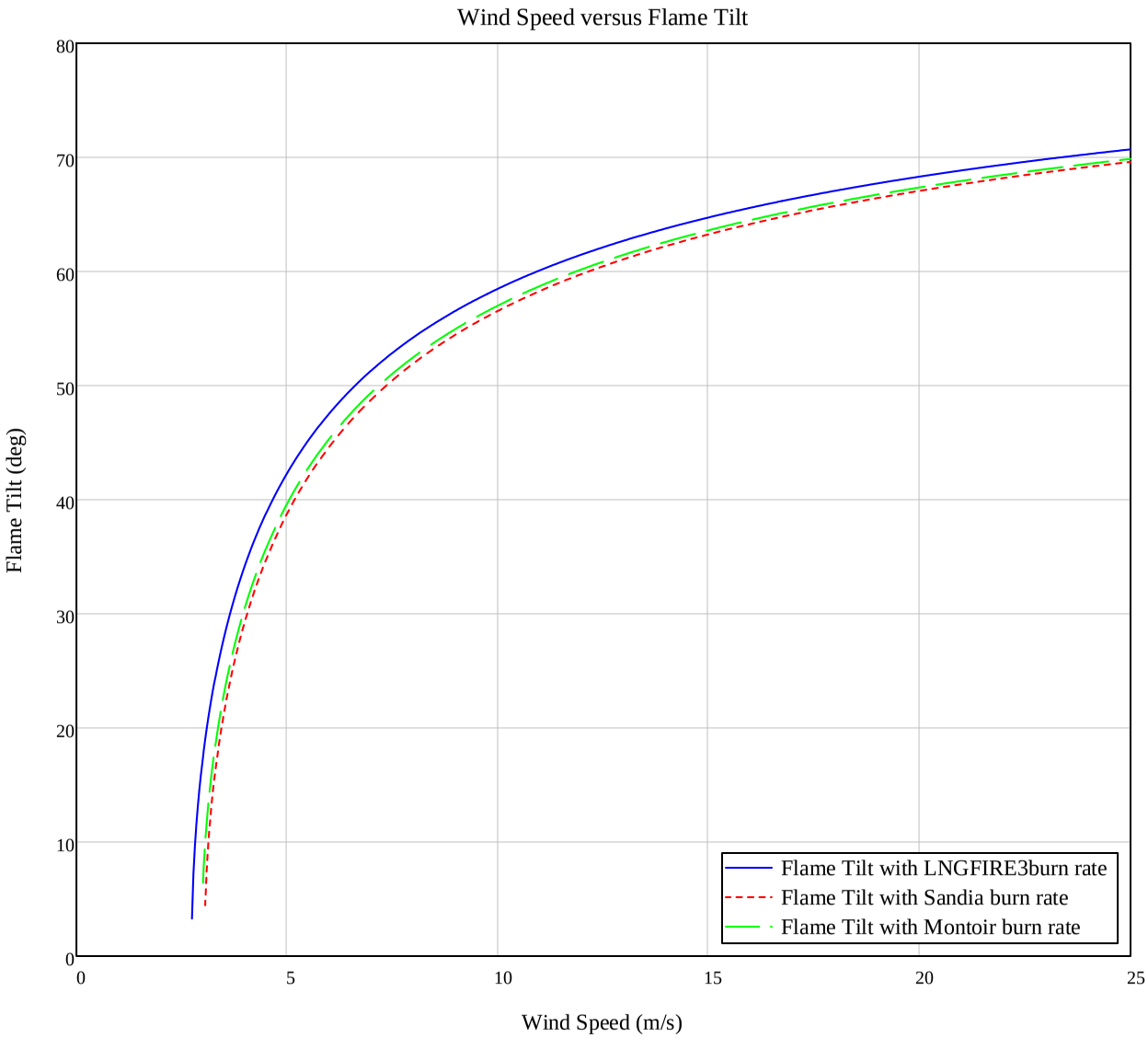
Wind Speed versus Flame Tilt
Flame Tilt (deg)
Wind Speed (m/s)
0
10
20
30
40
50
60
70
80
0
5
10
15
20
25
Flame Tilt with LNGFIRE3burn rate
Flame Tilt with Sandia burn rate
Flame Tilt with Montoir burn rate

Drag ratio
(extension of base of the flame downwind)

$$DR_{frontLNGFIRE3} := \begin{| DR \leftarrow 1.5 \cdot \left(\frac{u_{wLNGFIRE3} \left(Z_f + Z_r \right)^2}{g \cdot d} \right)^{0.069} \quad \text{if } p_s = 1 \\ DR \leftarrow 2.2 \cdot FR_{LNGFIRE3}^{0.329} \cdot (AR)^{0.205} \quad \text{if } p_s = 2 \\ DR \leftarrow 1 \quad \text{if } DR < 1 \vee Z_f > 2m \\ DR \end{|}$$

$$DR_{frontLNGFIRE3} = 1.348$$

$$DR_{sideLNGFIRE3} := \begin{| DR \leftarrow 1.5 \cdot \left(\frac{u_{wLNGFIRE3} \left(Z_f + Z_r \right)^2}{g \cdot d} \right)^{0.069} \quad \text{if } p_s = 1 \\ DR \leftarrow \left[2.2 \cdot \left(\frac{u_{wLNGFIRE3} \left(Z_f + Z_r \right)}{2\sqrt{g \cdot l}} \right)^{0.329} \cdot \left(\frac{l}{l} \right)^{0.205} \right] \quad \text{if } p_s = 2 \\ DR \leftarrow 1 \quad \text{if } DR < 1 \vee Z_f > 2m \\ DR \end{|}$$

$$DR_{frontFERC} := \begin{cases} DR_f \leftarrow 1.5 \cdot \left(\frac{u_{wFERC} \left(Z_f + Z_r \right)^2}{g \cdot d} \right)^{0.069} & \text{if } p_s = 1 \\ DR_f \leftarrow \left[2.2 \cdot FR_{FERC}{}^{0.329} \cdot (AR)^{0.205} \right] & \text{if } p_s = 2 \\ DR_f \leftarrow 1 \quad \text{if } DR_f < 1 \\ DR_f \end{cases}$$

$$DR_{frontFERC} = 1.348$$

$$DR_{sideFERC} := \begin{cases} DR_s \leftarrow 1.5 \cdot \left(\frac{u_{wFERC} \left(Z_f + Z_r \right)^2}{g \cdot d} \right)^{0.069} & \text{if } p_s = 1 \\ DR_s \leftarrow \left[2.2 \cdot \left(\frac{u_{wFERC} \left(Z_f + Z_r \right)}{2\sqrt{g \cdot l}} \right)^{0.329} \cdot \left(\frac{l}{l} \right)^{0.205} \right] & \text{if } p_s = 2 \\ DR_s \leftarrow 1 \quad \text{if } DR_s < 1 \\ DR_s \end{cases}$$

$$DR_{sideFERC} = 1.348$$

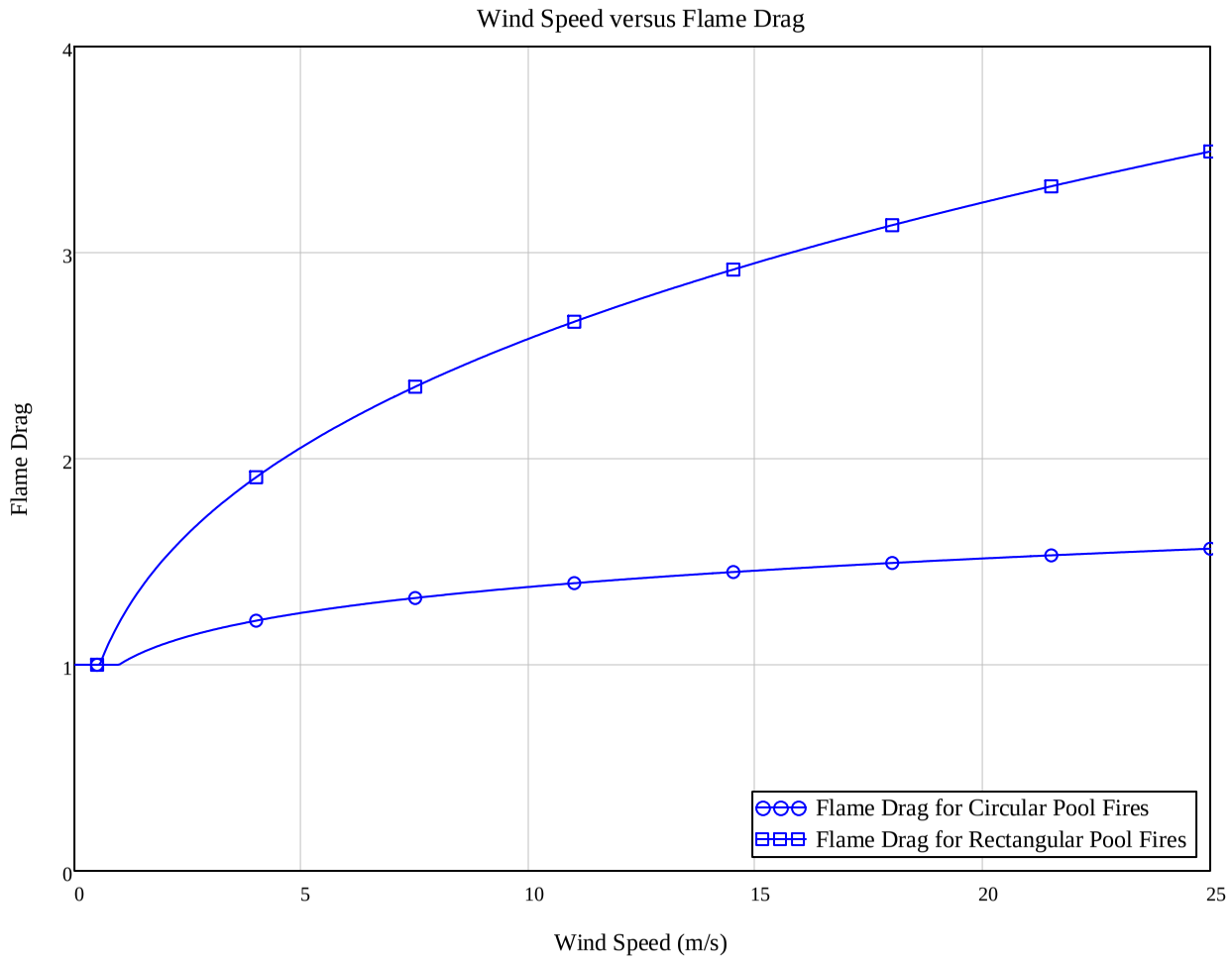
Wind Speed versus Flame Drag
Flame Drag
Wind Speed (m/s)
0
1
2
3
4
0
5
10
15
20
25
Flame Drag for Circular Pool Fires
Flame Drag for Rectangular Pool Fires

Flame Width

$$w_{f.frontLNGFIRE3} := \begin{cases} t_{f.f} \leftarrow d \cdot DR_{frontLNGFIRE3} & \text{if } p_s = 1 \\ t_{f.f} \leftarrow w \cdot DR_{frontLNGFIRE3} & \text{if } p_s = 2 \\ t_{f.f} \end{cases}$$

$$w_{f.sideLNGFIRE3} := \begin{cases} t_{f.s} \leftarrow d \cdot DR_{sideLNGFIRE3} & \text{if } p_s = 1 \\ t_{f.s} \leftarrow l \cdot DR_{sideLNGFIRE3} & \text{if } p_s = 2 \\ t_{f.s} \end{cases}$$

$$w_{f.frontLNGFIRE3} = 47.186\,\text{m}$$

$$w_{f.sideLNGFIRE3} = 47.186\,\text{m}$$

$$w_{f.frontFERC} := \begin{cases} t_{f.f} \leftarrow d \cdot DR_{frontFERC} & \text{if } p_s = 1 \\ t_{f.f} \leftarrow w \cdot DR_{frontFERC} & \text{if } p_s = 2 \\ t_{f.f} \end{cases}$$

$$w_{f.sideFERC} := \begin{cases} t_{f.s} \leftarrow d \cdot DR_{sideFERC} & \text{if } p_s = 1 \\ t_{f.s} \leftarrow l \cdot DR_{sideFERC} & \text{if } p_s = 2 \\ t_{f.s} \end{cases}$$

$$w_{f.frontFERC} = 47.186\,\text{m}$$

$$w_{f.sideFERC} = 47.186\,\text{m}$$

flame emissivity

$$\varepsilon_{w.frontLNGFIRE3} := 1 - e^{-0.3 \cdot \frac{w_{f.frontLNGFIRE3}}{m}}$$

$$\varepsilon_{w.frontLNGFIRE3} = 1$$

$$\varepsilon_{w.sideLNGFIRE3} := 1 - e^{-0.3 \cdot \frac{w_{f.sideLNGFIRE3}}{m}}$$

$$\varepsilon_{w.sideLNGFIRE3} = 1$$

$$\varepsilon_{w.frontFERC} := 1 - e^{-0.3 \cdot \frac{w_{f.frontFERC}}{m}}$$

$$\varepsilon_{w.frontFERC} = 1$$

$$\varepsilon_{w.sideFERC} := 1 - e^{-0.3 \cdot \frac{w_{f.sideFERC}}{m}}$$

$$\varepsilon_{w.sideFERC} = 1$$

SEP

$$E_{sLNGFIRE3} := 190 \frac{kW}{m^2} \quad E_{sSandia} := 286 \frac{kW}{m^2} \quad E_{sMontoir} := 265 \frac{kW}{m^2} \quad E_{sFit} := 125 \frac{kW}{m^2}$$

SEP adjusted downward to compensate for view factor over-prediction to match thermal radiation data

$$E_{s.frontLNGFIRE3}(E_{smax}) := E_{smax} \cdot \varepsilon_{w.frontLNGFIRE3}$$

$$E_{s.sideLNGFIRE3}(E_{smax}) := E_{smax} \cdot \varepsilon_{w.sideLNGFIRE3}$$

$$E_{s.frontFERC}(E_{smax}) := E_{smax} \cdot \varepsilon_{w.frontFERC}$$

$$E_{s.sideFERC}(E_{smax}) := E_{smax} \cdot \varepsilon_{w.sideFERC}$$

$$E_{s.frontLNGFIRE3}(E_{sLNGFIRE3}) = 190 \cdot \frac{kW}{m^2}$$

$$E_{s.sideLNGFIRE3}(E_{sLNGFIRE3}) = 190 \cdot \frac{kW}{m^2}$$

$$E_{s.frontFERC}(E_{sFit}) = 125 \cdot \frac{kW}{m^2}$$

$$E_{s.sideFERC}(E_{sFit}) = 125 \cdot \frac{kW}{m^2}$$

$$E_{s.frontLNGFIRE3}(E_{sMontoir}) = 265 \cdot \frac{kW}{m^2}$$

$$E_{s.sideLNGFIRE3}(E_{sMontoir}) = 265 \cdot \frac{kW}{m^2}$$

$$E_{s.frontFERC}(E_{sMontoir}) = 265 \cdot \frac{kW}{m^2}$$

$$E_{s.sideFERC}(E_{sMontoir}) = 265 \cdot \frac{kW}{m^2}$$

$$E_{s.frontLNGFIRE3}(E_{sSandia}) = 286 \cdot \frac{kW}{m^2}$$

$$E_{s.sideLNGFIRE3}(E_{sSandia}) = 286 \cdot \frac{kW}{m^2}$$

$$E_{s.frontFERC}(E_{sSandia}) = 286 \cdot \frac{kW}{m^2}$$

$$E_{s.sideFERC}(E_{sSandia}) = 286 \cdot \frac{kW}{m^2}$$

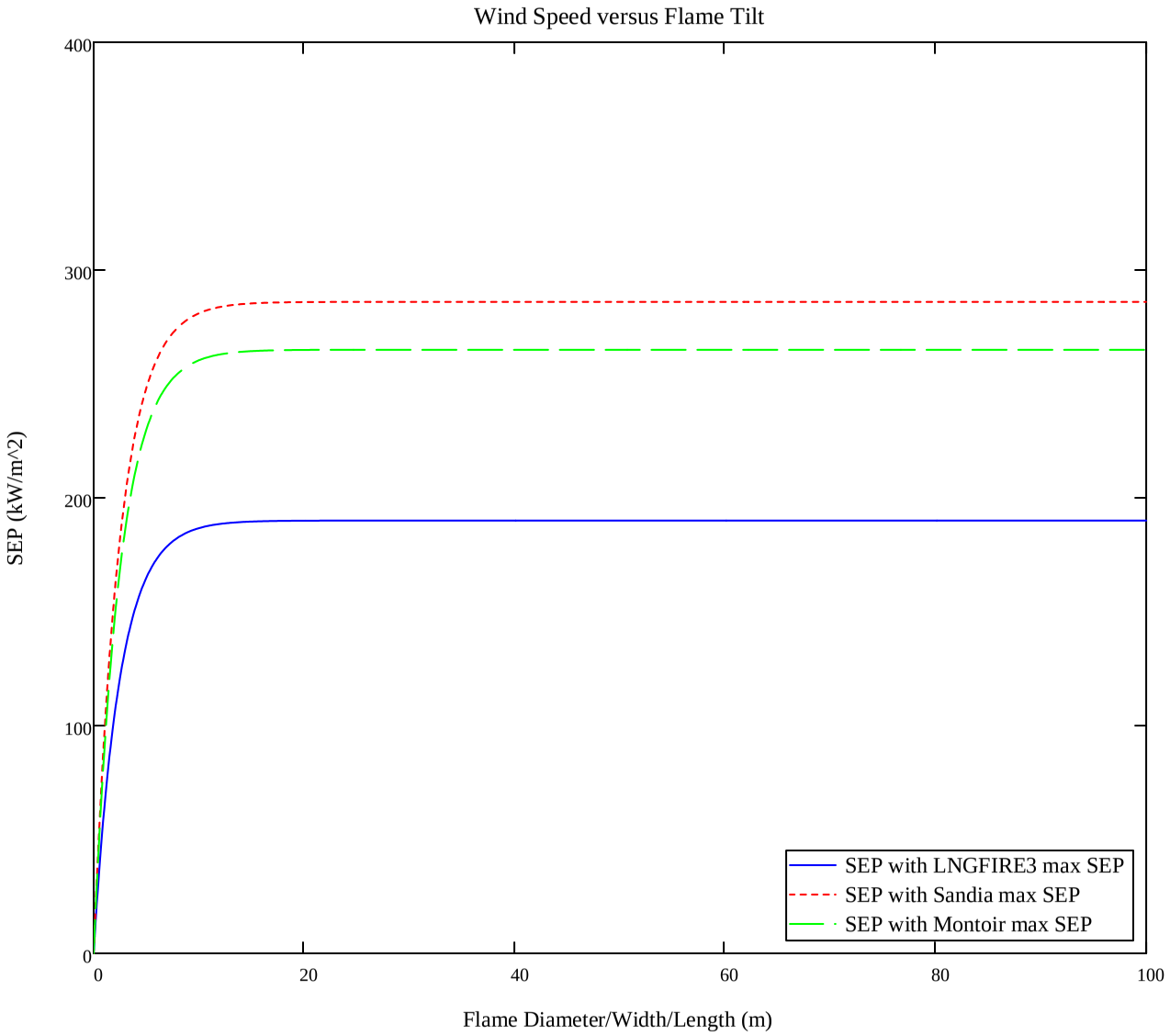
Wind Speed versus Flame Tilt
SEP (kW/m^2)
400
300
200
100
0
0
20
40
60
80
100
Flame Diameter/Width/Length (m)
SEP with LNGFIRE3 max SEP
SEP with Sandia max SEP
SEP with Montoir max SEP

Atmospheric Transmissivity

saturated water vapor pressure $P_{v\_water} := \left| \begin{array}{l} P_v \leftarrow e^{14.4114 - \frac{9590.563}{\left(\frac{T_a}{R}\right)}} \cdot RH \cdot atm \\ P_v \end{array} \right.$

$P_{v\_water} = 0.013 \cdot atm$

$P_{v\_waterSandia} := \begin{pmatrix} 4.65430 - \frac{1435.264}{\frac{T_a}{K} - 64.848} \\ 10 \end{pmatrix} \cdot RH \cdot bar$

$P_{v\_waterSandia} = 0.013 \cdot atm$

$P_{vL}(X, width) := \left| \begin{array}{l} P_{vL} \leftarrow P_{v\_water} \cdot \frac{T_{flame}}{T_a} \cdot (X - 0) \quad \text{if } p_s = 1 \\ P_{vL} \leftarrow P_{v\_water} \cdot \frac{T_{flame}}{T_a} \cdot (X - width) \quad \text{if } p_s = 2 \\ P_{vL} \end{array} \right.$

$P_{vL}(1m, 1m) = 0.059 \cdot atm \cdot m \qquad P_{vL}(X, width)$

absorptivity of water vapor

$$a_w(X, width) :=$$

$a_w \leftarrow 0 \quad \text{if} \quad RH \le 0 \vee P_{vL}(X, width) < 0.00005 atm \cdot m$

$\text{if} \quad RH > 0 \wedge P_{vL}(X, width) > 0$

$$P_{log} \leftarrow \frac{\ln\left(\frac{P_{vL}(X, width)}{atm \cdot m}\right)}{2.302585093}$$

$$E1 \leftarrow 10^{-0.4685 + 0.34729 P_{log} - 0.0864 P_{log}^2}$$

$$E1 \leftarrow 1.24 - \frac{0.642}{P_{log}} \quad \text{if} \quad P_{vL}(X, width) > 10 \cdot atm \cdot m \wedge P_{vL}(X, width) \le 453 \cdot atm \cdot m$$

$E1 \leftarrow 1 \quad \text{if} \quad P_{vL}(X, width) > 453 \cdot atm \cdot m$

$$E21 \leftarrow 0.72 + 0.16 P_{log}$$

$$E21 \leftarrow \frac{1.24 \cdot P_{log} - 0.72}{1.24 \cdot P_{log} - 0.642} \quad \text{if} \quad P_{vL}(X, width) > 10 \cdot atm \cdot m \wedge P_{vL}(X, width) \le 453 \cdot atm \cdot m$$

$$E21 \leftarrow 1.24 - \frac{0.72}{P_{log}} \quad \text{if} \quad P_{vL}(X, width) > 453 atm \cdot m \wedge P_{vL}(X, width) \le 1000 \cdot atm \cdot m$$

$E21 \leftarrow 1 \quad \text{if} \quad P_{vL}(X, width) > 1000 \cdot atm \cdot m$

$$F1 \leftarrow \ln(E21)$$

$$F2 \leftarrow \ln\left(\frac{T_a}{500R}\right)$$

$$\varepsilon_w \leftarrow E1 \cdot e^{\frac{F1 \cdot F2}{\ln(3)}}$$

$$a_w \leftarrow \varepsilon_w \cdot \left(\frac{T_a}{T_{flame}}\right)^{.45}$$

$a_w \leftarrow 1 \quad \text{if} \quad a_w \ge 1$

$a \leftarrow 0 \quad \text{if} \quad a \le 0 \vee X \le width$

$a_w \leftarrow 0 \text{ if } a_w \le 0 \vee X \ge \text{width}$

a_w

$$a_{w.frontLNGFIRE3}(X) := \begin{cases} a_{w.f} \leftarrow a_w\left(X, \frac{DR_{frontLNGFIRE3} \cdot d}{2}\right) & \text{if } p_s = 1 \\ a_{w.f} \leftarrow a_w\left(X, \frac{DR_{frontLNGFIRE3} \cdot w}{2}\right) & \text{if } p_s = 2 \\ a_{w.f} \end{cases}$$

$$a_{w.sideLNGFIRE3}(X) := \begin{cases} a_{w.s} \leftarrow a_w\left(X, \frac{DR_{sideLNGFIRE3} \cdot d}{2}\right) & \text{if } p_s = 1 \\ a_{w.s} \leftarrow a_w\left(X, \frac{DR_{sideLNGFIRE3} \cdot l}{2}\right) & \text{if } p_s = 2 \\ a_{w.s} \end{cases}$$

$a_{w.frontLNGFIRE3}\left(100m + \frac{DR_{sideLNGFIRE3} \cdot d}{2}\right) = 0.297$ $a_{w.sideLNGFIRE3}\left(100m + \frac{DR_{sideLNGFIRE3} \cdot d}{2}\right) = 0.29$

$a_{w.frontLNGFIRE3}\left(100m + \frac{DR_{sideLNGFIRE3} \cdot w}{2}\right) = 0.285$ $a_{w.sideLNGFIRE3}\left(100m + \frac{DR_{sideLNGFIRE3} \cdot l}{2}\right) = 0.29$

Define function for atmospheric transmissivity

$\tau_{frontLNGFIRE3}(X) := 1 - a_{w.frontLNGFIRE3}(X)$ $\tau_{sideLNGFIRE3}(X) := 1 - a_{w.sideLNGFIRE3}(X)$

$\tau_{frontLNGFIRE3}\left(100m + \frac{DR_{frontLNGFIRE3} \cdot d}{2}\right) = 0.703$ $\tau_{sideLNGFIRE3}\left(100m + \frac{DR_{sideLNGFIRE3} \cdot d}{2}\right) = 0.703$

$\tau_{frontLNGFIRE3}\left(100m + \frac{DR_{frontLNGFIRE3} \cdot w}{2}\right) = 0.715$ $\tau_{sideLNGFIRE3}\left(100m + \frac{DR_{sideLNGFIRE3} \cdot l}{2}\right) = 0.707$

Amount of Water Vapor along Path Length

$$\chi_{H2O}(X) := \frac{\frac{P_{v\_waterSandia} \cdot X}{\left(in\_Hg \cdot \frac{mm}{in}\right) m} \cdot 2.8865 \cdot 10^2}{\frac{T_a}{K}} \qquad \chi_{H2O}(100m) = 987$$

Amount of Carbon Dioxide along Path Length

$$\chi_{CO2}(X) := \frac{273K}{T_a} \cdot \frac{X}{m} \qquad \chi_{CO2}(100m) = 92.81$$

$$\tau_{Sandia}(X, width) := \left| \begin{array}{l} \text{if } X > width \\ \quad \left| \begin{array}{l} \tau \leftarrow 1.006 - 0.0117 \log\left(\chi_{H2O}(X - width)\right) - 0.02368 \log\left(\chi_{H2O}(X - width)\right)^2 - 0.03188 \log\left(\chi_{CO2}(X - width)\right) + 0.001164 \log\left(\chi_{CC} \right. \\ \tau \leftarrow 1.006 - 0.03188 \log\left(\chi_{CO2}(X - width)\right) + 0.001164 \log\left(\chi_{CO2}(X - width)\right)^2 \text{ if } RH = 0 \end{array} \right. \\ \tau \leftarrow 1 \text{ if } X \le width \vee \tau \ge 1 \\ \tau \end{array} \right.$$

$$\tau_{Sandia.front}(X) := \left| \begin{array}{l} \tau_{S.f} \leftarrow \tau_{Sandia}\left(X, \frac{DR_{frontLNGFIRE3} \cdot d}{2}\right) \text{ if } \\ \tau_{S.f} \leftarrow \tau_{Sandia}\left(X, \frac{DR_{frontLNGFIRE3} \cdot w}{2}\right) \text{ if} \\ \tau_{S.f} \end{array} \right. \qquad \tau_{Sandia.side}(X) := \left| \begin{array}{l} \tau_{S.s} \leftarrow \tau_{Sandia}\left(X, \frac{DR_{sideLNGFIRE3} \cdot d}{2}\right) \text{ if } p_s = 1 \\ \tau_{S.s} \leftarrow \tau_{Sandia}\left(X, \frac{DR_{sideLNGFIRE3} \cdot l}{2}\right) \text{ if } p_s = 2 \\ \tau_{S.s} \end{array} \right.$$

$$\tau_{Sandia.front}\left(100m + \frac{DR_{frontLNGFIRE3} \cdot d}{2}\right) = 0 \qquad \tau_{Sandia.side}\left(100m + \frac{DR_{sideLNGFIRE3} \cdot d}{2}\right) = 0.7$$

$$\tau_{Sandia.front}\left(100m + \frac{DR_{frontLNGFIRE3} \cdot w}{2}\right) = 0 \qquad \tau_{Sandia.side}\left(100m + \frac{DR_{sideLNGFIRE3} \cdot l}{2}\right) = 0.707$$

$$\tau_{frontFERC}(X) := \begin{cases} \tau_{F.f} \leftarrow \tau_{Sandia}\left(X, \frac{DR_{frontFERC} \cdot d}{2}\right) & \text{if } p_s = 1 \\ \tau_{F.f} \leftarrow \tau_{Sandia}\left(X, \frac{DR_{frontFERC} \cdot w}{2}\right) & \text{if } p_s = 2 \\ \tau_{F.f} \end{cases}$$

$$\tau_{sideFERC}(X) := \begin{cases} \tau_{F.s} \leftarrow \tau_{Sandia}\left(X, \frac{DR_{sideFERC} \cdot d}{2}\right) & \text{if } p_s = 1 \\ \tau_{F.s} \leftarrow \tau_{Sandia}\left(X, \frac{DR_{sideFERC} \cdot l}{2}\right) & \text{if } p_s = 2 \\ \tau_{F.s} \end{cases}$$

$$\tau_{frontFERC}\left(100m + \frac{DR_{frontFERC} \cdot d}{2}\right) = 0.7 \qquad \tau_{frontFERC}\left(100m + \frac{DR_{sideFERC} \cdot d}{2}\right) = 0.7$$

$$\tau_{frontFERC}\left(100m + \frac{DR_{frontFERC} \cdot w}{2}\right) = 0.72 \qquad \tau_{frontFERC}\left(100m + \frac{DR_{sideFERC} \cdot l}{2}\right) = 0.707$$

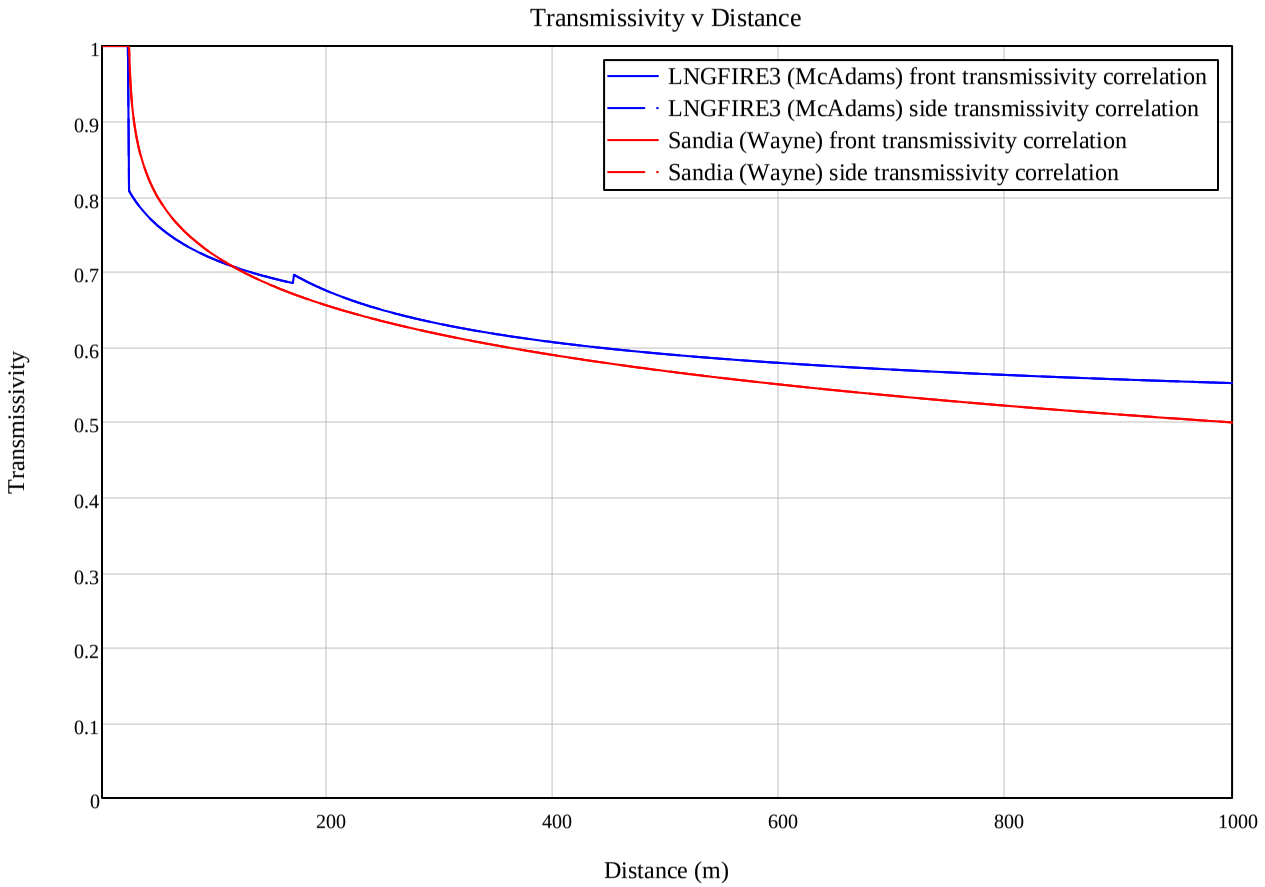
Transmissivity v Distance
LNGFIRE3 (McAdams) front transmissivity correlation
LNGFIRE3 (McAdams) side transmissivity correlation
Sandia (Wayne) front transmissivity correlation
Sandia (Wayne) side transmissivity correlation
Transmissivity
Distance (m)
0
0.1
0.2
0.3
0.4
0.5
0.6
0.7
0.8
0.9
1
200
400
600
800
1000

View Factors

$FH_{circ}(\theta, r, LFH, X, l_f) :=$

$HH \leftarrow \frac{LFH}{r}$

$S \leftarrow \frac{X}{r}$

$TA \leftarrow HH^2 + (S+1)^2 - 2 \cdot HH \cdot (S+1) \cdot \sin(\theta)$

$TB \leftarrow HH^2 + (S-1)^2 - 2 \cdot HH \cdot (S-1) \cdot \sin(\theta)$

$TC \leftarrow 1 + \left(S^2 - 1\right) \cdot \cos(\theta)^2$

$TE \leftarrow \sqrt{\frac{S-1}{S+1}}$

$TF \leftarrow \frac{HH^2 + (S+1)^2 - 2 \cdot (S + 1 + HH \cdot S \cdot \sin(\theta))}{\sqrt{TA \cdot TB}}$

$TG \leftarrow \frac{HH \cdot S - \left(S^2 - 1\right) \cdot \sin(\theta)}{\sqrt{S^2 - 1} \cdot \sqrt{TC}}$

$TH \leftarrow \frac{\sqrt{S^2 - 1} \cdot \sin(\theta)}{\sqrt{TC}}$

$TJ \leftarrow \frac{\sin(\theta)}{\sqrt{TC}}$

$TK \leftarrow TE \cdot \sqrt{\frac{TA}{TB}}$

$VAL1 \leftarrow \operatorname{atan}(TG) + \operatorname{atan}(TH)$

$VAL2 \leftarrow TF \cdot \operatorname{atan}(TK)$

$VAL3 \leftarrow \sqrt{\frac{S+1}{S-1}}$

$FH \leftarrow \frac{1}{\pi} \cdot (\operatorname{atan}(VAL3) + TJ \cdot VAL1 - VAL2)$

FH

$FV_{circ}(\theta, r, LFV, X, l_f) :=$

$HV \leftarrow \frac{LFV}{r}$

$S \leftarrow \frac{X}{r}$

$TA1 \leftarrow HV^2 + (S+1)^2 - 2 \cdot HV \cdot (S+1) \cdot \sin(\theta)$

$TB1 \leftarrow HV^2 + (S-1)^2 - 2 \cdot HV \cdot (S-1) \cdot \sin(\theta)$

$TC1 \leftarrow 1 + \left(S^2 - 1\right) \cdot \cos(\theta)^2$

$TD1 \leftarrow \frac{HV \cdot \cos(\theta)}{S - HV \cdot \sin(\theta)}$

$TE1 \leftarrow \sqrt{\frac{S-1}{S+1}}$

$TF1 \leftarrow \frac{HV^2 + (S+1)^2 - 2 \cdot S \cdot (1 + HV \cdot \sin(\theta))}{\sqrt{TA1 \cdot TB1}}$

$TG1 \leftarrow \frac{HV \cdot S - \left(S^2 - 1\right) \cdot \sin(\theta)}{\sqrt{S^2 - 1} \cdot \sqrt{TC1}}$

$TH1 \leftarrow \frac{\sqrt{S^2 - 1} \cdot \sin(\theta)}{\sqrt{TC1}}$

$TI1 \leftarrow \frac{\cos(\theta)}{\sqrt{TC1}}$

$TK1 \leftarrow TE1 \cdot \sqrt{\frac{TA1}{TB1}}$

$VAL11 \leftarrow \operatorname{atan}(TG1) + \operatorname{atan}(TH1)$

$VAL21 \leftarrow TF1 \cdot \operatorname{atan}(TK1)$

$FV \leftarrow \frac{1}{\pi} \cdot (-TD1 \cdot \operatorname{atan}(TE1) + TD1 \cdot VAL21 + TI1 \cdot$

FV

$$FHZ_{rect}(X, H, XL, \theta) := \left| \begin{array}{l} P \leftarrow 2 \cdot \frac{H}{XL} \\ Q \leftarrow 2 \cdot \frac{X}{XL} \\ V \leftarrow \frac{1}{\sqrt{P^2 + Q^2 - 2 \cdot P \cdot Q \cdot \cos(\theta)}} \\ W \leftarrow \sqrt{1 + Q^2 \cdot \sin(\theta)^2} \\ A \leftarrow \operatorname{atan}\left(\frac{1}{Q}\right) + V \cdot (P \cdot \cos(\theta) - Q) \cdot \operatorname{atan}(V) \\ B \leftarrow \frac{\cos(\theta)}{W} \\ C \leftarrow \operatorname{atan}\left(\frac{P - Q \cdot \cos(\theta)}{W}\right) + \operatorname{atan}\left(\frac{Q \cdot \cos(\theta)}{W}\right) \\ FHZ \leftarrow \frac{A + B \cdot C}{\pi} \\ FHZ \end{array} \right.$$

$$FVZ_{rect}(X, H, XL) := \left| \begin{array}{l} P \leftarrow \frac{H}{X} \\ Q \leftarrow \frac{XL}{2 \cdot X} \\ P1 \leftarrow \sqrt{1 + P^2} \\ Q1 \leftarrow \sqrt{1 + Q^2} \\ FVZ \leftarrow \frac{\frac{P}{P1} \operatorname{atan}\left(\frac{Q}{P1}\right) + \frac{Q}{Q1} \operatorname{atan}\left(\frac{P}{Q1}\right)}{\pi} \\ FVZ \end{array} \right.$$

$$
\begin{aligned}
&F_{circ}(X, l_f, \theta) := \\
&\quad XP \leftarrow X - ZZ \cdot \tan(\theta) \\
&\quad LFH1_{circ}(l_f, \theta) \leftarrow l_f - \frac{ZZ}{\cos(\theta)} \\
&\quad LFH2_{circ}(l_f, \theta) \leftarrow \frac{|ZZ|}{\cos(\theta)} \\
&\quad LFV1_{circ}(l_f, \theta) \leftarrow l_f - \frac{ZZ}{\cos(\theta)} \\
&\quad LFV2_{circ}(l_f, \theta) \leftarrow \frac{|ZZ|}{\cos(\theta)} \\
&\quad FH \leftarrow FH_{circ}(\theta, r, LFH1_{circ}(l_f, \theta), XP, l_f) - FH_{circ}(\theta, r, LFH2_{circ}(l_f, \theta), XP, l_f) \text{ if } Z_T \le Z_f \\
&\quad FH \leftarrow FH_{circ}(\theta, r, LFH1_{circ}(l_f, \theta), XP, l_f) \text{ if } Z_T > Z_f \wedge Z_T < Z_f + l_f \cdot \cos(\theta) \\
&\quad FV \leftarrow FV_{circ}(\theta, r, LFV1_{circ}(l_f, \theta), XP, l_f) - FV_{circ}(\theta, r, LFV2_{circ}(l_f, \theta), XP, l_f) \text{ if } Z_T \le Z_f \\
&\quad FV \leftarrow FV_{circ}(\theta, r, LFV1_{circ}(l_f, \theta), XP, l_f) + FV_{circ}(-\theta, r, LFV2_{circ}(l_f, \theta), XP, l_f) \text{ if } Z_T > Z_f \wedge Z_T < Z_f + l_f \cdot \cos(\theta) \\
&\quad F_{circ} \leftarrow \sqrt{FH^2 + FV^2} \\
&\quad F_{circ} \leftarrow 1 \text{ if } F_{circ} \ge 1 \\
&\quad F_{circ}
\end{aligned}
$$

$$F_{rect}(X, l_f, XL, \theta) :=$$

$\beta \leftarrow \frac{\pi}{2} - \theta$

$XP \leftarrow X - ZZ \cdot \tan(\theta)$

$H1 \leftarrow l_f - \frac{ZZ}{\cos(\theta)}$

$H2 \leftarrow H1 - l_f$

$FHX1 \leftarrow FHZ_{rect}(XP, H1, XL, \beta)$

$FHX1 \leftarrow 0 \quad \text{if} \quad FHX1 \le 0$

$FHX1 \leftarrow 0 \quad \text{if} \quad H1 \le 0$

$FHX2 \leftarrow FHZ_{rect}(XP, H2, XL, \beta)$

$FHX2 \leftarrow 0 \quad \text{if} \quad FHX1 \le 0$

$FHX2 \leftarrow 0 \quad \text{if} \quad H2 \le 0$

$FHX \leftarrow FHX1 - FHX2 \quad \text{if} \quad XP > 0$

$FHX \leftarrow 0 \quad \text{if} \quad XP \le 0$

if $\theta = 0$

- $H1 \leftarrow |ZZ|$
- $H2 \leftarrow l_f - ZZ$
- $FVX1 \leftarrow FVZ_{rect}(XP, H1, XL)$
- $FVX2 \leftarrow FVZ_{rect}(XP, H2, XL)$
- $FVX \leftarrow FVX1 + FVX2 \quad \text{if} \quad ZZ > 0$
- $FVX \leftarrow FVX2 - FVX1 \quad \text{if} \quad ZZ \le 0$

if $\theta \neq 0$

- $XCR \leftarrow l_f \cdot \sin(\theta)$
- if $X > XCR$
  - $H1 \leftarrow \frac{X}{\cos(\beta)}$

$Y1 \leftarrow X \cdot \tan(\beta)$

$Y \leftarrow Y1 - ZZ$

$FVX1 \leftarrow FHZ_{rect}(Y, H1, XL, \theta)$

$H2 \leftarrow H1 - l_f$

$FVX2 \leftarrow FHZ_{rect}(Y, H2, XL, \theta)$

$FVX \leftarrow FVX1 - FVX2$

if $X \le XCR$

$H1 \leftarrow \frac{X}{\sin(\theta)}$

$Y1 \leftarrow \frac{X}{\tan(\theta)}$

$Y \leftarrow Y1 - ZZ$

$FVX \leftarrow FHZ_{rect}(Y, H1, XL, \theta)$

$FVX \leftarrow 0$ if $FVX \le 0$

$F_{rect} \leftarrow \sqrt{FHX^2 + FVX^2}$

$F_{rect} \leftarrow 1$ if $F_{rect} \ge 1$

F_{rect}

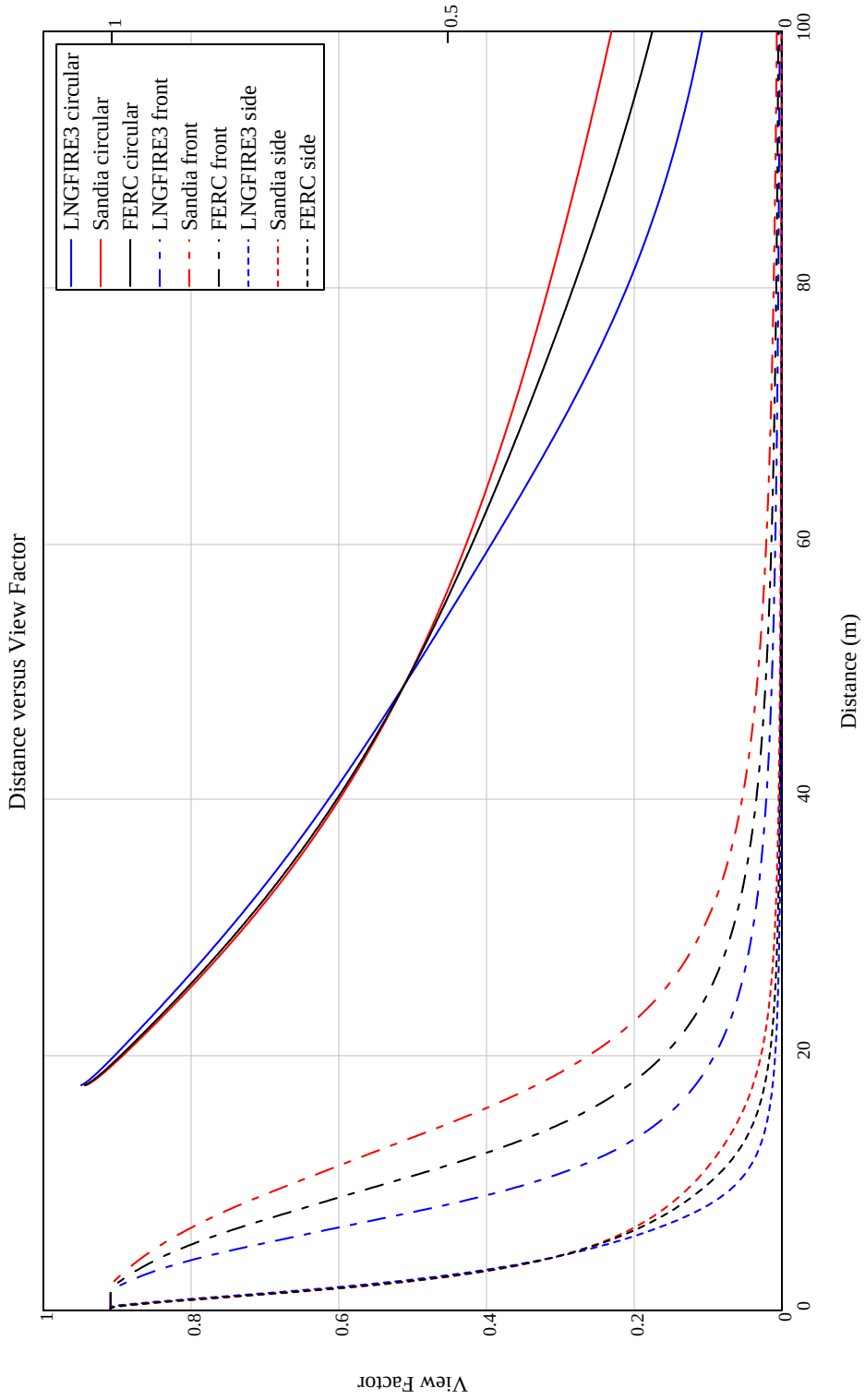
Distance versus View Factor
View Factor
Distance (m)
LNGFIRE3 circular
Sandia circular
FERC circular
LNGFIRE3 front
Sandia front
FERC front
LNGFIRE3 side
Sandia side
FERC side
0
0.2
0.4
0.6
0.8
1
0
20
40
60
80
100
0.5
1

Calculate Thermal Flux Downwind

X is distance from CENTER of pool

$$I_{th.front.LNGFIRE3}(X) := \left| \begin{array}{l} I_{th}(X) \leftarrow \tau_{frontLNGFIRE3}(X) \cdot E_{s.frontLNGFIRE3}\left(E_{sLNGFIRE3}\right) \cdot F_{circ}\left(X, L_f\left(d, m_{bLNGFIRE3}\left(m_{bmaxLNGFIRE3}\right)\right), \alpha_{frontLNG}\right. \\ I_{th}(X) \leftarrow \tau_{frontLNGFIRE3}(X) \cdot E_{s.frontLNGFIRE3}\left(E_{sLNGFIRE3}\right) \cdot F_{rect}\left(X, L_f\left(w, m_{bLNGFIRE3}\left(m_{bmaxLNGFIRE3}\right)\right), l, \alpha_{frontLN}\right. \\ I_{th}(X) \end{array} \right.$$

$$I_{th.side.LNGFIRE3}(X) := \left| \begin{array}{l} I_{th}(X) \leftarrow \tau_{sideLNGFIRE3}(X) \cdot E_{s.sideLNGFIRE3}\left(E_{sLNGFIRE3}\right) \cdot F_{circ}\left(X, L_f\left(d, m_{bLNGFIRE3}\left(m_{bmaxLNGFIRE3}\right)\right), \alpha_{sideLNGFII}\right. \\ I_{th}(X) \leftarrow \tau_{sideLNGFIRE3}(X) \cdot E_{s.sideLNGFIRE3}\left(E_{sLNGFIRE3}\right) \cdot F_{rect}\left(X, L_f\left(w, m_{bLNGFIRE3}\left(m_{bmaxLNGFIRE3}\right)\right), w, \alpha_{sideLNG}\right. \\ I_{th}(X) \end{array} \right.$$

$$I_{th.front.Sandia}(X) := \left| \begin{array}{l} I_{th}(X) \leftarrow \tau_{Sandia.front}(X) \cdot E_{s.frontLNGFIRE3}\left(E_{sSandia}\right) \cdot F_{circ}\left(X, L_{fSandia}\left(d, m_{bLNGFIRE3}\left(m_{bmaxSandia}\right)\right), \alpha_{frontLNGFIRE3}\left(m_{bL}\right.\right. \\ I_{th}(X) \leftarrow \tau_{Sandia.front}(X) \cdot E_{s.frontLNGFIRE3}\left(E_{sSandia}\right) \cdot F_{rect}\left(X, L_{fSandia}\left(w, m_{bLNGFIRE3}\left(m_{bmaxSandia}\right)\right), l, \alpha_{frontLNGFIRE3}\left(m_{t}\right.\right. \\ I_{th}(X) \end{array} \right.$$

$$I_{th.side.Sandia}(X) := \left| \begin{array}{l} I_{th}(X) \leftarrow \tau_{Sandia.side}(X) \cdot E_{s.sideLNGFIRE3}\left(E_{sSandia}\right) \cdot F_{circ}\left(X, L_{fSandia}\left(d, m_{bLNGFIRE3}\left(m_{bmaxSandia}\right)\right), \alpha_{sideLNGFIRE3}\left(m_{bLNG}\right.\right. \\ I_{th}(X) \leftarrow \tau_{Sandia.side}(X) \cdot E_{s.sideLNGFIRE3}\left(E_{sSandia}\right) \cdot F_{rect}\left(X, L_{fSandia}\left(w, m_{bLNGFIRE3}\left(m_{bmaxSandia}\right)\right), w, \alpha_{sideLNGFIRE3}\left(m_{bL}\right.\right. \\ I_{th}(X) \end{array} \right.$$

$$I_{th.front.Montoir}(X) := \begin{cases} I_{th}(X) \leftarrow \tau_{Sandia.front}(X) \cdot E_{s.frontLNGFIRE3}\left(E_{sMontoir}\right) \cdot F_{circ}\left(X, L_{fSandia}\left(d, m_{bLNGFIRE3}\left(m_{bmaxMontoir}\right)\right), \alpha_{frontLNGFIRE3}\left(\right.\right. \\ I_{th}(X) \leftarrow \tau_{Sandia.front}(X) \cdot E_{s.frontLNGFIRE3}\left(E_{sMontoir}\right) \cdot F_{rect}\left(X, L_{fSandia}\left(w, m_{bLNGFIRE3}\left(m_{bmaxMontoir}\right)\right), l, \alpha_{frontLNGFIRE3}\right. \\ I_{th}(X) \end{cases}$$

$$I_{th.side.Montoir}(X) := \begin{cases} I_{th}(X) \leftarrow \tau_{Sandia.side}(X) \cdot E_{s.sideLNGFIRE3}\left(E_{sMontoir}\right) \cdot F_{circ}\left(X, L_{fSandia}\left(d, m_{bLNGFIRE3}\left(m_{bmaxMontoir}\right)\right), \alpha_{sideLNGFIRE3}\left(m_{bI}\right.\right. \\ I_{th}(X) \leftarrow \tau_{Sandia.side}(X) \cdot E_{s.sideLNGFIRE3}\left(E_{sMontoir}\right) \cdot F_{rect}\left(X, L_{fSandia}\left(w, m_{bLNGFIRE3}\left(m_{bmaxMontoir}\right)\right), w, \alpha_{sideLNGFIRE3}\left(\right.\right. \\ I_{th}(X) \end{cases}$$

$$I_{th.front.FERC}(X) := \begin{cases} I_{th}(X) \leftarrow \tau_{Sandia.front}(X) \cdot E_{s.frontFERC}\left(E_{sFit}\right) \cdot F_{circ}\left(X, L_{fFERC}\left(d, m_{bFERC}\left(m_{bmaxFERC}\right)\right), \alpha_{frontFERC}\left(m_{bFERC}\left(m_{bmaxFERC}\right)\right)\right. \\ I_{th}(X) \leftarrow \tau_{Sandia.front}(X) \cdot E_{s.frontFERC}\left(E_{sFit}\right) \cdot F_{rect}\left(X, L_{fFERC}\left(w, m_{bFERC}\left(m_{bmaxFERC}\right)\right), l, \alpha_{frontFERC}\left(m_{bFERC}\left(m_{bmaxFERC}\right)\right.\right. \\ I_{th}(X) \end{cases}$$

$$I_{th.side.FERC}(X) := \begin{cases} I_{th}(X) \leftarrow \tau_{Sandia.side}(X) \cdot E_{s.sideFERC}\left(E_{sFit}\right) \cdot F_{circ}\left(X, L_{fFERC}\left(d, m_{bFERC}\left(m_{bmaxFERC}\right)\right), \alpha_{sideFERC}\left(m_{bFERC}\left(m_{bmaxFERC}\right)\right)\right) & \text{if} \\ I_{th}(X) \leftarrow \tau_{Sandia.side}(X) \cdot E_{s.sideFERC}\left(E_{sFit}\right) \cdot F_{rect}\left(X, L_{fFERC}\left(w, m_{bFERC}\left(m_{bmaxFERC}\right)\right), w, \alpha_{sideFERC}\left(m_{bFERC}\left(m_{bmaxFERC}\right)\right)\right) \\ I_{th}(X) \end{cases}$$

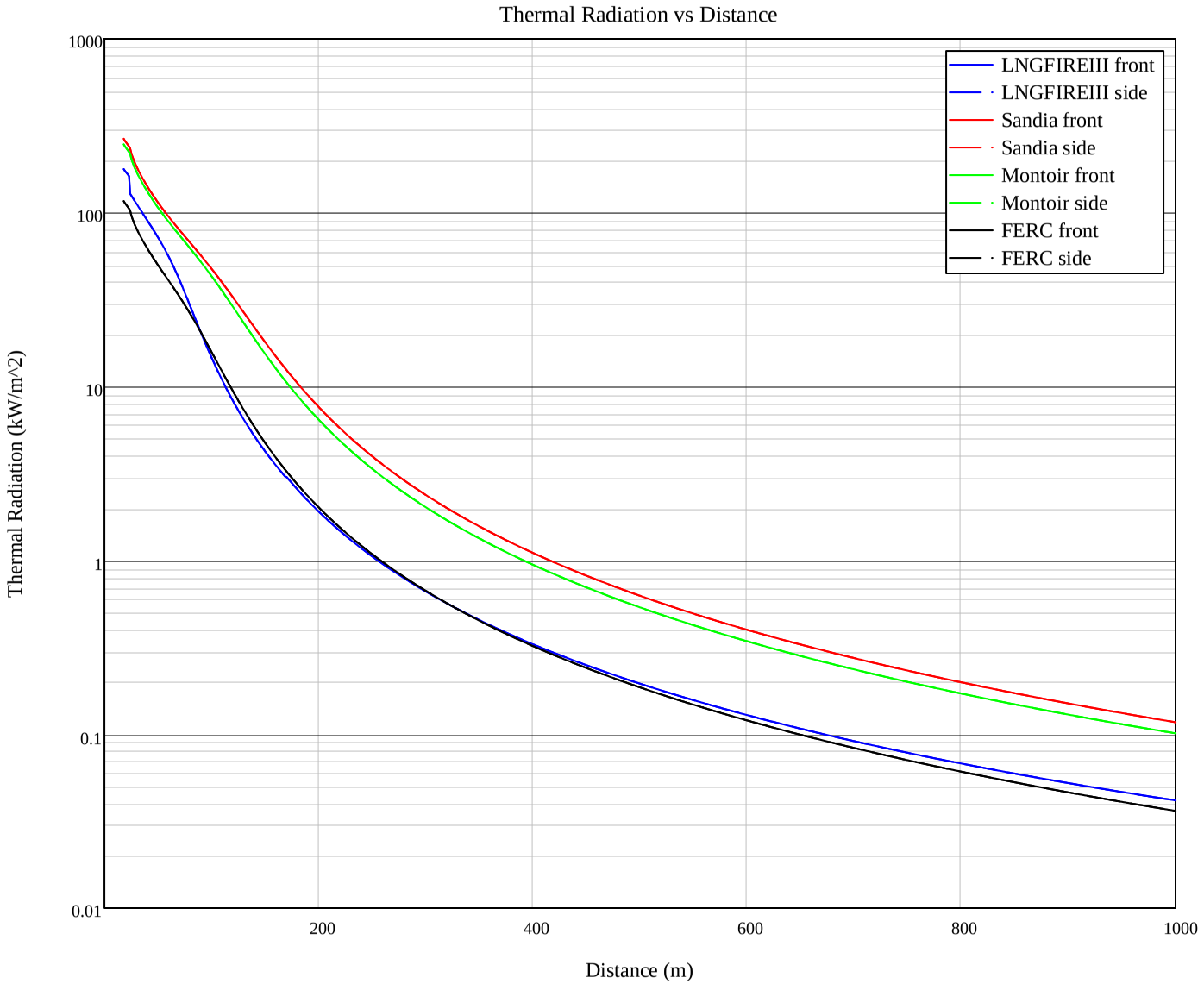
Thermal Radiation vs Distance
Thermal Radiation (kW/m^2)
1000
100
10
1
0.1
0.01
200
400
600
800
1000
Distance (m)
LNGFIREIII front
LNGFIREIII side
Sandia front
Sandia side
Montoir front
Montoir side
FERC front
FERC side

$q_{frontLNGFIRE3} :=$

$i \leftarrow 0$

$step \leftarrow \frac{DR_{frontLNGFIRE3} \cdot d}{200}$ if $p_s = 1$

$step \leftarrow \frac{DR_{frontLNGFIRE3} \cdot w}{200}$ if $p_s = 2$

$x_0 \leftarrow DR_{frontLNGFIRE3} \cdot d - \frac{d}{2} + step$ if $p_s = 1$

$x_0 \leftarrow 0 + step$ if $p_s = 2$

$q_0 \leftarrow I_{th.front.LNGFIRE3}(x_0)$

$q_{max_0} \leftarrow q_0$

while $q_i \geq 5 \frac{kW}{m^2} \vee x_i \leq 500m$

- $i \leftarrow i + 1$
- $q_i \leftarrow I_{th.front.LNGFIRE3}(x_{i-1})$
- $q_{max_i} \leftarrow \max(q_i, q_{max_{i-1}})$
- $x_i \leftarrow x_{i-1} + step$
- $x_{max_i} \leftarrow x_i$ if $q_i \geq q_{max_{i-1}}$
- $x_{max_i} \leftarrow x_{max_{i-1}}$ if $q_i < q_{max_{i-1}}$

$M^{\langle 0 \rangle} \leftarrow \frac{x + \left(\frac{d}{2} - \frac{DR_{frontLNGFIRE3} \cdot d}{2}\right)}{m}$ if $p_s = 1$

$M^{\langle 0 \rangle} \leftarrow \frac{x + \left(DR_{frontLNGFIRE3} \cdot w - \frac{w}{2}\right)}{m}$ if $p_s = 2$

$M^{\langle 1 \rangle} \leftarrow \frac{q}{}$

$q_{sideLNGFIRE3} :=$

$i \leftarrow 0$

$step \leftarrow \frac{DR_{sideLNGFIRE3} \cdot d}{200}$ if $p_s = 1$

$step \leftarrow \frac{DR_{sideLNGFIRE3} \cdot l}{200}$ if $p_s = 2$

$x_0 \leftarrow DR_{frontLNGFIRE3} \cdot d - \frac{d}{2} + step$ if p_s

$x_0 \leftarrow 0 + step$ if $p_s = 2$

$q_0 \leftarrow I_{th.side.LNGFIRE3}(x_0)$

$q_{max_0} \leftarrow q_0$

while $q_i \geq 5 \frac{kW}{m^2} \vee x_i \leq 500m$

- $i \leftarrow i + 1$
- $q_i \leftarrow I_{th.side.LNGFIRE3}(x_{i-1})$
- $q_{max_i} \leftarrow \max(q_i, q_{max_{i-1}})$
- $x_i \leftarrow x_{i-1} + step$
- $x_{max_i} \leftarrow x_i$ if $q_i \geq q_{max_{i-1}}$
- $x_{max_i} \leftarrow x_{max_{i-1}}$ if $q_i < q_{max_{i-1}}$

$M^{\langle 0 \rangle} \leftarrow \frac{x + \left(\frac{d}{2} - \frac{DR_{sideLNGFIRE3} \cdot d}{2}\right)}{m}$ if

$M^{\langle 0 \rangle} \leftarrow \frac{x + \left(DR_{sideLNGFIRE3} \cdot l - \frac{l}{2}\right)}{m}$ if p_s

$M^{\langle 1 \rangle} \leftarrow \frac{q}{}$

$$M^{\langle 1\rangle} \leftarrow \frac{kW}{m^2}$$

$$M^{\langle 2\rangle} \leftarrow \frac{x_{max} + \left(\frac{d}{2} - \frac{DR_{frontLNGFIRE3} \cdot d}{2}\right)}{m} \quad \text{if } p_s = 1$$

$$M^{\langle 2\rangle} \leftarrow \frac{x_{max} + \left(DR_{frontLNGFIRE3} \cdot w - \frac{w}{2}\right)}{m} \quad \text{if } p_s = 2$$

$$M^{\langle 3\rangle} \leftarrow \frac{q_{max}}{\frac{kW}{m^2}}$$

$$M^{\langle 1\rangle} \leftarrow \frac{kW}{m^2}$$

$$M^{\langle 2\rangle} \leftarrow \frac{x_{max} + \left(\frac{d}{2} - \frac{DR_{sideLNGFIRE3} \cdot d}{2}\right)}{m}$$

$$M^{\langle 2\rangle} \leftarrow \frac{x_{max} + \left(DR_{sideLNGFIRE3} \cdot l - \frac{l}{2}\right)}{m} \quad \text{i}$$

$$M^{\langle 3\rangle} \leftarrow \frac{q_{max}}{\frac{kW}{m^2}}$$

$q_{frontLNGFIRE3}^{\langle 1\rangle}$

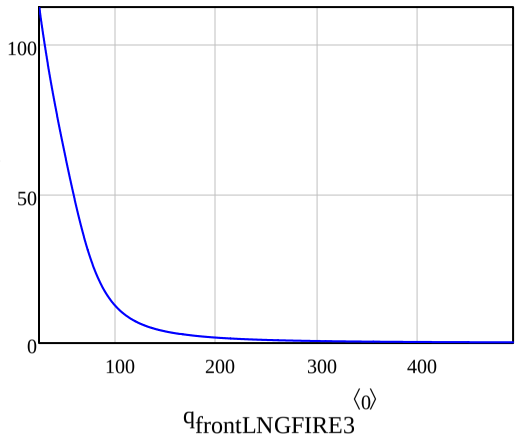

$q_{sideLNGFIRE3}^{\langle 1\rangle}$

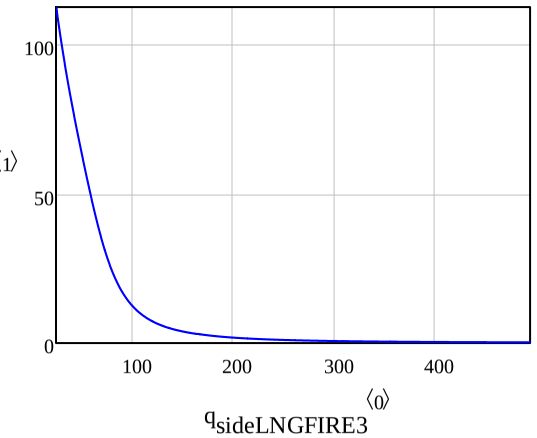

$q_{frontLNGFIRE3} =$

	0	1	2	3
0	23.829	112.604	-6.093	112.604
1	24.065	112.604	24.065	112.604
2	24.301	112.018	24.065	…

$q_{sideLNGFIRE3} =$

	0	1	2	3
0	23.829	112.604	-6.093	112.6
1	24.065	112.604	24.065	112.6
2	24.301	112.018	24.065	

$x_{min} := \min\left(q_{frontLNGFIRE3}^{\langle 0 \rangle}\right) m = 23.829\,m$

$x_{qmax} := \max\left(q_{frontLNGFIRE3}^{\langle 2 \rangle}\right) m = 24.065\,m$

$q_{max} := \max\left(q_{frontLNGFIRE3}^{\langle 3 \rangle}\right) \frac{kW}{m^2} = 112.604 \cdot \frac{kW}{m^2}$

$x_{smin} := \min\left(q_{sideLNGFIRE3}^{\langle 0 \rangle}\right) m = 23.829\,m$

$x_{sqmax} := \max\left(q_{sideLNGFIRE3}^{\langle 2 \rangle}\right) m = 24.065\,m$

$q_{smax} := \max\left(q_{sideLNGFIRE3}^{\langle 3 \rangle}\right) \frac{kW}{m^2} = 112.604 \cdot \frac{kW}{m^2}$

Determine the thermal flux level(s) at distances of the concern

$X_{loc1} := 105m$

$$I_{th.front.LNGFIRE3}\left(X_{loc1} + \frac{d}{2} - \frac{DR_{frontLNGFIRE3} \cdot d}{2}\right) = 15.206 \cdot \frac{kW}{m^2} \qquad I_{th.front.Sandia}\left(X_{loc1} + \frac{d}{2} - \frac{DR_{frontLNGFIRE3} \cdot d}{2}\right) = 48.54 \cdot \frac{kW}{m^2}$$

$$I_{th.side.LNGFIRE3}\left(X_{loc1} + \frac{d}{2} - \frac{DR_{sideLNGFIRE3} \cdot d}{2}\right) = 15.206 \cdot \frac{kW}{m^2} \qquad I_{th.side.Sandia}\left(X_{loc1} + \frac{d}{2} - \frac{DR_{sideLNGFIRE3} \cdot d}{2}\right) = 48.54 \cdot \frac{kW}{m^2}$$

$$I_{th.front.LNGFIRE3}\left(X_{loc1} - DR_{frontLNGFIRE3} \cdot w + \frac{w}{2}\right) = 13.179 \cdot \frac{kW}{m^2} \qquad I_{th.front.Sandia}\left(X_{loc1} - DR_{frontLNGFIRE3} \cdot w + \frac{w}{2}\right) = 44.684 \cdot \frac{kW}{m^2}$$

$$I_{th.side.LNGFIRE3}\left(X_{loc1} - DR_{sideLNGFIRE3} \cdot l + \frac{l}{2}\right) = 24.318 \cdot \frac{kW}{m^2} \qquad I_{th.side.Sandia}\left(X_{loc1} - DR_{sideLNGFIRE3} \cdot l + \frac{l}{2}\right) = 61.751 \cdot \frac{kW}{m^2}$$

$$I_{th.front.Montoir}\left(X_{loc1} + \frac{d}{2} - \frac{DR_{frontLNGFIRE3} \cdot d}{2}\right) = 44.096 \cdot \frac{kW}{m^2} \qquad I_{th.front.FERC}\left(X_{loc1} + \frac{d}{2} - \frac{DR_{frontFERC} \cdot d}{2}\right) = 16.281 \cdot \frac{kW}{m^2}$$

$$I_{th.side.Montoir}\left(X_{loc1} + \frac{d}{2} - \frac{DR_{sideLNGFIRE3} \cdot d}{2}\right) = 44.096 \cdot \frac{kW}{m^2} \qquad I_{th.side.FERC}\left(X_{loc1} + \frac{d}{2} - \frac{DR_{sideFERC} \cdot d}{2}\right) = 16.281 \cdot \frac{kW}{m^2}$$

$$I_{th.front.Montoir}\left(X_{loc1} - DR_{frontLNGFIRE3} \cdot w + \frac{w}{2}\right) = 40.338 \cdot \frac{kW}{m^2} \qquad I_{th.front.FERC}\left(X_{loc1} - DR_{frontFERC} \cdot w + \frac{w}{2}\right) = 14.433 \cdot \frac{kW}{m^2}$$

$$I_{th.side.Montoir}\left(X_{loc1} - DR_{sideLNGFIRE3} \cdot l + \frac{l}{2}\right) = 56.992 \cdot \frac{kW}{m^2} \qquad I_{th.side.FERC}\left(X_{loc1} - DR_{sideFERC} \cdot l + \frac{l}{2}\right) = 23.245 \cdot \frac{kW}{m^2}$$

$X_{loc2} := 135m$

$$I_{th.front.LNGFIRE3}\left(X_{loc2} + \frac{d}{2} - \frac{DR_{frontLNGFIRE3}\cdot d}{2}\right) = 6.638\cdot\frac{kW}{m^2} \qquad I_{th.front.Sandia}\left(X_{loc2} + \frac{d}{2} - \frac{DR_{frontLNGFIRE3}\cdot d}{2}\right) = 27.3\cdot\frac{kW}{m^2}$$

$$I_{th.side.LNGFIRE3}\left(X_{loc2} + \frac{d}{2} - \frac{DR_{frontLNGFIRE3}\cdot d}{2}\right) = 6.638\cdot\frac{kW}{m^2} \qquad I_{th.side.Sandia}\left(X_{loc2} + \frac{d}{2} - \frac{DR_{frontLNGFIRE3}\cdot d}{2}\right) = 27.305\cdot\frac{kW}{m^2}$$

$$I_{th.front.LNGFIRE3}\left(X_{loc2} - DR_{frontLNGFIRE3}\cdot w + \frac{w}{2}\right) = 5.978\cdot\frac{kW}{m^2} \qquad I_{th.front.Sandia}\left(X_{loc2} - DR_{frontLNGFIRE3}\cdot w + \frac{w}{2}\right) = 24.931\cdot\frac{kW}{m^2}$$

$$I_{th.side.LNGFIRE3}\left(X_{loc2} - DR_{sideLNGFIRE3}\cdot l + \frac{l}{2}\right) = 9.428\cdot\frac{kW}{m^2} \qquad I_{th.side.Sandia}\left(X_{loc2} - DR_{sideLNGFIRE3}\cdot l + \frac{l}{2}\right) = 35.898\cdot\frac{kW}{m^2}$$

$$I_{th.front.Montoir}\left(X_{loc2} + \frac{d}{2} - \frac{DR_{frontLNGFIRE3}\cdot d}{2}\right) = 23.8\cdot\frac{kW}{m^2} \qquad I_{th.front.FERC}\left(X_{loc2} + \frac{d}{2} - \frac{DR_{frontFERC}\cdot d}{2}\right) = 7.56\cdot\frac{kW}{m^2}$$

$$I_{th.side.Montoir}\left(X_{loc2} + \frac{d}{2} - \frac{DR_{frontLNGFIRE3}\cdot d}{2}\right) = 23.801\cdot\frac{kW}{m^2} \qquad I_{th.side.FERC}\left(X_{loc2} + \frac{d}{2} - \frac{DR_{sideFERC}\cdot d}{2}\right) = 7.56\cdot\frac{kW}{m^2}$$

$$I_{th.front.Montoir}\left(X_{loc2} - DR_{frontLNGFIRE3}\cdot w + \frac{w}{2}\right) = 21.623\cdot\frac{kW}{m^2} \qquad I_{th.front.FERC}\left(X_{loc2} - DR_{frontFERC}\cdot w + \frac{w}{2}\right) = 6.792\cdot\frac{kW}{m^2}$$

$$I_{th.side.Montoir}\left(X_{loc2} - DR_{sideLNGFIRE3}\cdot l + \frac{l}{2}\right) = 31.868\cdot\frac{kW}{m^2} \qquad I_{th.side.FERC}\left(X_{loc2} - DR_{sideFERC}\cdot l + \frac{l}{2}\right) = 10.658\cdot\frac{kW}{m^2}$$

$X_{loc3} := 100m$

$$I_{th.front.LNGFIRE3}\left(X_{loc3} + \frac{d}{2} - \frac{DR_{frontLNGFIRE3} \cdot d}{2}\right) = 17.916 \cdot \frac{kW}{m^2} \qquad I_{th.front.Sandia}\left(X_{loc3} + \frac{d}{2} - \frac{DR_{frontLNGFIRE3} \cdot d}{2}\right) = 53.03 \cdot \frac{kW}{m^2}$$

$$I_{th.side.LNGFIRE3}\left(X_{loc3} + \frac{d}{2} - \frac{DR_{frontLNGFIRE3} \cdot d}{2}\right) = 17.916 \cdot \frac{kW}{m^2} \qquad I_{th.side.Sandia}\left(X_{loc3} + \frac{d}{2} - \frac{DR_{frontLNGFIRE3} \cdot d}{2}\right) = 53.035 \cdot \frac{kW}{m^2}$$

$$I_{th.front.LNGFIRE3}\left(X_{loc3} - DR_{frontLNGFIRE3} \cdot w + \frac{w}{2}\right) = 15.424 \cdot \frac{kW}{m^2} \qquad I_{th.front.Sandia}\left(X_{loc3} - DR_{frontLNGFIRE3} \cdot w + \frac{w}{2}\right) = 48.926 \cdot \frac{kW}{m^2}$$

$$I_{th.side.LNGFIRE3}\left(X_{loc3} - DR_{sideLNGFIRE3} \cdot l + \frac{l}{2}\right) = 29.022 \cdot \frac{kW}{m^2} \qquad I_{th.side.Sandia}\left(X_{loc3} - DR_{sideLNGFIRE3} \cdot l + \frac{l}{2}\right) = 67.165 \cdot \frac{kW}{m^2}$$

$$I_{th.front.Montoir}\left(X_{loc3} + \frac{d}{2} - \frac{DR_{frontLNGFIRE3} \cdot d}{2}\right) = 48.49 \cdot \frac{kW}{m^2} \qquad I_{th.front.FERC}\left(X_{loc3} + \frac{d}{2} - \frac{DR_{frontFERC} \cdot d}{2}\right) = 18.561 \cdot \frac{kW}{m^2}$$

$$I_{th.side.Montoir}\left(X_{loc3} + \frac{d}{2} - \frac{DR_{frontLNGFIRE3} \cdot d}{2}\right) = 48.487 \cdot \frac{kW}{m^2} \qquad I_{th.side.FERC}\left(X_{loc3} + \frac{d}{2} - \frac{DR_{sideFERC} \cdot d}{2}\right) = 18.561 \cdot \frac{kW}{m^2}$$

$$I_{th.front.Montoir}\left(X_{loc3} - DR_{frontLNGFIRE3} \cdot w + \frac{w}{2}\right) = 44.473 \cdot \frac{kW}{m^2} \qquad I_{th.front.FERC}\left(X_{loc3} - DR_{frontFERC} \cdot w + \frac{w}{2}\right) = 16.472 \cdot \frac{kW}{m^2}$$

$$I_{th.side.Montoir}\left(X_{loc3} - DR_{sideLNGFIRE3} \cdot l + \frac{l}{2}\right) = 62.246 \cdot \frac{kW}{m^2} \qquad I_{th.side.FERC}\left(X_{loc3} - DR_{sideFERC} \cdot l + \frac{l}{2}\right) = 26.226 \cdot \frac{kW}{m^2}$$

$X_{loc4} := 155m$

$$I_{th.front.LNGFIRE3}\left(X_{loc4} + \frac{d}{2} - \frac{DR_{frontLNGFIRE3} \cdot d}{2}\right) = 4.329 \cdot \frac{kW}{m^2} \qquad I_{th.front.Sandia}\left(X_{loc4} + \frac{d}{2} - \frac{DR_{frontLNGFIRE3} \cdot d}{2}\right) = 18.392 \cdot \frac{kW}{m^2}$$

$$I_{th.side.LNGFIRE3}\left(X_{loc4} + \frac{d}{2} - \frac{DR_{frontLNGFIRE3} \cdot d}{2}\right) = 4.329 \cdot \frac{kW}{m^2} \qquad I_{th.side.Sandia}\left(X_{loc4} + \frac{d}{2} - \frac{DR_{frontLNGFIRE3} \cdot d}{2}\right) = 18.392 \cdot \frac{kW}{m^2}$$

$$I_{th.front.LNGFIRE3}\left(X_{loc4} - DR_{frontLNGFIRE3} \cdot w + \frac{w}{2}\right) = 3.969 \cdot \frac{kW}{m^2} \qquad I_{th.front.Sandia}\left(X_{loc4} - DR_{frontLNGFIRE3} \cdot w + \frac{w}{2}\right) = 16.853 \cdot \frac{kW}{m^2}$$

$$I_{th.side.LNGFIRE3}\left(X_{loc4} - DR_{sideLNGFIRE3} \cdot l + \frac{l}{2}\right) = 5.771 \cdot \frac{kW}{m^2} \qquad I_{th.side.Sandia}\left(X_{loc4} - DR_{sideLNGFIRE3} \cdot l + \frac{l}{2}\right) = 24.16 \cdot \frac{kW}{m^2}$$

$$I_{th.front.Montoir}\left(X_{loc4} + \frac{d}{2} - \frac{DR_{frontLNGFIRE3} \cdot d}{2}\right) = 15.746 \cdot \frac{kW}{m^2} \qquad I_{th.front.FERC}\left(X_{loc4} + \frac{d}{2} - \frac{DR_{frontFERC} \cdot d}{2}\right) = 4.851 \cdot \frac{kW}{m^2}$$

$$I_{th.side.Montoir}\left(X_{loc4} + \frac{d}{2} - \frac{DR_{frontLNGFIRE3} \cdot d}{2}\right) = 15.746 \cdot \frac{kW}{m^2} \qquad I_{th.side.FERC}\left(X_{loc4} + \frac{d}{2} - \frac{DR_{sideFERC} \cdot d}{2}\right) = 4.851 \cdot \frac{kW}{m^2}$$

$$I_{th.front.Montoir}\left(X_{loc4} - DR_{frontLNGFIRE3} \cdot w + \frac{w}{2}\right) = 14.389 \cdot \frac{kW}{m^2} \qquad I_{th.front.FERC}\left(X_{loc4} - DR_{frontFERC} \cdot w + \frac{w}{2}\right) = 4.424 \cdot \frac{kW}{m^2}$$

$$I_{th.side.Montoir}\left(X_{loc4} - DR_{sideLNGFIRE3} \cdot l + \frac{l}{2}\right) = 20.919 \cdot \frac{kW}{m^2} \qquad I_{th.side.FERC}\left(X_{loc4} - DR_{sideFERC} \cdot l + \frac{l}{2}\right) = 6.55 \cdot \frac{kW}{m^2}$$

$X_{loc5} := 125m$

$$I_{th.front.LNGFIRE3}\left(X_{loc5} + \frac{d}{2} - \frac{DR_{frontLNGFIRE3} \cdot d}{2}\right) = 8.505 \cdot \frac{kW}{m^2}$$

$$I_{th.front.Sandia}\left(X_{loc5} + \frac{d}{2} - \frac{DR_{frontLNGFIRE3} \cdot d}{2}\right) = 33.291 \cdot \frac{kW}{m^2}$$

$$I_{th.side.LNGFIRE3}\left(X_{loc5} + \frac{d}{2} - \frac{DR_{frontLNGFIRE3} \cdot d}{2}\right) = 8.51 \cdot \frac{kW}{m^2}$$

$$I_{th.side.Sandia}\left(X_{loc5} + \frac{d}{2} - \frac{DR_{frontLNGFIRE3} \cdot d}{2}\right) = 33.291 \cdot \frac{kW}{m^2}$$

$$I_{th.front.LNGFIRE3}\left(X_{loc5} - DR_{frontLNGFIRE3} \cdot w + \frac{w}{2}\right) = 7.573 \cdot \frac{kW}{m^2}$$

$$I_{th.front.Sandia}\left(X_{loc5} - DR_{frontLNGFIRE3} \cdot w + \frac{w}{2}\right) = 30.427 \cdot \frac{kW}{m^2}$$

$$I_{th.side.LNGFIRE3}\left(X_{loc5} - DR_{sideLNGFIRE3} \cdot l + \frac{l}{2}\right) = 12.561 \cdot \frac{kW}{m^2}$$

$$I_{th.side.Sandia}\left(X_{loc5} - DR_{sideLNGFIRE3} \cdot l + \frac{l}{2}\right) = 43.401 \cdot \frac{kW}{m^2}$$

$$I_{th.front.Montoir}\left(X_{loc5} + \frac{d}{2} - \frac{DR_{frontLNGFIRE3} \cdot d}{2}\right) = 29.393 \cdot \frac{kW}{m^2}$$

$$I_{th.front.FERC}\left(X_{loc5} + \frac{d}{2} - \frac{DR_{frontFERC} \cdot d}{2}\right) = 9.658 \cdot \frac{kW}{m^2}$$

$$I_{th.side.Montoir}\left(X_{loc5} + \frac{d}{2} - \frac{DR_{frontLNGFIRE3} \cdot d}{2}\right) = 29.393 \cdot \frac{kW}{m^2}$$

$$I_{th.side.FERC}\left(X_{loc5} + \frac{d}{2} - \frac{DR_{sideFERC} \cdot d}{2}\right) = 9.658 \cdot \frac{kW}{m^2}$$

$$I_{th.front.Montoir}\left(X_{loc5} - DR_{frontLNGFIRE3} \cdot w + \frac{w}{2}\right) = 26.701 \cdot \frac{kW}{m^2}$$

$$I_{th.front.FERC}\left(X_{loc5} - DR_{frontFERC} \cdot w + \frac{w}{2}\right) = 8.62 \cdot \frac{kW}{m^2}$$

$$I_{th.side.Montoir}\left(X_{loc5} - DR_{sideLNGFIRE3} \cdot l + \frac{l}{2}\right) = 39.092 \cdot \frac{kW}{m^2}$$

$$I_{th.side.FERC}\left(X_{loc5} - DR_{sideFERC} \cdot l + \frac{l}{2}\right) = 13.843 \cdot \frac{kW}{m^2}$$

$X_{loc6} := 75m$

$$I_{th.front.LNGFIRE3}\left(X_{loc6} + \frac{d}{2} - \frac{DR_{frontLNGFIRE3} \cdot d}{2}\right) = 42.56 \cdot \frac{kW}{m^2} \qquad I_{th.front.Sandia}\left(X_{loc6} + \frac{d}{2} - \frac{DR_{frontLNGFIRE3} \cdot d}{2}\right) = 81.008 \cdot \frac{kW}{m^2}$$

$$I_{th.side.LNGFIRE3}\left(X_{loc6} + \frac{d}{2} - \frac{DR_{frontLNGFIRE3} \cdot d}{2}\right) = 42.56 \cdot \frac{kW}{m^2} \qquad I_{th.side.Sandia}\left(X_{loc6} + \frac{d}{2} - \frac{DR_{frontLNGFIRE3} \cdot d}{2}\right) = 81.008 \cdot \frac{kW}{m^2}$$

$$I_{th.front.LNGFIRE3}\left(X_{loc6} - DR_{frontLNGFIRE3} \cdot w + \frac{w}{2}\right) = 36.529 \cdot \frac{kW}{m^2} \qquad I_{th.front.Sandia}\left(X_{loc6} - DR_{frontLNGFIRE3} \cdot w + \frac{w}{2}\right) = 74.993 \cdot \frac{kW}{m^2}$$

$$I_{th.side.LNGFIRE3}\left(X_{loc6} - DR_{sideLNGFIRE3} \cdot l + \frac{l}{2}\right) = 63.723 \cdot \frac{kW}{m^2} \qquad I_{th.side.Sandia}\left(X_{loc6} - DR_{sideLNGFIRE3} \cdot l + \frac{l}{2}\right) = 103.75 \cdot \frac{kW}{m^2}$$

$$I_{th.front.Montoir}\left(X_{loc6} + \frac{d}{2} - \frac{DR_{frontLNGFIRE3} \cdot d}{2}\right) = 75.538 \cdot \frac{kW}{m^2} \qquad I_{th.front.FERC}\left(X_{loc6} + \frac{d}{2} - \frac{DR_{frontFERC} \cdot d}{2}\right) = 33.688 \cdot \frac{kW}{m^2}$$

$$I_{th.side.Montoir}\left(X_{loc6} + \frac{d}{2} - \frac{DR_{frontLNGFIRE3} \cdot d}{2}\right) = 75.538 \cdot \frac{kW}{m^2} \qquad I_{th.side.FERC}\left(X_{loc6} + \frac{d}{2} - \frac{DR_{sideFERC} \cdot d}{2}\right) = 33.688 \cdot \frac{kW}{m^2}$$

$$I_{th.front.Montoir}\left(X_{loc6} - DR_{frontLNGFIRE3} \cdot w + \frac{w}{2}\right) = 69.786 \cdot \frac{kW}{m^2} \qquad I_{th.front.FERC}\left(X_{loc6} - DR_{frontFERC} \cdot w + \frac{w}{2}\right) = 30.496 \cdot \frac{kW}{m^2}$$

$$I_{th.side.Montoir}\left(X_{loc6} - DR_{sideLNGFIRE3} \cdot l + \frac{l}{2}\right) = 97.034 \cdot \frac{kW}{m^2} \qquad I_{th.side.FERC}\left(X_{loc6} - DR_{sideFERC} \cdot l + \frac{l}{2}\right) = 44.968 \cdot \frac{kW}{m^2}$$

$X_{loc7} := 190m$

$$I_{th.front.LNGFIRE3}\left(X_{loc7} + \frac{d}{2} - \frac{DR_{frontLNGFIRE3} \cdot d}{2}\right) = 2.414 \cdot \frac{kW}{m^2} \qquad I_{th.front.Sandia}\left(X_{loc7} + \frac{d}{2} - \frac{DR_{frontLNGFIRE3} \cdot d}{2}\right) = 9.822 \cdot \frac{kW}{m^2}$$

$$I_{th.side.LNGFIRE3}\left(X_{loc7} + \frac{d}{2} - \frac{DR_{frontLNGFIRE3} \cdot d}{2}\right) = 2.414 \cdot \frac{kW}{m^2} \qquad I_{th.side.Sandia}\left(X_{loc7} + \frac{d}{2} - \frac{DR_{frontLNGFIRE3} \cdot d}{2}\right) = 9.822 \cdot \frac{kW}{m^2}$$

$$I_{th.front.LNGFIRE3}\left(X_{loc7} - DR_{frontLNGFIRE3} \cdot w + \frac{w}{2}\right) = 2.253 \cdot \frac{kW}{m^2} \qquad I_{th.front.Sandia}\left(X_{loc7} - DR_{frontLNGFIRE3} \cdot w + \frac{w}{2}\right) = 9.124 \cdot \frac{kW}{m^2}$$

$$I_{th.side.LNGFIRE3}\left(X_{loc7} - DR_{sideLNGFIRE3} \cdot l + \frac{l}{2}\right) = 3.021 \cdot \frac{kW}{m^2} \qquad I_{th.side.Sandia}\left(X_{loc7} - DR_{sideLNGFIRE3} \cdot l + \frac{l}{2}\right) = 12.433 \cdot \frac{kW}{m^2}$$

$$I_{th.front.Montoir}\left(X_{loc7} + \frac{d}{2} - \frac{DR_{frontLNGFIRE3} \cdot d}{2}\right) = 8.312 \cdot \frac{kW}{m^2} \qquad I_{th.front.FERC}\left(X_{loc7} + \frac{d}{2} - \frac{DR_{frontFERC} \cdot d}{2}\right) = 2.58 \cdot \frac{kW}{m^2}$$

$$I_{th.side.Montoir}\left(X_{loc7} + \frac{d}{2} - \frac{DR_{frontLNGFIRE3} \cdot d}{2}\right) = 8.312 \cdot \frac{kW}{m^2} \qquad I_{th.side.FERC}\left(X_{loc7} + \frac{d}{2} - \frac{DR_{sideFERC} \cdot d}{2}\right) = 2.58 \cdot \frac{kW}{m^2}$$

$$I_{th.front.Montoir}\left(X_{loc7} - DR_{frontLNGFIRE3} \cdot w + \frac{w}{2}\right) = 7.718 \cdot \frac{kW}{m^2} \qquad I_{th.front.FERC}\left(X_{loc7} - DR_{frontFERC} \cdot w + \frac{w}{2}\right) = 2.398 \cdot \frac{kW}{m^2}$$

$$I_{th.side.Montoir}\left(X_{loc7} - DR_{sideLNGFIRE3} \cdot l + \frac{l}{2}\right) = 10.547 \cdot \frac{kW}{m^2} \qquad I_{th.side.FERC}\left(X_{loc7} - DR_{sideFERC} \cdot l + \frac{l}{2}\right) = 3.247 \cdot \frac{kW}{m^2}$$

$X_{loc8} := 180m$

$$I_{th.front.LNGFIRE3}\left(X_{loc8} + \frac{d}{2} - \frac{DR_{frontLNGFIRE3} \cdot d}{2}\right) = 2.831 \cdot \frac{kW}{m^2} \qquad I_{th.front.Sandia}\left(X_{loc8} + \frac{d}{2} - \frac{DR_{frontLNGFIRE3} \cdot d}{2}\right) = 11.622 \cdot \frac{kW}{m^2}$$

$$I_{th.side.LNGFIRE3}\left(X_{loc8} + \frac{d}{2} - \frac{DR_{frontLNGFIRE3} \cdot d}{2}\right) = 2.831 \cdot \frac{kW}{m^2} \qquad I_{th.side.Sandia}\left(X_{loc8} + \frac{d}{2} - \frac{DR_{frontLNGFIRE3} \cdot d}{2}\right) = 11.622 \cdot \frac{kW}{m^2}$$

$$I_{th.front.LNGFIRE3}\left(X_{loc8} - DR_{frontLNGFIRE3} \cdot w + \frac{w}{2}\right) = 2.629 \cdot \frac{kW}{m^2} \qquad I_{th.front.Sandia}\left(X_{loc8} - DR_{frontLNGFIRE3} \cdot w + \frac{w}{2}\right) = 10.751 \cdot \frac{kW}{m^2}$$

$$I_{th.side.LNGFIRE3}\left(X_{loc8} - DR_{sideLNGFIRE3} \cdot l + \frac{l}{2}\right) = 3.522 \cdot \frac{kW}{m^2} \qquad I_{th.side.Sandia}\left(X_{loc8} - DR_{sideLNGFIRE3} \cdot l + \frac{l}{2}\right) = 14.896 \cdot \frac{kW}{m^2}$$

$$I_{th.front.Montoir}\left(X_{loc8} + \frac{d}{2} - \frac{DR_{frontLNGFIRE3} \cdot d}{2}\right) = 9.85 \cdot \frac{kW}{m^2} \qquad I_{th.front.FERC}\left(X_{loc8} + \frac{d}{2} - \frac{DR_{frontFERC} \cdot d}{2}\right) = 3.037 \cdot \frac{kW}{m^2}$$

$$I_{th.side.Montoir}\left(X_{loc8} + \frac{d}{2} - \frac{DR_{frontLNGFIRE3} \cdot d}{2}\right) = 9.85 \cdot \frac{kW}{m^2} \qquad I_{th.side.FERC}\left(X_{loc8} + \frac{d}{2} - \frac{DR_{sideFERC} \cdot d}{2}\right) = 3.037 \cdot \frac{kW}{m^2}$$

$$I_{th.front.Montoir}\left(X_{loc8} - DR_{frontLNGFIRE3} \cdot w + \frac{w}{2}\right) = 9.105 \cdot \frac{kW}{m^2} \qquad I_{th.front.FERC}\left(X_{loc8} - DR_{frontFERC} \cdot w + \frac{w}{2}\right) = 2.813 \cdot \frac{kW}{m^2}$$

$$I_{th.side.Montoir}\left(X_{loc8} - DR_{sideLNGFIRE3} \cdot l + \frac{l}{2}\right) = 12.679 \cdot \frac{kW}{m^2} \qquad I_{th.side.FERC}\left(X_{loc8} - DR_{sideFERC} \cdot l + \frac{l}{2}\right) = 3.895 \cdot \frac{kW}{m^2}$$

$X_{loc9} := 115m$

$$I_{th.front.LNGFIRE3}\left(X_{loc9} + \frac{d}{2} - \frac{DR_{frontLNGFIRE3}\cdot d}{2}\right) = 11.202\cdot\frac{kW}{m^2} \qquad I_{th.front.Sandia}\left(X_{loc9} + \frac{d}{2} - \frac{DR_{frontLNGFIRE3}\cdot d}{2}\right) = 40.373\cdot\frac{kW}{m^2}$$

$$I_{th.side.LNGFIRE3}\left(X_{loc9} + \frac{d}{2} - \frac{DR_{frontLNGFIRE3}\cdot d}{2}\right) = 11.202\cdot\frac{kW}{m^2} \qquad I_{th.side.Sandia}\left(X_{loc9} + \frac{d}{2} - \frac{DR_{frontLNGFIRE3}\cdot d}{2}\right) = 40.373\cdot\frac{kW}{m^2}$$

$$I_{th.front.LNGFIRE3}\left(X_{loc9} - DR_{frontLNGFIRE3}\cdot w + \frac{w}{2}\right) = 9.845\cdot\frac{kW}{m^2} \qquad I_{th.front.Sandia}\left(X_{loc9} - DR_{frontLNGFIRE3}\cdot w + \frac{w}{2}\right) = 37.009\cdot\frac{kW}{m^2}$$

$$I_{th.side.LNGFIRE3}\left(X_{loc9} - DR_{sideLNGFIRE3}\cdot l + \frac{l}{2}\right) = 17.251\cdot\frac{kW}{m^2} \qquad I_{th.side.Sandia}\left(X_{loc9} - DR_{sideLNGFIRE3}\cdot l + \frac{l}{2}\right) = 51.989\cdot\frac{kW}{m^2}$$

$$I_{th.front.Montoir}\left(X_{loc9} + \frac{d}{2} - \frac{DR_{frontLNGFIRE3}\cdot d}{2}\right) = 36.161\cdot\frac{kW}{m^2} \qquad I_{th.front.FERC}\left(X_{loc9} + \frac{d}{2} - \frac{DR_{frontFERC}\cdot d}{2}\right) = 12.503\cdot\frac{kW}{m^2}$$

$$I_{th.side.Montoir}\left(X_{loc9} + \frac{d}{2} - \frac{DR_{frontLNGFIRE3}\cdot d}{2}\right) = 36.161\cdot\frac{kW}{m^2} \qquad I_{th.side.FERC}\left(X_{loc9} + \frac{d}{2} - \frac{DR_{sideFERC}\cdot d}{2}\right) = 12.503\cdot\frac{kW}{m^2}$$

$$I_{th.front.Montoir}\left(X_{loc9} - DR_{frontLNGFIRE3}\cdot w + \frac{w}{2}\right) = 32.93\cdot\frac{kW}{m^2} \qquad I_{th.front.FERC}\left(X_{loc9} - DR_{frontFERC}\cdot w + \frac{w}{2}\right) = 11.101\cdot\frac{kW}{m^2}$$

$$I_{th.side.Montoir}\left(X_{loc9} - DR_{sideLNGFIRE3}\cdot l + \frac{l}{2}\right) = 47.465\cdot\frac{kW}{m^2} \qquad I_{th.side.FERC}\left(X_{loc9} - DR_{sideFERC}\cdot l + \frac{l}{2}\right) = 18.02\cdot\frac{kW}{m^2}$$

$X_{loc10} := 100m$

$I_{th.front.LNGFIRE3}\left(X_{loc10} + \frac{d}{2} - \frac{DR_{frontLNGFIRE3} \cdot d}{2}\right) = 17.916 \cdot \frac{kW}{m^2}$ $I_{th.front.Sandia}\left(X_{loc10} + \frac{d}{2} - \frac{DR_{frontLNGFIRE3} \cdot d}{2}\right) = 53.035 \cdot \frac{kW}{m^2}$

$I_{th.side.LNGFIRE3}\left(X_{loc10} + \frac{d}{2} - \frac{DR_{frontLNGFIRE3} \cdot d}{2}\right) = 17.916 \cdot \frac{kW}{m^2}$ $I_{th.side.Sandia}\left(X_{loc10} + \frac{d}{2} - \frac{DR_{frontLNGFIRE3} \cdot d}{2}\right) = 53.035 \cdot \frac{kW}{m^2}$

$I_{th.front.LNGFIRE3}\left(X_{loc10} - DR_{frontLNGFIRE3} \cdot w + \frac{w}{2}\right) = 15.424 \cdot \frac{kW}{m^2}$ $I_{th.front.Sandia}\left(X_{loc10} - DR_{frontLNGFIRE3} \cdot w + \frac{w}{2}\right) = 48.926 \cdot \frac{kW}{m^2}$

$I_{th.side.LNGFIRE3}\left(X_{loc10} - DR_{sideLNGFIRE3} \cdot l + \frac{l}{2}\right) = 29.022 \cdot \frac{kW}{m^2}$ $I_{th.side.Sandia}\left(X_{loc10} - DR_{sideLNGFIRE3} \cdot l + \frac{l}{2}\right) = 67.165 \cdot \frac{kW}{m^2}$

$I_{th.front.Montoir}\left(X_{loc10} + \frac{d}{2} - \frac{DR_{frontLNGFIRE3} \cdot d}{2}\right) = 48.487 \cdot \frac{kW}{m^2}$ $I_{th.front.FERC}\left(X_{loc10} + \frac{d}{2} - \frac{DR_{frontFERC} \cdot d}{2}\right) = 18.561 \cdot \frac{kW}{m^2}$

$I_{th.side.Montoir}\left(X_{loc10} + \frac{d}{2} - \frac{DR_{frontLNGFIRE3} \cdot d}{2}\right) = 48.487 \cdot \frac{kW}{m^2}$ $I_{th.side.FERC}\left(X_{loc10} + \frac{d}{2} - \frac{DR_{sideFERC} \cdot d}{2}\right) = 18.561 \cdot \frac{kW}{m^2}$

$I_{th.front.Montoir}\left(X_{loc10} - DR_{frontLNGFIRE3} \cdot w + \frac{w}{2}\right) = 44.473 \cdot \frac{kW}{m^2}$ $I_{th.front.FERC}\left(X_{loc10} - DR_{frontFERC} \cdot w + \frac{w}{2}\right) = 16.472 \cdot \frac{kW}{m^2}$

$I_{th.side.Montoir}\left(X_{loc10} - DR_{sideLNGFIRE3} \cdot l + \frac{l}{2}\right) = 62.246 \cdot \frac{kW}{m^2}$ $I_{th.side.FERC}\left(X_{loc10} - DR_{sideFERC} \cdot l + \frac{l}{2}\right) = 26.226 \cdot \frac{kW}{m^2}$

Determine the distances to the thermal flux level(s) of concern

(initial guess) $x_{rf} := \begin{cases} x_{rf} \leftarrow x_{qmax} + \dfrac{DR_{frontLNGFIRE3} \cdot d}{3} & \text{if } p_s = 1 \\ x_{rf} \leftarrow x_{qmax} + \dfrac{DR_{frontLNGFIRE3} \cdot w}{9} & \text{if } p_s = 2 \\ x_{rf} \end{cases}$ $x_{rs} := \begin{cases} x_{rs} \leftarrow x_{sqmax} + \dfrac{DR_{sideLNGFIRE3} \cdot d}{3} & \text{if } p_s = 1 \\ x_{rs} \leftarrow x_{sqmax} + \dfrac{DR_{sideLNGFIRE3} \cdot l}{9} & \text{if } p_s = 2 \\ x_{rs} \end{cases}$

Determine the ground-level distances to the thermal flux level(s) of concern using maximum radius

$R_{loc.front}(I_{loc}) := root(I_{loc} - I_{th.front.LNGFIRE3}(x_{rf}), x_{rf})$

$R_{loc.side}(I_{loc}) := root(I_{loc} - I_{th.side.LNGFIRE3}(x_{rs}), x_{rs})$

$R_{loc.f.Montoir}(I_{loc}) := root(I_{loc} - I_{th.front.Montoir}(x_{rf}), x_{rf})$

$R_{loc.s.Montoir}(I_{loc}) := root(I_{loc} - I_{th.side.Montoir}(x_{rs}), x_{rs})$

$R_{loc.f.Sandia}(I_{loc}) := root(I_{loc} - I_{th.front.Sandia}(x_{rf}), x_{rf})$

$R_{loc.s.Sandia}(I_{loc}) := root(I_{loc} - I_{th.side.Sandia}(x_{rs}), x_{rs})$

$R_{loc.f.FERC}(I_{loc}) := root(I_{loc} - I_{th.front.FERC}(x_{rf}), x_{rf})$

$R_{loc.s.FERC}(I_{loc}) := root(I_{loc} - I_{th.side.FERC}(x_{rs}), x_{rs})$

Distances to the thermal flux levels of concern

31.5 kW/m² $I_{loc1} := 31.5 \cdot \frac{kW}{m^2}$ $I_{loc1} = 9985 \cdot \frac{BTU}{hr \cdot ft^2}$

$$R_{loc.front1} := \begin{cases} R_{loc.front}(I_{loc1}) + \left(\frac{DR_{frontLNGFIRE3} \cdot d}{2} - \frac{d}{2}\right) & \text{if } p_s = 1 \\ R_{loc.front}(I_{loc1}) + \left(DR_{frontLNGFIRE3} \cdot w - \frac{w}{2}\right) & \text{if } p_s = 2 \end{cases}$$

$$R_{loc.f.Sandia1} := \begin{cases} R_{loc.f.Sandia}(I_{loc1}) + \left(\frac{DR_{frontLNGFIRE3} \cdot d}{2} - \frac{d}{2}\right) & \text{if } p_s \\ R_{loc.f.Sandia}(I_{loc1}) + \left(DR_{frontLNGFIRE3} \cdot w - \frac{w}{2}\right) & \text{if } p_s \end{cases}$$

$$R_{loc.side1} := \begin{cases} R_{loc.side}(I_{loc1}) + \left(\frac{DR_{sideLNGFIRE3} \cdot d}{2} - \frac{d}{2}\right) & \text{if } p_s = 1 \\ R_{loc.side}(I_{loc1}) + \left(DR_{sideLNGFIRE3} \cdot l - \frac{l}{2}\right) & \text{if } p_s = 2 \end{cases}$$

$$R_{loc.s.Sandia1} := \begin{cases} R_{loc.s.Sandia}(I_{loc1}) + \left(\frac{DR_{sideLNGFIRE3} \cdot d}{2} - \frac{d}{2}\right) & \text{if } p_s \\ R_{loc.s.Sandia}(I_{loc1}) + \left(DR_{sideLNGFIRE3} \cdot l - \frac{l}{2}\right) & \text{if } p_s = \end{cases}$$

$R_{loc.front1} = 83.8 \cdot m$ $R_{loc.side1} = 83.8 \cdot m$

$R_{loc.f.Sandia1} = 128 \cdot m$ $R_{loc.s.Sandia1} = 128 \cdot m$

$$R_{loc.f.Montoir1} := \begin{cases} R_{loc.f.Montoir}(I_{loc1}) + \left(\frac{DR_{frontLNGFIRE3} \cdot d}{2} - \frac{d}{2}\right) & \text{if } p_s = 1 \\ R_{loc.f.Montoir}(I_{loc1}) + \left(DR_{frontLNGFIRE3} \cdot w - \frac{w}{2}\right) & \text{if } p_s = 2 \end{cases}$$

$$R_{loc.f.FERC1} := \begin{cases} R_{loc.f.FERC}(I_{loc1}) + \left(\frac{DR_{frontFERC} \cdot d}{2} - \frac{d}{2}\right) & \text{if } p_s \\ R_{loc.f.FERC}(I_{loc1}) + \left(DR_{frontFERC} \cdot w - \frac{w}{2}\right) & \text{if } p_s \end{cases}$$

$$R_{loc.s.Montoir1} := \begin{cases} R_{loc.s.Montoir}(I_{loc1}) + \left(\frac{DR_{sideLNGFIRE3} \cdot d}{2} - \frac{d}{2}\right) & \text{if } p_s = 1 \\ R_{loc.s.Montoir}(I_{loc1}) + \left(DR_{sideLNGFIRE3} \cdot l - \frac{l}{2}\right) & \text{if } p_s = 2 \end{cases}$$

$$R_{loc.s.FERC1} := \begin{cases} R_{loc.s.FERC}(I_{loc1}) + \left(\frac{DR_{sideFERC} \cdot d}{2} - \frac{d}{2}\right) & \text{if } p_s \\ R_{loc.s.FERC}(I_{loc1}) + \left(DR_{sideFERC} \cdot l - \frac{l}{2}\right) & \text{if } p_s = \end{cases}$$

$R_{loc.f.Montoir1} = 122 \cdot m$ $R_{loc.s.Montoir1} = 122 \cdot m$

$R_{loc.f.FERC1} = 78 \cdot m$ $R_{loc.s.FERC1} = 78 \cdot m$

21.1 kW/m² $I_{loc2} := 21.1 \cdot \frac{kW}{m^2}$ $I_{loc2} = 6689 \cdot \frac{BTU}{hr \cdot ft^2}$

$$R_{loc.front2} := \begin{cases} R_{loc.front}(I_{loc2}) + \left(\frac{DR_{frontLNGFIRE3} \cdot d}{2} - \frac{d}{2}\right) & \text{if } p_s = 1 \\ R_{loc.front}(I_{loc2}) + \left(DR_{frontLNGFIRE3} \cdot w - \frac{w}{2}\right) & \text{if } p_s = 2 \end{cases} \quad R_{loc.f.Sandia2} := \begin{cases} R_{loc.f.Sandia}(I_{loc2}) + \left(\frac{DR_{frontLNGFIRE3} \cdot d}{2} - \frac{d}{2}\right) & \text{if } p_s = \\ R_{loc.f.Sandia}(I_{loc2}) + \left(DR_{frontLNGFIRE3} \cdot w - \frac{w}{2}\right) & \text{if } p_s = \end{cases}$$

$$R_{loc.side2} := \begin{cases} R_{loc.side}(I_{loc2}) + \left(\frac{DR_{sideLNGFIRE3} \cdot d}{2} - \frac{d}{2}\right) & \text{if } p_s = 1 \\ R_{loc.side}(I_{loc2}) + \left(DR_{sideLNGFIRE3} \cdot l - \frac{l}{2}\right) & \text{if } p_s = 2 \end{cases} \quad R_{loc.s.Sandia2} := \begin{cases} R_{loc.s.Sandia}(I_{loc2}) + \left(\frac{DR_{sideLNGFIRE3} \cdot d}{2} - \frac{d}{2}\right) & \text{if } p_s = \\ R_{loc.s.Sandia}(I_{loc2}) + \left(DR_{sideLNGFIRE3} \cdot l - \frac{l}{2}\right) & \text{if } p_s = 2 \end{cases}$$

$R_{loc.front2} = 95.2 \cdot m$ $R_{loc.side2} = 95.2 \cdot m$ $R_{loc.f.Sandia2} = 148 \cdot m$ $R_{loc.s.Sandia2} = 148 \cdot m$

$$R_{loc.f.Montoir2} := \begin{cases} R_{loc.f.Montoir}(I_{loc2}) + \left(\frac{DR_{frontLNGFIRE3} \cdot d}{2} - \frac{d}{2}\right) \\ R_{loc.f.Montoir}(I_{loc2}) + \left(DR_{frontLNGFIRE3} \cdot w - \frac{w}{2}\right) \end{cases} \quad R_{loc.f.FERC2} := \begin{cases} R_{loc.f.FERC}(I_{loc2}) + \left(\frac{DR_{frontFERC} \cdot d}{2} - \frac{d}{2}\right) & \text{if } p_s = 1 \\ R_{loc.f.FERC}(I_{loc2}) + \left(DR_{frontFERC} \cdot w - \frac{w}{2}\right) & \text{if } p_s = 2 \end{cases}$$

$$R_{loc.s.Montoir2} := \begin{cases} R_{loc.s.Montoir}(I_{loc2}) + \left(\frac{DR_{sideLNGFIRE3} \cdot d}{2} - \frac{d}{2}\right) & \text{if } p_s = 1 \\ R_{loc.s.Montoir}(I_{loc2}) + \left(DR_{sideLNGFIRE3} \cdot l - \frac{l}{2}\right) & \text{if } p_s = 2 \end{cases} \quad \text{RC2} := \begin{cases} R_{loc.s.FERC}(I_{loc2}) + \left(\frac{DR_{sideFERC} \cdot d}{2} - \frac{d}{2}\right) & \text{if } p_s = 1 \\ R_{loc.s.FERC}(I_{loc2}) + \left(DR_{sideFERC} \cdot l - \frac{l}{2}\right) & \text{if } p_s = 2 \end{cases}$$

$R_{loc.f.Montoir2} = 141 \cdot m$ $R_{loc.s.Montoir2} = 141 \cdot m$ $R_{loc.f.FERC2} = 95 \cdot m$ $R_{loc.s.FERC2} = 95 \cdot m$

12.6 kW/m² $I_{loc3} := 12.6 \cdot \frac{kW}{m^2}$ $I_{loc3} = 3994 \cdot \frac{BTU}{hr \cdot ft^2}$

$$R_{loc.front3} := \begin{cases} R_{loc.front}(I_{loc3}) + \left(\frac{DR_{frontLNGFIRE3} \cdot d}{2} - \frac{d}{2}\right) & \text{if } p_s = 1 \\ R_{loc.front}(I_{loc3}) + \left(DR_{frontLNGFIRE3} \cdot w - \frac{w}{2}\right) & \text{if } p_s = 2 \end{cases} \quad R_{loc.f.Sandia3} := \begin{cases} R_{loc.f.Sandia}(I_{loc3}) + \left(\frac{DR_{frontLNGFIRE3} \cdot d}{2} - \frac{d}{2}\right) & \text{if } p_s \\ R_{loc.f.Sandia}(I_{loc3}) + \left(DR_{frontLNGFIRE3} \cdot w - \frac{w}{2}\right) & \text{if } p_s \end{cases}$$

$$R_{loc.side3} := \begin{cases} R_{loc.side}(I_{loc3}) + \left(\frac{DR_{sideLNGFIRE3} \cdot d}{2} - \frac{d}{2}\right) & \text{if } p_s = 1 \\ R_{loc.side}(I_{loc3}) + \left(DR_{sideLNGFIRE3} \cdot l - \frac{l}{2}\right) & \text{if } p_s = 2 \end{cases} \quad R_{loc.s.Sandia3} := \begin{cases} R_{loc.s.Sandia}(I_{loc3}) + \left(\frac{DR_{sideLNGFIRE3} \cdot d}{2} - \frac{d}{2}\right) & \text{if } p_s \\ R_{loc.s.Sandia}(I_{loc3}) + \left(DR_{sideLNGFIRE3} \cdot l - \frac{l}{2}\right) & \text{if } p_s = \end{cases}$$

$R_{loc.front3} = 111.0 \cdot m$ $R_{loc.side3} = 111.0 \cdot m$ $R_{loc.f.Sandia3} = 175 \cdot m$ $R_{loc.s.Sandia3} = 175 \cdot m$

$$R_{loc.f.Montoir3} := \begin{cases} R_{loc.f.Montoir}(I_{loc3}) + \left(\frac{DR_{frontLNGFIRE3} \cdot d}{2} - \frac{d}{2}\right) & \text{if } p_s \\ R_{loc.f.Montoir}(I_{loc3}) + \left(DR_{frontLNGFIRE3} \cdot w - \frac{w}{2}\right) & \text{if } p_s \end{cases} \quad R_{loc.f.FERC3} := \begin{cases} R_{loc.f.FERC}(I_{loc3}) + \left(\frac{DR_{frontFERC} \cdot d}{2} - \frac{d}{2}\right) & \text{if } p_s = \\ R_{loc.f.FERC}(I_{loc3}) + \left(DR_{frontFERC} \cdot w - \frac{w}{2}\right) & \text{if } p_s = \end{cases}$$

$$R_{loc.s.Montoir3} := \begin{cases} R_{loc.s.Montoir}(I_{loc3}) + \left(\frac{DR_{sideLNGFIRE3} \cdot d}{2} - \frac{d}{2}\right) & \text{if } p_s \\ R_{loc.s.Montoir}(I_{loc3}) + \left(DR_{sideLNGFIRE3} \cdot l - \frac{l}{2}\right) & \text{if } p_s = \end{cases} \quad R_{loc.s.FERC3} := \begin{cases} R_{loc.s.FERC}(I_{loc3}) + \left(\frac{DR_{sideFERC} \cdot d}{2} - \frac{d}{2}\right) & \text{if } p_s = \\ R_{loc.s.FERC}(I_{loc3}) + \left(DR_{sideFERC} \cdot l - \frac{l}{2}\right) & \text{if } p_s = 2 \end{cases}$$

$R_{loc.f.Montoir3} = 166 \cdot m$ $R_{loc.s.Montoir3} = 166 \cdot m$ $R_{loc.f.FERC3} = 115 \cdot m$ $R_{loc.s.FERC3} = 115 \cdot m$

5.0 kW/m²

$I_{loc4} := 5.05 \cdot \frac{kW}{m^2}$ $I_{loc4} = 1601 \cdot \frac{BTU}{hr \cdot ft^2}$

$$R_{loc.front4} := \begin{cases} R_{loc.front}(I_{loc4}) + \left(\frac{DR_{frontLNGFIRE3} \cdot d}{2} - \frac{d}{2}\right) & \text{if } p_s = 1 \\ R_{loc.front}(I_{loc4}) + \left(DR_{frontLNGFIRE3} \cdot w - \frac{w}{2}\right) & \text{if } p_s = 2 \end{cases}$$

$$R_{loc.f.Sandia4} := \begin{cases} R_{loc.f.Sandia}(I_{loc4}) + \left(\frac{DR_{frontLNGFIRE3} \cdot d}{2} - \frac{d}{2}\right) & \text{if } p_s \\ R_{loc.f.Sandia}(I_{loc4}) + \left(DR_{frontLNGFIRE3} \cdot w - \frac{w}{2}\right) & \text{if } p_s \end{cases}$$

$$R_{loc.side4} := \begin{cases} R_{loc.side}(I_{loc4}) + \left(\frac{DR_{sideLNGFIRE3} \cdot d}{2} - \frac{d}{2}\right) & \text{if } p_s = 1 \\ R_{loc.side}(I_{loc4}) + \left(DR_{sideLNGFIRE3} \cdot l - \frac{l}{2}\right) & \text{if } p_s = 2 \end{cases}$$

$$R_{loc.s.Sandia4} := \begin{cases} R_{loc.s.Sandia}(I_{loc4}) + \left(\frac{DR_{sideLNGFIRE3} \cdot d}{2} - \frac{d}{2}\right) & \text{if } p_s \\ R_{loc.s.Sandia}(I_{loc4}) + \left(DR_{sideLNGFIRE3} \cdot l - \frac{l}{2}\right) & \text{if } p_s = \end{cases}$$

$R_{loc.front4} = 147.3 \cdot m$ $R_{loc.side4} = 147.3 \cdot m$ $R_{loc.f.Sandia4} = 236 \cdot m$ $R_{loc.s.Sandia4} = 236 \cdot m$

$$R_{loc.f.Montoir4} := \begin{cases} R_{loc.f.Montoir}(I_{loc4}) + \left(\frac{DR_{frontLNGFIRE3} \cdot d}{2} - \frac{d}{2}\right) & \text{if } p \\ R_{loc.f.Montoir}(I_{loc4}) + \left(DR_{frontLNGFIRE3} \cdot w - \frac{w}{2}\right) & \text{if } p \end{cases}$$

$$R_{loc.f.FERC4} := \begin{cases} R_{loc.f.FERC}(I_{loc4}) + \left(\frac{DR_{frontFERC} \cdot d}{2} - \frac{d}{2}\right) & \text{if } p_s = 1 \\ R_{loc.f.FERC}(I_{loc4}) + \left(DR_{frontFERC} \cdot w - \frac{w}{2}\right) & \text{if } p_s = 2 \end{cases}$$

$$R_{loc.s.Montoir4} := \begin{cases} R_{loc.s.Montoir}(I_{loc4}) + \left(\frac{DR_{sideLNGFIRE3} \cdot d}{2} - \frac{d}{2}\right) & \text{if } p_s \\ R_{loc.s.Montoir}(I_{loc4}) + \left(DR_{sideLNGFIRE3} \cdot l - \frac{l}{2}\right) & \text{if } p_s \end{cases}$$

$$R_{loc.s.FERC4} := \begin{cases} R_{loc.s.FERC}(I_{loc4}) + \left(\frac{DR_{sideFERC} \cdot d}{2} - \frac{d}{2}\right) & \text{if } p_s = 1 \\ R_{loc.s.FERC}(I_{loc4}) + \left(DR_{sideFERC} \cdot l - \frac{l}{2}\right) & \text{if } p_s = 2 \end{cases}$$

$R_{loc.f.Montoir4} = 223 \cdot m$ $R_{loc.s.Montoir4} = 223 \cdot m$ $R_{loc.f.FERC4} = 153 \cdot m$ $R_{loc.s.FERC4} = 153 \cdot m$

10,000 BTU/hr/ft² $I_{loc7} := 10000 \cdot \frac{BTU}{hr \cdot ft^2}$ $I_{loc7} = 31.55 \cdot \frac{kW}{m^2}$

$$R_{loc.front7} := \begin{cases} R_{loc.front}(I_{loc7}) + \left(\frac{DR_{frontLNGFIRE3} \cdot d}{2} - \frac{d}{2}\right) & \text{if } p_s = 1 \\ R_{loc.front}(I_{loc7}) + \left(DR_{frontLNGFIRE3} \cdot w - \frac{w}{2}\right) & \text{if } p_s = 2 \end{cases} \quad R_{loc.f.Sandia7} := \begin{cases} R_{loc.f.Sandia}(I_{loc7}) + \left(\frac{DR_{frontLNGFIRE3} \cdot d}{2} - \frac{d}{2}\right) & \text{if } p_s = \\ R_{loc.f.Sandia}(I_{loc7}) + \left(DR_{frontLNGFIRE3} \cdot w - \frac{w}{2}\right) & \text{if } p_s = \end{cases}$$

$$R_{loc.side7} := \begin{cases} R_{loc.side}(I_{loc7}) + \left(\frac{DR_{sideLNGFIRE3} \cdot d}{2} - \frac{d}{2}\right) & \text{if } p_s = 1 \\ R_{loc.side}(I_{loc7}) + \left(DR_{sideLNGFIRE3} \cdot l - \frac{l}{2}\right) & \text{if } p_s = 2 \end{cases} \quad R_{loc.s.Sandia7} := \begin{cases} R_{loc.s.Sandia}(I_{loc7}) + \left(\frac{DR_{sideLNGFIRE3} \cdot d}{2} - \frac{d}{2}\right) & \text{if } p_s = \\ R_{loc.s.Sandia}(I_{loc7}) + \left(DR_{sideLNGFIRE3} \cdot l - \frac{l}{2}\right) & \text{if } p_s = 2 \end{cases}$$

$R_{loc.front7} = 275 \cdot ft$ $R_{loc.side7} = 275 \cdot ft$ $R_{loc.f.Sandia7} = 419 \cdot ft$ $R_{loc.s.Sandia7} = 419 \cdot ft$

$$R_{loc.f.Montoir7} := \begin{cases} R_{loc.f.Montoir}(I_{loc7}) + \left(\frac{DR_{frontLNGFIRE3} \cdot d}{2} - \frac{d}{2}\right) & \text{if } p \\ R_{loc.f.Montoir}(I_{loc7}) + \left(DR_{frontLNGFIRE3} \cdot w - \frac{w}{2}\right) & \text{if } p \end{cases} \quad R_{loc.f.FERC7} := \begin{cases} R_{loc.f.FERC}(I_{loc7}) + \left(\frac{DR_{frontFERC} \cdot d}{2} - \frac{d}{2}\right) & \text{if } p_s = 1 \\ R_{loc.f.FERC}(I_{loc7}) + \left(DR_{frontFERC} \cdot w - \frac{w}{2}\right) & \text{if } p_s = 2 \end{cases}$$

$$R_{loc.s.Montoir7} := \begin{cases} R_{loc.s.Montoir}(I_{loc7}) + \left(\frac{DR_{sideLNGFIRE3} \cdot d}{2} - \frac{d}{2}\right) & \text{if } p_s \\ R_{loc.s.Montoir}(I_{loc7}) + \left(DR_{sideLNGFIRE3} \cdot l - \frac{l}{2}\right) & \text{if } p_s : \end{cases} \quad R_{loc.s.FERC7} := \begin{cases} R_{loc.s.FERC}(I_{loc7}) + \left(\frac{DR_{sideFERC} \cdot d}{2} - \frac{d}{2}\right) & \text{if } p_s = 1 \\ R_{loc.s.FERC}(I_{loc7}) + \left(DR_{sideFERC} \cdot l - \frac{l}{2}\right) & \text{if } p_s = 2 \end{cases}$$

$R_{loc.f.Montoir7} = 399 \cdot ft$ $R_{loc.s.Montoir7} = 399 \cdot ft$ $R_{loc.f.FERC7} = 256 \cdot ft$ $R_{loc.s.FERC7} = 256 \cdot ft$

3,000 BTU/hr/ft^2 $I_{loc6} := 3000 \frac{BTU}{hr \cdot ft^2}$ $I_{loc6} = 9.46 \cdot \frac{kW}{m^2}$

$$R_{loc.front6} := \begin{cases} R_{loc.front}(I_{loc6}) + \left(\frac{DR_{frontLNGFIRE3} \cdot d}{2} - \frac{d}{2}\right) & \text{if } p_s = 1 \\ R_{loc.front}(I_{loc6}) + \left(DR_{frontLNGFIRE3} \cdot w - \frac{w}{2}\right) & \text{if } p_s = 2 \end{cases} \quad R_{loc.f.Sandia6} := \begin{cases} R_{loc.f.Sandia}(I_{loc6}) + \left(\frac{DR_{frontLNGFIRE3} \cdot d}{2} - \frac{d}{2}\right) & \text{if } p_s = \\ R_{loc.f.Sandia}(I_{loc6}) + \left(DR_{frontLNGFIRE3} \cdot w - \frac{w}{2}\right) & \text{if } p_s = \end{cases}$$

$$R_{loc.side6} := \begin{cases} R_{loc.side}(I_{loc6}) + \left(\frac{DR_{sideLNGFIRE3} \cdot d}{2} - \frac{d}{2}\right) & \text{if } p_s = 1 \\ R_{loc.side}(I_{loc6}) + \left(DR_{sideLNGFIRE3} \cdot l - \frac{l}{2}\right) & \text{if } p_s = 2 \end{cases} \quad R_{loc.s.Sandia6} := \begin{cases} R_{loc.s.Sandia}(I_{loc6}) + \left(\frac{DR_{sideLNGFIRE3} \cdot d}{2} - \frac{d}{2}\right) & \text{if } p_s = \\ R_{loc.s.Sandia}(I_{loc6}) + \left(DR_{sideLNGFIRE3} \cdot l - \frac{l}{2}\right) & \text{if } p_s = 2 \end{cases}$$

$R_{loc.front6} = 397 \cdot ft$ $R_{loc.side6} = 397 \cdot ft$ $R_{loc.f.Sandia6} = 631 \cdot ft$ $R_{loc.s.Sandia6} = 631 \cdot ft$

$$R_{loc.f.Montoir6} := \begin{cases} R_{loc.f.Montoir}(I_{loc6}) + \left(\frac{DR_{frontLNGFIRE3} \cdot d}{2} - \frac{d}{2}\right) & \text{if p} \\ R_{loc.f.Montoir}(I_{loc6}) + \left(DR_{frontLNGFIRE3} \cdot w - \frac{w}{2}\right) & \text{if p} \end{cases} \quad R_{loc.f.FERC6} := \begin{cases} R_{loc.f.FERC}(I_{loc6}) + \left(\frac{DR_{frontFERC} \cdot d}{2} - \frac{d}{2}\right) & \text{if } p_s = 1 \\ R_{loc.f.FERC}(I_{loc6}) + \left(DR_{frontFERC} \cdot w - \frac{w}{2}\right) & \text{if } p_s = 2 \end{cases}$$

$$R_{loc.s.Montoir6} := \begin{cases} R_{loc.s.Montoir}(I_{loc6}) + \left(\frac{DR_{sideLNGFIRE3} \cdot d}{2} - \frac{d}{2}\right) & \text{if } p_s = 1 \\ R_{loc.s.Montoir}(I_{loc6}) + \left(DR_{sideLNGFIRE3} \cdot l - \frac{l}{2}\right) & \text{if } p_s = 2 \end{cases} \quad \text{s.FERC6} := \begin{cases} R_{loc.s.FERC}(I_{loc6}) + \left(\frac{DR_{sideFERC} \cdot d}{2} - \frac{d}{2}\right) & \text{if } p_s = 1 \\ R_{loc.s.FERC}(I_{loc6}) + \left(DR_{sideFERC} \cdot l - \frac{l}{2}\right) & \text{if } p_s = 2 \end{cases}$$

$R_{loc.f.Montoir6} = 598 \cdot ft$ $R_{loc.s.Montoir6} = 598 \cdot ft$ $R_{loc.f.FERC6} = 413 \cdot ft$ $R_{loc.s.FERC6} = 413 \cdot ft$

1,600 BTU/hr/ft^2 $I_{loc5} := 1600 \cdot \frac{BTU}{hr \cdot ft^2}$ $I_{loc5} = 5.05 \cdot \frac{kW}{m^2}$

$$R_{loc.front5} := \begin{cases} R_{loc.front}(I_{loc5}) + \left(\frac{DR_{frontLNGFIRE3} \cdot d}{2} - \frac{d}{2}\right) & \text{if } p_s = 1 \\ R_{loc.front}(I_{loc5}) + \left(DR_{frontLNGFIRE3} \cdot w - \frac{w}{2}\right) & \text{if } p_s = 2 \end{cases} \quad R_{loc.f.Sandia5} := \begin{cases} R_{loc.f.Sandia}(I_{loc5}) + \left(\frac{DR_{frontLNGFIRE3} \cdot d}{2} - \frac{d}{2}\right) & \text{if } p_s = \\ R_{loc.f.Sandia}(I_{loc5}) + \left(DR_{frontLNGFIRE3} \cdot w - \frac{w}{2}\right) & \text{if } p_s = \end{cases}$$

$$R_{loc.side5} := \begin{cases} R_{loc.side}(I_{loc5}) + \left(\frac{DR_{sideLNGFIRE3} \cdot d}{2} - \frac{d}{2}\right) & \text{if } p_s = 1 \\ R_{loc.side}(I_{loc5}) + \left(DR_{sideLNGFIRE3} \cdot l - \frac{l}{2}\right) & \text{if } p_s = 2 \end{cases} \quad R_{loc.s.Sandia5} := \begin{cases} R_{loc.s.Sandia}(I_{loc5}) + \left(\frac{DR_{sideLNGFIRE3} \cdot d}{2} - \frac{d}{2}\right) & \text{if } p_s = \\ R_{loc.s.Sandia}(I_{loc5}) + \left(DR_{sideLNGFIRE3} \cdot l - \frac{l}{2}\right) & \text{if } p_s = 2 \end{cases}$$

$R_{loc.front5} = 484 \cdot ft$ $R_{loc.side5} = 484 \cdot ft$ $R_{loc.f.Sandia5} = 775 \cdot ft$ $R_{loc.s.Sandia5} = 775 \cdot ft$

$$R_{loc.f.Montoir5} := \begin{cases} R_{loc.f.Montoir}(I_{loc5}) + \left(\frac{DR_{frontLNGFIRE3} \cdot d}{2} - \frac{d}{2}\right) & \text{if } p_s = \\ R_{loc.f.Montoir}(I_{loc5}) + \left(DR_{frontLNGFIRE3} \cdot w - \frac{w}{2}\right) & \text{if } p_s = \end{cases} \quad R_{loc.f.FERC5} := \begin{cases} R_{loc.f.FERC}(I_{loc5}) + \left(\frac{DR_{frontFERC} \cdot d}{2} - \frac{d}{2}\right) & \text{if } p_s = \\ R_{loc.f.FERC}(I_{loc5}) + \left(DR_{frontFERC} \cdot w - \frac{w}{2}\right) & \text{if } p_s = \end{cases}$$

$$R_{loc.s.Montoir5} := \begin{cases} R_{loc.s.Montoir}(I_{loc5}) + \left(\frac{DR_{sideLNGFIRE3} \cdot d}{2} - \frac{d}{2}\right) & \text{if } p_s = \\ R_{loc.s.Montoir}(I_{loc5}) + \left(DR_{sideLNGFIRE3} \cdot l - \frac{l}{2}\right) & \text{if } p_s = 2 \end{cases} \quad R_{loc.s.FERC5} := \begin{cases} R_{loc.s.FERC}(I_{loc5}) + \left(\frac{DR_{sideFERC} \cdot d}{2} - \frac{d}{2}\right) & \text{if } p_s = \\ R_{loc.s.FERC}(I_{loc5}) + \left(DR_{sideFERC} \cdot l - \frac{l}{2}\right) & \text{if } p_s = \end{cases}$$

$R_{loc.f.Montoir5} = 733 \cdot ft$ $R_{loc.s.Montoir5} = 733 \cdot ft$ $R_{loc.f.FERC5} = 502 \cdot ft$ $R_{loc.s.FERC5} = 502 \cdot ft$

Summary of Inputs

Pool Fire Characteristics

Pool shape
(1 = circle 2 = semicircle)

$p_s = 1$

Pool dimensions

$d = 35\,m$

OR

$l = 23.53\,m$ $w = 1.81\,m$

Pool height

$Z_f = 0 \cdot m$

Target height

$Z_T = 0 \cdot m$

LNG Properties

Molecular Weight

$MW_{LNG} = 17 \cdot \frac{kg}{10^3 mol}$

Boiling Point

$T_b = -258.07 \cdot °F$

Heat of Combustion

$H_c = 50000 \cdot \frac{kJ}{kg}$

Flame Temperature

$T_{flame} = 1300 \cdot K$

Density of Liquid
(at T_b)

$\rho_l = 432 \frac{kg}{m^3}$

Ambient Conditions

Ambient air density $\rho_a = 1.197 \frac{kg}{m^3}$

Temperature $T_a = 69.8 \cdot °F$

Relative humidity $RH = 54 \cdot \%$

Wind speed $u_{wr} = 8.55 \cdot \frac{m}{s}$ $u_{wFERC}(Z_r) = 8.55 \cdot \frac{m}{s}$ $u_{wFERC}(Z_f + Z_r) = 8.55 \cdot \frac{m}{s}$ $u_{wFERC}(Z_r)$

Summary of Output and Calculations

Pool Fire Calculations

Burning rate

$$m_{bLNGFIRE3}\left(m_{bmaxLNGFIRE3}\right) = 0.11\,\frac{kg}{m^2 \cdot s}$$

$$m_{bLNGFIRE3}\left(m_{bmaxSandia}\right) = 0.15119998\,\frac{kg}{m^2 \cdot s}$$

$$\frac{m_{bLNGFIRE3}\left(m_{bmaxSandia}\right)}{m_{bLNGFIRE3}\left(m_{bmaxLNGFIRE3}\right)} - 1 = 37 \cdot \%$$

$$m_{bFERC}\left(m_{bmaxFERC}\right) = 0.13999999\,\frac{kg}{m^2 \cdot s}$$

$$\frac{m_{bFERC}\left(m_{bmaxFERC}\right)}{m_{bLNGFIRE3}\left(m_{bmaxLNGFIRE3}\right)} - 1 = 27 \cdot \%$$

Flame Height

$$L_f\left(d, m_{bLNGFIRE3}\left(m_{bmaxLNGFIRE3}\right)\right) = 57.75\,m$$

$$L_f\left(w, m_{bLNGFIRE3}\left(m_{bmaxLNGFIRE3}\right)\right) = 7.37\,m$$

$$L_{fSandia}\left(d, m_{bLNGFIRE3}\left(m_{bmaxSandia}\right)\right) = 107\,m$$

$$L_{fSandia}\left(w, m_{bLNGFIRE3}\left(m_{bmaxSandia}\right)\right) = 14.3 \cdot m$$

$$\frac{L_{fSandia}\left(d, m_{bLNGFIRE3}\left(m_{bmaxSandia}\right)\right)}{L_f\left(d, m_{bLNGFIRE3}\left(m_{bmaxLNGFIRE3}\right)\right)} - 1 = 85 \cdot \%$$

$$\frac{L_{fSandia}\left(w, m_{bLNGFIRE3}\left(m_{bmaxSandia}\right)\right)}{L_f\left(w, m_{bLNGFIRE3}\left(m_{bmaxLNGFIRE3}\right)\right)} - 1 = 94 \cdot \%$$

$$L_{fFERC}\left(d, m_{bFERC}\left(m_{bmaxFERC}\right)\right) = 79\,m$$

$$L_{fFERC}\left(w, m_{bFERC}\left(m_{bmaxFERC}\right)\right) = 10.5 \cdot m$$

$$\frac{L_{fFERC}\left(d, m_{bFERC}\left(m_{bmaxFERC}\right)\right)}{L_f\left(d, m_{bLNGFIRE3}\left(m_{bmaxLNGFIRE3}\right)\right)} - 1 = 37 \cdot \%$$

$$\frac{L_{fFERC}\left(w, m_{bFERC}\left(m_{bmaxFERC}\right)\right)}{L_f\left(w, m_{bLNGFIRE3}\left(m_{bmaxLNGFIRE3}\right)\right)} - 1 = 43 \cdot \%$$

Pool Fire Calculations (continued)

Flame Tilt

$\alpha_{frontLNGFIRE3}\left(m_{bLNGFIRE3}\left(m_{bmaxLNGFIRE3}\right)\right) = 55.59 \cdot deg$

$\alpha_{frontLNGFIRE3}\left(m_{bLNGFIRE3}\left(m_{bmaxMontoir}\right)\right) = 53.94 \cdot deg$

$\alpha_{sideLNGFIRE3}\left(m_{bLNGFIRE3}\left(m_{bmaxLNGFIRE3}\right)\right) = 55.59 \cdot deg$

$\alpha_{sideLNGFIRE3}\left(m_{bLNGFIRE3}\left(m_{bmaxMontoir}\right)\right) = 53.94 \cdot deg$

$\alpha_{frontLNGFIRE3}\left(m_{bLNGFIRE3}\left(m_{bmaxSandia}\right)\right) = 53.42 \cdot deg$

$\alpha_{frontFERC}\left(m_{bFERC}\left(m_{bmaxFERC}\right)\right) = 54 \cdot deg$

$\alpha_{sideLNGFIRE3}\left(m_{bLNGFIRE3}\left(m_{bmaxSandia}\right)\right) = 53 \cdot deg$

$\alpha_{sideFERC}\left(m_{bFERC}\left(m_{bmaxFERC}\right)\right) = 54 \cdot deg$

$\frac{\alpha_{frontLNGFIRE3}\left(m_{bLNGFIRE3}\left(m_{bmaxSandia}\right)\right)}{\alpha_{frontLNGFIRE3}\left(m_{bLNGFIRE3}\left(m_{bmaxLNGFIRE3}\right)\right)} - 1 = -4 \cdot \%$

$\frac{\alpha_{frontFERC}\left(m_{bFERC}\left(m_{bmaxFERC}\right)\right)}{\alpha_{sideLNGFIRE3}\left(m_{bLNGFIRE3}\left(m_{bmaxLNGFIRE3}\right)\right)} - 1 = -3 \cdot$

$\frac{\alpha_{sideLNGFIRE3}\left(m_{bLNGFIRE3}\left(m_{bmaxSandia}\right)\right)}{\alpha_{sideLNGFIRE3}\left(m_{bLNGFIRE3}\left(m_{bmaxLNGFIRE3}\right)\right)} - 1 = -4 \cdot \%$

$\frac{\alpha_{sideFERC}\left(m_{bFERC}\left(m_{bmaxFERC}\right)\right)}{\alpha_{sideLNGFIRE3}\left(m_{bLNGFIRE3}\left(m_{bmaxLNGFIRE3}\right)\right)} - 1 = -3 \cdot$

Flame drag

$DR_{frontLNGFIRE3} = 1.35$

$DR_{sideLNGFIRE3} = 1.348$

$DR_{frontFERC} = 1.35$

$DR_{sideFERC} = 1.348$

$\frac{DR_{frontFERC}}{DR_{frontLNGFIRE3}} - 1 = 0 \cdot \%$

$\frac{DR_{sideFERC}}{DR_{sideLNGFIRE3}} - 1 = 0 \cdot \%$

SEP

$$E_{s.frontLNGFIRE3}\left(E_{sLNGFIRE3}\right) = 190\cdot\frac{kW}{m^2}$$

$$E_{s.sideLNGFIRE3}\left(E_{sLNGFIRE3}\right) = 190\cdot\frac{kW}{m^2}$$

$$E_{s.frontLNGFIRE3}\left(E_{sMontoir}\right) = 265\cdot\frac{kW}{m^2}$$

$$E_{s.sideLNGFIRE3}\left(E_{sMontoir}\right) = 265\cdot\frac{kW}{m^2}$$

$$E_{s.frontFERC}\left(E_{sSandia}\right) = 286\cdot\frac{kW}{m^2}$$

$$E_{s.sideFERC}\left(E_{sSandia}\right) = 286\cdot\frac{kW}{m^2}$$

$$\frac{E_{s.frontFERC}\left(E_{sSandia}\right)}{E_{s.sideLNGFIRE3}\left(E_{sLNGFIRE3}\right)} - 1 = 51\cdot\%$$

$$\frac{E_{s.sideFERC}\left(E_{sSandia}\right)}{E_{s.sideLNGFIRE3}\left(E_{sLNGFIRE3}\right)} - 1 = 51\cdot\%$$

$$E_{s.frontFERC}\left(E_{sFit}\right) = 125\cdot\frac{kW}{m^2}$$

$$E_{s.sideFERC}\left(E_{sFit}\right) = 125\cdot\frac{kW}{m^2}$$

$$\frac{E_{s.frontFERC}\left(E_{sFit}\right)}{E_{s.sideLNGFIRE3}\left(E_{sLNGFIRE3}\right)} - 1 = -34\cdot\%$$

$$\frac{E_{s.sideFERC}\left(E_{sFit}\right)}{E_{s.sideLNGFIRE3}\left(E_{sLNGFIRE3}\right)} - 1 = -34\cdot\%$$

Hazard Distance Calculations

Distance to 10,000 BTU/hr-ft^2:

$R_{loc.front7} = 275 \cdot ft$

$R_{loc.side7} = 275 \cdot ft$

$R_{loc.f.Sandia7} = 419 \cdot ft$

$R_{loc.s.Sandia7} = 419 \cdot ft$

$\frac{R_{loc.f.Sandia7}}{R_{loc.front7}} - 1 = 52 \cdot \%$

$\frac{R_{loc.s.Sandia7}}{R_{loc.side7}} - 1 = 52 \cdot \%$

$R_{loc.f.FERC7} = 256 \cdot ft$

$R_{loc.s.FERC7} = 256 \cdot ft$

$\frac{R_{loc.f.FERC7}}{R_{loc.front7}} - 1 = -7 \cdot \%$

$\frac{R_{loc.s.FERC7}}{R_{loc.side7}} - 1 = -7 \cdot \%$

Distance to 3,000 BTU/hr-ft^2:

$R_{loc.front6} = 397 \cdot ft$

$R_{loc.side6} = 397 \cdot ft$

$R_{loc.f.Sandia6} = 631 \cdot ft$

$R_{loc.s.Sandia6} = 631 \cdot ft$

$\frac{R_{loc.f.Sandia6}}{R_{loc.front6}} - 1 = 59 \cdot \%$

$\frac{R_{loc.s.Sandia6}}{R_{loc.side6}} - 1 = 59 \cdot \%$

$R_{loc.f.FERC6} = 413 \cdot ft$

$R_{loc.s.FERC6} = 413 \cdot ft$

$\frac{R_{loc.f.FERC6}}{R_{loc.front6}} - 1 = 4 \cdot \%$

$\frac{R_{loc.s.FERC6}}{R_{loc.side6}} - 1 = 4 \cdot \%$

Distance to 1,600 BTU/hr-ft^2:

$R_{loc.front5} = 484 \cdot ft$

$R_{loc.side5} = 484 \cdot ft$

$R_{loc.f.Sandia5} = 775 \cdot ft$

$R_{loc.s.Sandia5} = 775 \cdot ft$

$\frac{R_{loc.f.Sandia5}}{R_{loc.front5}} - 1 = 60 \cdot \%$

$\frac{R_{loc.s.Sandia5}}{R_{loc.side5}} - 1 = 60 \cdot \%$

$R_{loc.f.FERC5} = 502 \cdot ft$

$R_{loc.s.FERC5} = 502 \cdot ft$

$\frac{R_{loc.f.FERC5}}{R_{loc.front5}} - 1 = 4 \cdot \%$

$\frac{R_{loc.s.FERC5}}{R_{loc.side5}} - 1 = 4 \cdot \%$

Hazard Distance Calculations (continued)

Distance to 31.5 kW/m^2:

$R_{loc.front1} = 83.81 \cdot m$

$R_{loc.side1} = 83.81 \cdot m$

$R_{loc.f.Sandia1} = 128 \cdot m$

$R_{loc.s.Sandia1} = 128 \cdot m$

$\frac{R_{loc.f.Sandia1}}{R_{loc.front1}} - 1 = 52 \cdot \%$

$\frac{R_{loc.s.Sandia1}}{R_{loc.side1}} - 1 = 52 \cdot \%$

$R_{loc.f.FERC1} = 78 \cdot m$

$R_{loc.s.FERC1} = 78 \cdot m$

$\frac{R_{loc.f.FERC1}}{R_{loc.front1}} - 1 = -7 \cdot \%$

$\frac{R_{loc.s.FERC1}}{R_{loc.side1}} - 1 = -7 \cdot \%$

Distance to 21.1 kW/m^2:

$R_{loc.front2} = 95.20 \cdot m$

$R_{loc.side2} = 95.20 \cdot m$

$R_{loc.f.Sandia2} = 148 \cdot m$

$R_{loc.s.Sandia2} = 148 \cdot m$

$\frac{R_{loc.f.Sandia2}}{R_{loc.front2}} - 1 = 55 \cdot \%$

$\frac{R_{loc.s.Sandia2}}{R_{loc.side2}} - 1 = 55 \cdot \%$

$R_{loc.f.FERC2} = 95 \cdot m$

$R_{loc.s.FERC2} = 95 \cdot m$

$\frac{R_{loc.f.FERC2}}{R_{loc.front2}} - 1 = -0 \cdot \%$

$\frac{R_{loc.s.FERC2}}{R_{loc.side2}} - 1 = -0 \cdot \%$

Distance to 12.6 kW/m^2:

$R_{loc.front3} = 111.03 \cdot m$

$R_{loc.side3} = 111.03 \cdot m$

$R_{loc.f.Sandia3} = 175 \cdot m$

$R_{loc.s.Sandia3} = 175 \cdot m$

$\frac{R_{loc.f.Sandia3}}{R_{loc.front3}} - 1 = 58 \cdot \%$

$\frac{R_{loc.s.Sandia3}}{R_{loc.side3}} - 1 = 58 \cdot \%$

$R_{loc.f.FERC3} = 115 \cdot m$

$R_{loc.s.FERC3} = 115 \cdot m$

$\frac{R_{loc.f.FERC3}}{R_{loc.front3}} - 1 = 3 \cdot \%$

$\frac{R_{loc.s.FERC3}}{R_{loc.side3}} - 1 = 3 \cdot \%$

Distance to 5.00 kW/m^2:

$R_{loc.front4} = 147.35 \cdot m$

$R_{loc.side4} = 147.35 \cdot m$

$R_{loc.f.Sandia4} = 236 \cdot m$

$R_{loc.s.Sandia4} = 236 \cdot m$

$\frac{R_{loc.f.Sandia4}}{R_{loc.front4}} - 1 = 60 \cdot \%$

$\frac{R_{loc.s.Sandia4}}{R_{loc.side4}} - 1 = 60 \cdot \%$

$R_{loc.f.FERC4} = 153 \cdot m$

$R_{loc.s.FERC4} = 153 \cdot m$

$\frac{R_{loc.f.FERC4}}{R_{loc.front4}} - 1 = 4 \cdot \%$

$\frac{R_{loc.s.FERC4}}{R_{loc.side4}} - 1 = 4 \cdot \%$

Transmissivities Calculations

Transmissivity at 10,000 BTU/hr-ft^2:

$\tau_{frontLNGFIRE3}(R_{loc.front7}) = 0.727$ $\tau_{Sandia.front}(R_{loc.f.Sandia7}) = 0.697$

$\tau_{sideLNGFIRE3}(R_{loc.side7}) = 0.727$ $\tau_{Sandia.side}(R_{loc.s.Sandia7}) = 0.697$

$$\frac{\tau_{Sandia.front}(R_{loc.f.Sandia7})}{\tau_{frontLNGFIRE3}(R_{loc.front7})} - 1 = -4\cdot\%$$

$$\frac{\tau_{Sandia.side}(R_{loc.f.Sandia7})}{\tau_{sideLNGFIRE3}(R_{loc.front7})} - 1 = -4\cdot\%$$

Transmissivity at 3,000 BTU/hr-ft^2:

$\tau_{frontLNGFIRE3}(R_{loc.front6}) = 0.704$ $\tau_{Sandia.front}(R_{loc.f.Sandia6}) = 0.658$

$\tau_{sideLNGFIRE3}(R_{loc.side6}) = 0.704$ $\tau_{Sandia.side}(R_{loc.s.Sandia6}) = 0.658$

$$\frac{\tau_{Sandia.front}(R_{loc.f.Sandia6})}{\tau_{frontLNGFIRE3}(R_{loc.front6})} - 1 = -7\cdot\%$$

$$\frac{\tau_{Sandia.side}(R_{loc.f.Sandia6})}{\tau_{sideLNGFIRE3}(R_{loc.front6})} - 1 = -7\cdot\%$$

Transmissivity at 1,600 BTU/hr-ft^2:

$\tau_{frontLNGFIRE3}(R_{loc.front5}) = 0.693$ $\tau_{Sandia.front}(R_{loc.f.Sandia5}) = 0.639$

$\tau_{sideLNGFIRE3}(R_{loc.side5}) = 0.693$ $\tau_{Sandia.side}(R_{loc.s.Sandia5}) = 0.639$

$$\frac{\tau_{Sandia.front}(R_{loc.f.Sandia5})}{\tau_{frontLNGFIRE3}(R_{loc.front5})} - 1 = -8\cdot\%$$

$$\frac{\tau_{Sandia.side}(R_{loc.f.Sandia5})}{\tau_{sideLNGFIRE3}(R_{loc.front5})} - 1 = -8\cdot\%$$

Transmissivities Calculations (continued)

Transmissivity at 31.5 kW/m^2:

$\tau_{frontLNGFIRE3}(R_{loc.front1}) = 0.727$ $\tau_{Sandia.front}(R_{loc.f.Sandia1}) = 0.697$

$\tau_{sideLNGFIRE3}(R_{loc.side1}) = 0.727$ $\tau_{Sandia.side}(R_{loc.s.Sandia1}) = 0.697$

$$\frac{\tau_{Sandia.front}(R_{loc.f.Sandia1})}{\tau_{frontLNGFIRE3}(R_{loc.front1})} - 1 = -4\cdot\%$$

$$\frac{\tau_{Sandia.side}(R_{loc.f.Sandia1})}{\tau_{sideLNGFIRE3}(R_{loc.front1})} - 1 = -4\cdot\%$$

Transmissivity at 21.1 kW/m^2:

$\tau_{frontLNGFIRE3}(R_{loc.front2}) = 0.719$ $\tau_{Sandia.front}(R_{loc.f.Sandia2}) = 0.683$

$\tau_{sideLNGFIRE3}(R_{loc.side2}) = 0.719$ $\tau_{Sandia.side}(R_{loc.s.Sandia2}) = 0.683$

$$\frac{\tau_{Sandia.front}(R_{loc.f.Sandia2})}{\tau_{frontLNGFIRE3}(R_{loc.front2})} - 1 = -5\cdot\%$$

$$\frac{\tau_{Sandia.side}(R_{loc.f.Sandia2})}{\tau_{sideLNGFIRE3}(R_{loc.front2})} - 1 = -5\cdot\%$$

Transmissivity at 12.6 kW/m^2:

$\tau_{frontLNGFIRE3}(R_{loc.front3}) = 0.709$ $\tau_{Sandia.front}(R_{loc.f.Sandia3}) = 0.667$

$\tau_{sideLNGFIRE3}(R_{loc.side3}) = 0.709$ $\tau_{Sandia.side}(R_{loc.s.Sandia3}) = 0.667$

$$\frac{\tau_{Sandia.front}(R_{loc.f.Sandia3})}{\tau_{frontLNGFIRE3}(R_{loc.front3})} - 1 = -6\cdot\%$$

$$\frac{\tau_{Sandia.side}(R_{loc.f.Sandia3})}{\tau_{sideLNGFIRE3}(R_{loc.front3})} - 1 = -6\cdot\%$$

Transmissivity at 5.00 kW/m^2:

$\tau_{frontLNGFIRE3}(R_{loc.front4}) = 0.693$ $\tau_{Sandia.front}(R_{loc.f.Sandia4}) = 0.639$

$\tau_{sideLNGFIRE3}(R_{loc.side4}) = 0.693$ $\tau_{Sandia.side}(R_{loc.s.Sandia4}) = 0.639$

$$\frac{\tau_{Sandia.front}(R_{loc.f.Sandia4})}{\tau_{frontLNGFIRE3}(R_{loc.front4})} - 1 = -8\cdot\%$$ $$\frac{\tau_{Sandia.side}(R_{loc.f.Sandia4})}{\tau_{sideLNGFIRE3}(R_{loc.front4})} - 1 = -8\cdot\%$$

APPENDIX B: REFERENCES

{THIS PAGE INTENTIONALLY LEFT BLANK}

REFERENCES

American Gas Association, *LNG Safety Program: Consequences of LNG Spills on Land*, IS-3-1, American Gas Association, Arlington, VA, July 1974. [AGA 1974]

Atallah, S., Shah, J., *LNGFIRE: A Thermal Radiation Model for LNG Fires*, GRI-89/0176. Gas Research Institute, 1990. [Atallah 1990]

Blanchat, T., Helmick, P., Jensen, R., Luketa, A., Deola, R., Suo-Anttila, S., Mercier, J., Miller, T., Ricks, A., Simpson, R., Demosthenous, B., Tieszen, S., and Hightower, M., *The Phoenix Series Large Scale LNG Pool Fire Experiments*, SAND2010-8676, Sandia National Laboratories, Albuquerque, NM, 2010. [Blanchat 2010]

Gas Research Institute, *LNGFIRE2: A Thermal Radiation Model for LNG Fires*, GRI-92/0532, 1992. [GRI 1992]

Gas Technology Institute, *LNGFIRE3: A Thermal Radiation Model for LNG Fires*, GTI-04/0032, 2004. [GTI 2004]

Kohout, A., *Evaluation of DEGADIS2.1 Using Advisory Bulletin ADB-10-07*, Federal Energy Regulatory Commission, July 2011. [Kohout 2011]

Luketa, A., *Recommendations on the Prediction of Thermal Hazard Distances from Large Liquefied Natural Gas Pool Fires on Water for Solid Flame Models*, SAND2011-9415, Sandia National Laboratories, Albuquerque, NM, 2011. [Luketa 2011]

Malvos, H., Raj, P., Details of 35 m Diameter LNG Fire Tests Conducted In Montoir, France in 1987, and Analysis of Fire Spectral and other Data, AIChE Spring National Meeting, Orlando, Florida, April 23-27, 2006. [Malvos 2006]

Raj, P., Spectrum of Fires in an LNG Facility: Assessments, Models and Consideration in Risk Evaluations, Final Technical Report, DTRS56-04-T-0005, U.S. Department of Transportation, December 5, 2006. [Raj 2006]

U.S. Department of Energy, *Liquefied Natural Gas Research*, Report to Congress, May 2012. [DOE 2012]

U.S. Department of Transportation, *Direct final rule: Liquefied Natural Gas Regulations—Miscellaneous Amendments*, Federal Register, 62 Fed. Reg. 8,402-8,043, February 25, 1997. [DOT 1997]

U.S. Department of Transportation, *Final rule: Pipeline Safety: Incorporation of Standard NFPA 59A in the Liquefied Natural Gas Regulations*, Federal Register, 65 Fed. Reg. 10,952, March 1, 2000. [DOT 2000]

U.S. Department of Transportation, *Final rule: Pipeline Safety: Periodic Updates of Regulatory References to Technical Standards and Miscellaneous Edits*, Federal Register, 75 Fed. Reg. 48,593, August 11, 2010. [DOT 2010a]

U.S. Department of Transportation, *Advisory Bulletin ADB-10-07 Liquefied Natural Gas Facilities: Obtaining Approval of Alternative Vapor-Gas Dispersion Models*, Federal Register, 75 Fed. Reg. 53,371-53,374 (August 31, 2010b). [DOT 2010b]

{THIS PAGE INTENTIONALLY LEFT BLANK}

APPENDIX C: LIST OF PREPARERS

{THIS PAGE INTENTIONALLY LEFT BLANK}

LIST OF PREPARERS

Kohout, Andrew

B.S., Mechanical Engineering, 2006, University of Maryland
B.S., Fire Protection Engineering, 2006, University of Maryland
M.S., Fire Protection Engineering, 2011, University of Maryland

Turpin, Terry

B.S., Civil Engineering, 1992, Virginia Polytechnic Institute & State University